APPENDIX B

THE DEVELOPMENT OF HIGH PERFORMANCE INSULATION SYSTEMS

PROGRAM PROGRESS REPORT NO. 14

Contract Number AF 04(647)-464

1 January through 31 March 1963

Prepared for

AIR FORCE BALLISTIC SYSTEMS DIVISION
AIR FORCE SYSTEMS COMMAND

1 APRIL 1963

C-62458

APPENDIX B

PROGRAM PROGRESS REPORT, NO. 14, 1 JAN - 31 MAR 63,

THE DEVELOPMENT OF HIGH PERFORMANCE INSULATION SYSTEMS. APPENDIX B.

Contract No. AF 04(647)-464

Work Completed

1 September 1960

Prepared for

AIR FORCE BALLISTIC SYSTEMS DIVISION

AIR FORCE SYSTEMS COMMAND

1 April 1963,

1 ft mo, C-62458

Arthur D. Little, Inc.

CONTENTS

I. SUMMARY 1

A. Introduction 1
B. Scope 1
C. Tests 2
D. Conclusions 2

II. STATE OF THE ART 3

III. THEORY 8

A. Nomenclature 8
B. Definition of Apparent Mean Thermal Conductivity 9
C. Modes of Heat Transfer 9
D. Discussion of Heat Transfer Analysis 10

IV. MATERIALS OF CONSTRUCTION 14

A. Radiation Shields 14
B. Spacers 14

V. EXPERIMENTAL APPARATUS AND TEST PROCEDURES 16

A. Single, Guarded, Cold-Plate Thermal-Conductivity Test Apparatus 16
B. 30-Liter Dewar 20

VI. TEST RESULTS 23

A. Tests with Single Guarded Cold-Plate Apparatus 23
B. Tests on 30-Liter Dewar 40
C. Outgassing of Insulating Material 42

VII. MANUFACTURING AND HANDLING TECHNIQUES 45

A. Radiation Shield Materials 45
B. Spacer Materials 45
C. Application Methods 45

VIII. LITERATURE SURVEY 47

IX. FURTHER DEVELOPMENT 48

X. CONCLUSIONS 49

XI. LIST OF REFERENCES 50

APPENDIX 52

TABLES

Table		Page
I.	Density and Thermal Conductivity of Insulating Materials	4
II.	Density and Thermal Conductivity of Insulating Materials	5
III.	Apparent Mean Thermal Conductivity of Various Power Insulations in Vacuum	7
IV.	Materials Tested as Radiation Shields	15
V.	Materials Tested as Spacers	15
VI.	Apparent Mean Thermal Conductivity	19
VII.	Insulations Tested on 30-Liter Dewar	22
VIII.	Tests of Insulations with Single Guarded Cold-Plate Apparatus	24
IX.	Emissivity of Surfaces and Foils	29
X.	Influence of Radiation Shield Choice on Total Heat Transfer	30
XI.	Influence of Spacer Choice on Total Heat Transfer.	34
XII.	Calculated Heat Transferred by Different Mechanisms Through Insulated Sample	35
XIII.	Tests on 30-Liter Dewar	41

I. SUMMARY

A. INTRODUCTION

The work reported in this appendix was completed in the fall of 1960. Subsequently it was decided that a detailed report on the development of high performance insulation systems was not required but that the information given in the quarterly progress reports was sufficient. Recently, interest in specific aspects of the test program has been shown and ADL was directed to issue the complete report as a part of this quarterly program progress report. A more recent report on a superinsulation system can be found in an ADL report to NASA (Contract No. NAS5-664) entitled "Liquid Propellant Losses During Space Flight," subtitled "Thermal Protection Systems for LH_2 Tanks," April 1963.

The growth of the cryogenics industry over the past ten years and the experience gained in the liquefaction of gases and the transportation and storage of cryogenic fluids have resulted in new industrial applications of these fluids. The use of liquefied gases such as methane, oxygen, nitrogen, and helium have become common in the steel, petroleum, chemical, electronics, and aircraft industries. The requirements for their transportation to the point of use and their storage for considerable periods has made the development of improved insulation techniques urgent. For a given application the type of insulation used depends primarily on the weight and space limitations, which may be classified as follows:

1. No space and weight limitation; e.g., stationary storage units of large capacity in the steel, mining, and chemical industries.

2. Space the paramount limitation, weight limitations, secondary; e.g., laboratory equipment, tanks for rail and highway transport, and for marine vessels.

3. Weight and space limitations paramount; e.g., cryogenic vessels for aircraft and space vehicles.

It is obvious that the development of an insulation technique for cryogenic vessels for aircraft and space vehicles presents the greatest challenge.

B. SCOPE

In 1958, Arthur D. Little, Inc., began a study (under Contract No. AF 33-(616)-5641) of the available insulation systems as well as of the feasibility of developing new insulation systems. The object was to find the most satisfactory means of achieving highly efficient insulation under severe weight and space limitations.

In the course of the study, the basic configuration of a high-efficiency, multilayer insulation was developed from a theoretical analysis.

Insulation samples were prepared and their performance evaluated by laboratory tests. These tests indicated that this new insulation would perform as predicted and a program for its development was undertaken under Contracts AF 04-(645)-34 and AF 04-(647)-464. This report discusses the selection of insulating materials, the methods of constructing samples of insulation systems, and the tests that were conducted for evaluating their effectiveness.

C. TESTS

Tests were conducted on small samples in a single-plate laboratory rig and on a 30-liter dewar. The single plate rig was used to establish the apparent conductivity of multilayer insulators made of various combinations of radiation shields and insulating spacers. The test on the 30-liter dewar established that results obtained in the single-plate rig applied to full-scale installations.

D. CONCLUSIONS

On the basis of our experimental work we can draw the following conclusions:

1. Good agreement exists between thermal conductivity data obtained in the single-plate thermal conductivity apparatus and the 30-liter insulated container.

2. The superiority of the multilayer radiation-shield insulation system over other insulation systems was established under laboratory conditions.

3. Immediate use of the multilayer radiation-shield insulation system in selected cases is possible and wide spread industrial use is feasible.

4. A combination of radiation shields and spacers suitable for a specific use may be selected on the basis of the information obtained.

5. Insulation effectiveness is greatly influenced by the degree of vacuum actually obtained in the insulation system. The vacuum is influenced by the prior history of outgassing and the materials used for the spacers and radiation shields of the insulation. The degree of cryopumping influences the effectiveness of the system.

II. STATE OF THE ART

Solids that have thermal conductivities of less than 10 $\frac{\text{Btu-in.}}{\text{hr-ft}^2\text{-}^\circ\text{F}}$ are customarily termed insulators. Experience in the handling of cryogenic materials has shown that the thermal conductivity cannot be reduced sufficiently by the use of a single insulator. Thus, an insulator must be modified or various insulation materials must be combined if sufficiently low values of thermal conductivity are to be attained. Combinations of insulation materials are called insulation systems. Superinsulation, maximum-efficiency insulation, multilayer radiation insulation, are terms that denote insulation systems in which the total heat transfer caused by gas conduction, solid-to-solid conduction, and radiation has been reduced to a minimum.

In an insulation system, several methods for reducing the heat transfer may be used. In many insulation systems the conduction path is broken up to reduce the heat conduction through the solid (e.g., the solid is pulverized or formed into fine fibers which are aligned perpendicularly to the heat flow). As long as the particles do not agglomerate, resistance to heat flow will exist at the surface of each particle. By this method the thermal conductivity has been reduced by one order of magnitude (see Table I). The thermal conductivity of a solid has also been reduced tenfold by decreasing the area of the solid conduction path; glass and plastic foams are examples of this method (Table II). Typical unevacuated powders, fibrous materials, and foam insulators have thermal conductivities between 0.5 and 0.1 $\frac{\text{Btu-in.}}{\text{hr-ft}^2\text{-}^\circ\text{F}}$.

As the lower limit of this range is approached, conduction through the gas filling the interstices of the material becomes the dominant contributor to the over-all heat flow (Reference 1). In general, large gas molecules have low thermal conductivity. Therefore, some benefit can be obtained from the use of a gas of high molecular weight, but the improvement in insulating value is limited to approximately the difference between the conductivity of the gas and that of the air (Reference 2).

A far greater improvement can be obtained by removal of the gas. The substantial gains to be obtained in this manner have already been recognized (References 3 and 4). Evacuation of the powder and fibrous insulations decreases the thermal conductivity by one order of magnitude to a range of 0.05 - 0.01 $\frac{\text{Btu-in.}}{\text{hr-ft}^2\text{-}^\circ\text{F}}$.

As the lower limit of this range is approached, the heat radiation, which originally accounted only for a few per cent of the total heat flow becomes the major contributing factor to the heat transport through the evacuated insulation. An increase of insulating effectiveness above the level obtained by the removal of the environmental air and by the breaking up of the conduction paths requires the attenuation of radiant energy that passes through the material. Radiation heat transfer may be reduced by the use of additives (to powders and fibrous materials), that act as absorbers

TABLE I

DENSITY AND THERMAL CONDUCTIVITY OF INSULATING MATERIALS*

(SOLID, POWDERED, AND FIBROUS FORMS)

Material	Solid		Powder		Fiber		Remarks
	k $\frac{\text{Btu-in.}}{\text{ft}^2\text{-hr-}^\circ\text{F}}$	ρ lb/ft^3	k $\frac{\text{Btu-in.}}{\text{ft}^2\text{-hr-}^\circ\text{F}}$	ρ lb/ft^3	k $\frac{\text{Btu-in.}}{\text{ft}^2\text{-hr-}^\circ\text{F}}$	ρ lb/ft^3	
Asbestos	1.3	112	-	-	0.24	-	
Glass	4 - 8	139	0.10 - 0.29	2 - 10	0.14-0.30	1 - 15	
Graphite	1100	-	1.2	30	-	-	
Ice-Snow	15.6	57.5	3.2	34.7	-	-	at 32°F
Wood	1.4 - 2.4	34 - 50	0.36	12	0.32	-	

* References 1 and 2. Values are for room temperature and pressure unless otherwise indicated.

TABLE II

DENSITY AND THERMAL CONDUCTIVITY OF INSULATING MATERIALS *

(SOLID AND FOAMED FORMS)

Material	Solid		Foam	
	k $\frac{\text{Btu-in.}}{\text{ft}^2\text{-hr-}^\circ\text{F}}$	ρ lb/ft^3	k $\frac{\text{Btu-in.}}{\text{ft}^2\text{-hr-}^\circ\text{F}}$	ρ lb/ft^3
Glass	4 - 8	139	0.40	4 - 10
Polyester	1.5	120	0.20 - 0.30	2 - 10
Polystrene	0.6	69	0.26	2.5 - 10.0
Epoxy	1.5	70	0.30	6
Rubber	1.1	75	0.19	7

* References 11, 12, 22, 23, and 24. All values are for room temperature and pressure.

and scatterers of radiation heat. Metal powders, such as aluminum and copper (Reference 5), and carbon powder (Reference 6) mixed with the insulation give satisfactory results as a radiation-absorbing medium. The thermal conductivity of insulations that use such additives decreases to approximately 0.005 $\frac{\text{Btu-in.}}{\text{hr-ft}^2\text{-}^\circ\text{F}}$ (See Table III.)

Until recently, this was the best available insulation. In 1951 Peter Peterson (Reference 7 and 8) at the University of Lund in Sweden found that approximately the same value of thermal conductivity (he reported 0.0057 $\frac{\text{Btu-in.}}{\text{hr-ft}^2\text{-}^\circ\text{F}}$) could be obtained by the use of successive radiation shields on thin aluminum foil, spirally wound with very fine glass-wool spacers. His test report, however, did not arouse any notable interest because the available powder insulation was cheaper, and at that time, its performance was regarded as highly satisfactory. However, because of the present-day requirements for maximum utilization of available space in missiles and in transportation facilities for light cryogenic fluids, such as hydrogen and helium*, a demand has been created for cryogenic insulations of the highest possible efficiency.

It was clear that it would not be possible to improve the insulations presently on the market to the desired degree and that a basically new approach to the problem, similar to the approach taken by P. Peterson, was necessary. A new insulation system greatly superior to the available powder insulation was developed. This system consists of an assembly of layers of radiation shields of high reflectivity separated by spacers of low thermal conductivity and is subjected to a high vacuum.

*Since these two fluids have very low heats of vaporization, a liquid-nitrogen shield is now used around the hydrogen or helium vessel to prevent high evaporation rate of these valuable fluids. This construction is expensive, heavy, and bulky.

TABLE III

APPARENT MEAN THERMAL CONDUCTIVITY

OF VARIOUS POWDER INSULATIONS IN VACUUM*

Base (% by weight)	Carbon (% by weight)	Density (lb/ft^3)	Warm Plate Temp. (^oF)	Apparent "k" $\left(\frac{Btu\text{-}in.}{ft^2\text{-}hr\text{-}^oF}\right)$
Perlite -- 100	-	10	50	.0105
**Cab-O-Sil -- 100	-	3.4	50	.010
Perlite -- 60	40	5	70	.0033
Cab-O-Sil -- 30	70	5	72	.0077
Cab-O-Sil -- 40	60	5	73.5	.0057
Cab-O-Sil -- 75	25	5	50	.0046
ADL -- 16	-	5	50	.0049

* Measurements were made with single guarded cold plate apparatus under the following conditions:

Emissivities of Hot and Cold Walls: 0.7

Temperature of Cold Wall: -320 F

Vacuum : 10^{-5} mm Hg

Assembly Thickness: 1/2"

** Cab-O-Sil is produced by Godfrey L. Cabot, Inc., Cambridge, Massachusetts

III. THEORY

A. NOMENCLATURE

A	Area - ft^2
a_1	Accommodation coefficient for gas at cold boundary temperature - dimensionless
a_2	Accommodation coefficient for gas at warm boundary temperature - dimensionless
C	Proportionality constant - 194 $Btu/hr\text{-}lb_f\text{-}\sqrt{^oR}$
e_s	Emissivity of radiation shield surface - dimensionless
e_w	Emissivity of boundary walls - dimensionless
k	Thermal conductivity of solid - $Btu\text{-}in./hr\text{-}ft^2\text{-}^oR$
k_a	Apparent thermal conductivity - $Btu\text{-}in./hr\text{-}ft^2\text{-}^oR$
ℓ	Thickness of insulation - inches
L	Thickness of the multilayer insulation - inches
M	Molecular weight of residual gas - dimensionless
n	Number of radiation shields - dimensionless
P	Gas pressure - lb/ft^2
Q	Rate of heat transfer - Btu/hr
q	Heat flux (Q/A) - $Btu/hr\text{-}ft^2$
T_1	Cold boundary temperature - ^oR
T_2	Warm boundary temperature - ^oR
T_p	Temperature at which gas pressure P is measured - ^oR
ΔT	Temperature difference between neighboring radiation shields - ^oR
γ	Ratio of gas specific heat (C_p/C_v) - dimensionless
σ	Stefan-Boltzmann constant - 0.1713×10^{-8} $Btu/hr\text{-}ft^2\text{-}R^4$

B. DEFINITION OF APPARENT MEAN THERMAL CONDUCTIVITY

The maximum efficiency insulation can be defined as an insulation that, for a given thickness applied to a given area, results in minimum heat transfer between two surfaces at given temperatures. The insulation thus has a minimum apparent mean thermal conductivity. The definition of the apparent mean thermal conductivity is:

$$k_A = \frac{Q_{Total} \ell}{A(T_2 - T_1)} \qquad (1)$$

The apparent conductivity, k_A, defined by equation (1) is not a property of the insulation system. It is used to combine three modes of heat transfer into one equation. Therefore, k_A, will change with T_1 and T_2 and with the thickness (ℓ). Nevertheless, this definition is commonly applied in the evaluation of powder insulations and is used freely in the literature for applications where the temperatures on the boundaries are known. Since the insulation is intended for use on vessels which can contain various cryogenic fluids, the k_A value corresponding to liquid oxygen, hydrogen, helium, or other temperatures can be determined experimentally and a selection can be made by comparing the different insulation systems for the actual boundary temperatures. We should bear in mind, however, that these k_A values are valid only for the specified temperatures.

C. MODES OF HEAT TRANSFER

In analyzing the effectiveness of an insulation system we must consider three mechanisms of heat transfer:

1. Heat conduction through the gas permeating the insulation.
2. Heat radiation between the surfaces.
3. Heat conduction through the solid.

The minimum heat transfer will be reached when the sum of all three is a minimum. We must, therefore, consider each of the mechanisms of heat transfer separately and determine the means to reduce each of them.

1. Gas Conduction

One can minimize the heat conduction through the gas medium quite easily by maintaining a high vacuum in the space enclosing an insulation layer. Once the mean free path of the gas molecules exceeds the surface spacing, the heat conduction rate per unit area through the gas becomes proportional to its pressure (Figure 1 and Reference 9) and can be expressed as follows:

$$q_{Gas} = Q_{Gas}/A_{Mean}$$

$$q_{Gas} = C \frac{a_1 a_2}{a_2 + a_1(1 - a_2)A_1/A_2} \left(\frac{\gamma + 1}{\gamma - 1} \right) \sqrt{\frac{P}{MT_p}} \Delta T \qquad (2)$$

We can see from equation (2) that heat conduction through the gas can be made as small as desired by decreasing the pressure. When a high vacuum is achieved, gas conduction is negligible. Gas convection also becomes negligible at low pressures and may be disregarded.

2. Radiation

The heat transmission rate by radiation can be expressed by the modified Stefan-Boltzmann equation:

$$q_{rad} = \frac{Q_{rad}}{A_{Mean}} = \sigma \frac{T_2^4 - T_1^4}{\left[(2/e_s) - 1 \right] n + (2/e_w) - 1} \qquad (3)$$

From this equation we deduce that the heat transferred by radiation can be decreased by increasing the number of radiation shields and by the use of materials of low emissivity as radiation shields.

3. Solid Conduction

The heat conduction rate per unit area, through a solid, is expressed by the equation:

$$q_{Solid} = \frac{Q_{Solid}}{A_{Mean}} = \frac{k}{\ell} \Delta T \qquad (4)$$

Consequently, a decrease of heat transfer through a solid may be achieved by reduction of the areas of contact between individual particles and by the use of materials of low thermal conductivity.

D. DISCUSSION OF HEAT TRANSFER ANALYSIS

From equation (3), we can see that high-efficiency insulation may theoretically be achieved by mounting in series a large number of low emissivity radiation shields. However, materials that have a low emissivity also have a high thermal conductivity. Thus we find from equation (4) that if adjacent shields are allowed to touch each other the resulting increase in solid conduction heat transfer may offset the decrease in

radiation heat transfer. It follows that if radiation shields are to be employed to reduce the heat transfer rate, means must be found to eliminate direct contact between the shields and between the boundaries and the shields. It also follows that materials used to separate the shields must be of the lowest possible thermal conductivity and that the area of contact with the shields must be minimized.

This discussion suggests that a maximum efficiency insulation can be developed in the following way:

1. Minimize radiation heat transfer by a series of radiation shields. A radiation shield is defined as a single thickness of material of low emissivity having no direct contact with adjoining shields or with the boundaries.

2. Separate the radiation shields by solid spacers having very low thermal conductivity and a minimum contact area with the shields.

3. Minimize heat transfer through the gas permeating the insulation by the use of a high vacuum.

The heat transfer through gas and through solid in a series of spacers can be analyzed by the application of equations (1) and (4). Assume that the number of radiation shields is n and the number of spacers is (n + 1). To simplify the analysis, also assume that the temperature drop, Δ T, through each spacer is the same. We then find that:

$$T_2 - T_1 = (n+1)\ \Delta T$$

$$\Delta T = \frac{T_2 - T_1}{n+1}$$

Thus equation (2) becomes:

$$q_{Gas} = C\ \frac{a_1 a_2}{a_2 + a_1\ (1 - a_2)\ A_1/A_2}\ \left(\frac{\gamma+1}{\gamma-1}\right)\sqrt{\frac{P}{MT_p}}\ \frac{T_2 - T_1}{n+1} \qquad (2a)$$

and the conduction of heat through the gas is inversely proportional to the number of spacers. Equation (4) remains unchanged when L, the thickness of the multilayer insulation, and $T_2 - T_1$ are substituted for $\mathcal{L}$ and ΔT respectively (since $\mathcal{L} = L/(n+1)$, $\Delta T = (T_2 - T_1)/(n+1)$). However, the resistance to heat conduction between spacer and radiation shield must now be taken into account. On the basis of experimental data (Reference 10), the correction factor for conductive resistance may be expressed by $1/\sqrt{n}$.

Equation (4) now becomes:

$$q_{Solid} = \frac{1}{\sqrt{n}} \frac{k}{L} (T_2 - T_1) \qquad (4a)$$

The heat conductivity of radiation shields is very high in comparison to that of the spacers and therefore it is assumed to be infinite, i.e., the temperature drop across the radiation shield is zero.

The total heat transfer rate in the system consisting of a series of radiation shields and spacers is then equal to the sum of equations (2a), (3), and (4a): $q_{Total} = q_{Gas} + q_{Rad} + q_{Solid}$.

$$q_{Total} = \left[C \frac{a_1 a_2 (\gamma + 1)/(\gamma - 1)}{a_2 + (A_1/A_2)(1-a_2)a_1} \frac{P}{\sqrt{MT_p}} \frac{1}{n+1} + \frac{k}{nL} \right] (T_2 - T_1)$$

$$+ \sigma \frac{T_2^4 - T_1^4}{\left[(2/e_s) - 1\right] n + (2/e_w) - 1} \qquad (5)$$

Equation (5) can be written in a simplified form if the residual gas and its pressure is established for all runs and if n is assumed to be a large number, i.e., if n becomes approximately equal to n + 1, then:

$$q_{Total} = \left[(C_1 + C_2 \sqrt{n})(T_2 - T_1) + C_3 (T_2^4 - T_1^4) \right] / n \qquad (5a)$$

where:

$$C_1 = C \frac{a_1 a_2}{a_2 + a_1(1 - a_2) A_1/A_2} \left(\frac{\gamma + 1}{\gamma - 1} \right) \frac{P}{\sqrt{MT_p}}$$

$$C_2 = k/L$$

$$C_3 = \sigma / \left[(2/e_s) - 1 \right]$$

Since n is large, the $(2/e_w - 1)$ term is small compared to $n\,(2/e_s) - 1$ and has been neglected in the denominator of the equation for C_3.

A sample calculation based on equation (5a) can be found in the Appendix, Chapter 1. Clearly, there are several sources of error present:

1. We assume that the heat flow is one-dimensional, and perpendicular to the plane of the shield and the spacer. In reality, lateral heat flow may be present, and the temperature of the shield (and spacer) may not be uniform. For instance we have calculated the heat transfer rate when a boundary at a temperature of 300 K is "seen" by the edges of the radiation shields. For a sample 2-3/4" diameter and 1/4" thick (10 shields) the heat transfer by radiation only (no physical contact exists between the boundary and the shields, and the gas is evacuated) is as much as $0.014\ \frac{Btu}{hr}$ or 20% of the total calculated one-dimensional heat flow through the same sample.

2. We assume that the pressure through the sample is uniform. In reality the vacuum on the surface of the specimen may differ by an order of magnitude from the vacuum in the interior of the specimen.

3. The simplified analysis is based on linear temperature distribution for conductive transfer, and on nonlinear temperature distribution for radiative transfer. Figure 2 shows the two temperature distributions. Since the real temperature distribution curve lies somewhere between these two curves, the heat transfer rates by conduction and by radiation will be somewhat different from the values used in establishing equation (5a).

IV. MATERIALS OF CONSTRUCTION

A. RADIATION SHIELDS

Several technically feasible arrangements incorporating the theoretical requirements for reducing the heat transfer rate can be suggested. There are publications available on materials with low emissivity surfaces (References 11 through 17). The materials of the lowest emissivity are in order of increasing emissivity; pure silver, pure gold, pure copper and pure aluminum. The cost of gold foil is prohibitive and silver and copper are difficult to obtain in sheet form. Highly reflective aluminum offers the most practical solution, since aluminum is readily available in foil thickness of the desired stiffness and strength. Stiffness and strength are important, for we have calculated that, to reduce the heat transfer through the spacers to the desired value, requires that contact between radiation shields be limited to points 1/8 to 1/4 inch apart. Such wide spacing requires mechanically stiff radiation shields. We found that H-19 tempered, aluminum foil 0.001 to 0.002 inches thick or metal coated Mylar (or acetate) films 0.003 to 0.005 inches thick exhibited the necessary stiffness. Further discussion of different radiation-shield materials is presented in Chapter VI, paragraph A-2. A list of material manufacturers contacted is given in the Appendix. Table IV lists the different materials used in the radiation shields that were tested.

B. SPACERS

Theoretically, the ideal method of separating the shields is to allow them to be suspended freely in the vacuum space. However, this method is not practicable so spacers are required to separate the shields.

Since 40 to 60 radiation shields of a known thickness per inch of insulation were to be employed, the allowable thickness of each spacer was established. Figures 3 through 9 show different schemes proposed for the spacers. The points of contact of the spacing material and the radiation shields should be kept as far apart as possible, the limiting distance being determined by the stiffness of the radiation shields. Boundary pressures to be encountered in practice must be taken into account, since pressure will cause an increase of contact area and will increase the heat conduction through the spacers. Boundary pressure will be increased if the insulation is subjected to compressive loads due to acceleration or atmospheric pressure. Therefore, glass or plastic spheres (preferably hollow) rather than a continuous sheet were considered as spacers for the radiation shields. Because no suitable adhesives could be obtained to maintain the spheres in the desired positions, we tried nettings of glass, nylon, and plastic-covered glass fibers. The nettings were quite easy to use with the aluminum shields, and, because of their low cost, seemed promising. Table V lists the spacers which were tested; Figures 10 through 12 show the spacer-shield combinations.

TABLE IV

MATERIALS TESTED AS RADIATION SHIELDS

1. 0.002-in. tempered Alcoa aluminum foil bright on both sides.
2. 0.00025-in. soft Alcoa aluminum foil.
3. 0.00025-in. soft Alcoa aluminum foil perforated (14% open).
4. 0.00025-in. Mylar, coated with aluminum on both sides.
5. 0.002-in. Mylar, coated with aluminum on one side.
6. 0.005-in. Mylar, coated with aluminum on one side.
7. 0.005-in. transparent Mylar.

TABLE V

MATERIALS TESTED AS SPACERS

1. 1/8 x 1/8 mesh, 0.010-in. dia. thread, resin covered fiberglass.
2. 1/4 x 1/4 mesh, 0.010-in. dia. thread, resin covered netting.
3. 0.10 x 0.10 mesh, 0.005-in. dia. thread, fortisan acetate, multi-strand netting.
4. Fiberglass AA - 8 lb/ft^3 density (Owens-Corning).
5. Polystyrene bonded fiberglass 0.010-in. thick, perforated (37% open).
6. Nylon stockings, 0.004-in. thick.
7. 0.008-in. thick Dexter paper.
8. 0.008-in. thick perforated (14 and 50% open area) Dexter paper.
9. Teflon washers, 0.015-in. thick, 0.050-in. O.D. x 0.027-in. I.D. spaced 3/4 in. apart.
10. 0.022-in. dia. glass beads 1/2 in. apart mounted on Mylar film.

V. EXPERIMENTAL APPARATUS AND TEST PROCEDURES

Two types of test apparatus were used: a single, guarded cold-plate apparatus for testing of the thermal conductivity of laboratory samples and a vessel for performance of the tests under simulated field conditions. Descriptions of the two types of apparatus follow.

A. SINGLE, GUARDED, COLD-PLATE THERMAL-CONDUCTIVITY TEST APPARATUS

1. Construction

The single-plate apparatus for the tests of low-temperature conductivity developed for this project is shown in Figure 13; design details are given in Figure 14. The apparatus consists of three main components:

1. A heat-source plate holding the specimen
2. A measuring vessel enclosed in a ring-shaped guard vessel
3. A bell-shaped covering jar

The brass heat-source plate (7-inch diameter and 1-inch thick), covered by a black paint of 0.74 emissivity (Reference 16), is placed on four micarta columns so that it is insulated from the ambient temperatures. The plate is kept at the desired constant temperature by water flowing through channels bored into it. Tap water, used for this purpose, passes first through copper coils placed in a thermostatically controlled water bath, then through a pressure regulator (which eliminates pulsation), then a flowmeter, and finally into the plate. The temperature of the water is measured by a thermometer at the entrance to the flowmeter and by four copper-constantan thermocouples attached to the plate. The thermocouples are installed in grooves and are made flush with the surface of the plate. A type K potentiometer is used for the thermocouple readings.

The 2-3/4 inch-diameter, 1/2-liter capacity stainless steel measuring vessel is enclosed in a ring-shaped guard vessel, also of stainless steel (2-7/8-inch inside diameter, 6-inch outside diameter, 5-1/4-liter capacity). The bottom surfaces of the measuring and guard vessels are painted with black paint of 0.74 emissivity to provide a means for determining radiation heat transfer. The bottom of the measuring vessel constitutes the cold plate. Four tie rods, used to lower the cold plate to a predetermined level over the heat-source plate, make it possible to regulate the mechanical pressure on the specimen.

Both vessels can withstand pressures ranging from a full vacuum to 200 psia. If additional temperature control is desired, a system of valving to raise or lower the pressure, and hence the boiling point of the cryogenic fluid, can be installed.

The vessels are vented by lines through the opening at the top of the enclosing jar. To decrease the possible inaccuracy in measurement due to heat-leak from vessel to vessel, a gap of 1/16 inch between the measuring and guard vessels is provided. Heat-leak along the measuring vessel's vent line, which passes through the guard vessel and forms the only metal-to-metal connection between the two, is minimized by its extremely small cross section (3/8-in. diameter, 0.015-in. thickness, 6-in. length).[1]

Since the guard vessel is filled to capacity with a cryogenic fluid, and the vent line is thus fully enclosed, the ambient-temperature heat-leak into the measuring vessel via the vent line is prevented, except by radiation heat transfer. (This heat loss has been decreased to less than 3×10^{-3} Btu per hour by the insertion of radiation shields in the vent-line neck.)

Because the heat-leak into the test chamber is insignificant, the measurement is not affected by a varying liquid level in the measuring vessel. However, if the heat-leak is to be kept small, the guard vessel must be kept full. Experiments have shown that the level in the guard vessel should not be allowed to drop more than 2 inches from the top.

The heat-source and cold-plate assembly are enclosed in a stainless steel, bell-shaped jar 8 inches in diameter and 22 inches high. The opening for the vent line at the top is encased in a rubber sleeve, which seals the atmosphere within the jar from the surrounding air. A diffusion pump attached to the jar evacuates it and the specimen within it. If the specimen is to be tested in a gas medium, the jar is filled with gas via the same line. Ionization and thermocouple vacuum gages are attached to the jar. The vent lines leading from both vessels are attached to rubber hose lines, which in turn are attached to capillary glass tubes placed under the inverted graduate in the low vapor-pressure oil bath (see Figure 15). The amount of oil displaced from the graduate per unit of time is an indication of the boil-off rate of the cryogenic fluid in the measuring vessel. The oil bath also prevents the diffusion and condensation of water vapor and air; moreover, the pressure within the measuring and guard vessels may be regulated by the degree to which the capillary tubes are immersed in the oil bath. Sensitive oil manometers connected to the vents on the vessels register the pressure inside; the pressure in the two vessels must be positive and equal if the vapors rising in the vent line are not to recondense. A radiation-shielded thermocouple is inserted in the graduate jar to measure the temperature of the boiled-off gas.

2. Check of Equipment Accuracy

Before we used the apparatus, we subjected it to a series of experiments designed to establish the actual temperature differences between the measuring and guard vessels. This was necessary for a check on the accuracy of the calculated heat leak of 1×10^{-3} Btu per hour (see Appendix, Chapter 3)

[1] See Section on "Check of Equipment Accuracy."

at an assumed temperature difference of 1 F. Such a heat-leak represents 1.5% of the total heat transfer through the best specimen. For these experiments we installed differential thermocouples (Figure 16) at the following locations:

1. On the vent line to the measuring vessel, one junction at the lower entrance to the guard vessel and the other at the neck of the measuring vessel.

2. One junction on the side surface of the guard vessel at the same level as the top of the measuring vessel, and the other on the top surface of the measuring vessel.

3. On the bottom surfaces of the guard and measuring vessels. Temperature differences of less than 1 F were registered at all points.

A copper-constantan thermocouple with an ice junction was attached to the cold plate (bottom surface of the measuring vessel). It showed that the cold plate's temperature differed from the liquid-nitrogen temperature by 1/2 F -- a reading corresponding to the calculated temperature difference.

All the thermocouples were removed after the successful tests because the heat transfer via the thermocouple wires was calculated to equal 0.15 Btu per hour, or 50% of the expected heat transfer through the insulation sample. Tests conducted with the same insulation specimen with and without the thermocouple systems bore out this assumption. Finally, the accuracy of the apparatus was checked by tests of Cab-O-Sil M-5, Santocel, and Perlite insulations, which were previously tested by NBS. Table VI compares the results obtained on ADL apparatus with the results published by NBS for the same materials. They show close agreement.

3. Experimental Procedure

The radiation shields and spacers were cut with a die. Radiation shields were carefully cleaned with a cleaning solvent to remove oil film The following solvents were tested: trichloroethylene, fumes and solution; carbon tetrachloride; and alkaline bath. All three solvents are about equally effective. The cleanliness of aluminum discs seems to depend mainly on the care with which they are handled by the operator.

A sample consisting of the alternate spacers and shields was placed on the heat source plate and a glass-wool guard ring of 6-inch OD x 2-13/16 inch ID was placed around it. The distance between the heat source and the cold plate was controlled by three micarta prisms 1/4 inch high that were equally spaced along the outer edge of the heat source plate (with apexes toward the cold plate). The cold plate (the measuring vessel surrounded by the ring-shaped guard vessel) was lowered in place. The enclosing bell jar was placed over the assembly and sealed. The diffusion pump and the water lines were connected. The bell jar was then evacuated. After vacuum was achieved, the measuring and guard vessels were filled with

TABLE VI

APPARENT MEAN THERMAL CONDUCTIVITY*

Material	Run No.	Investig.	Density lb/ft^3	Grade or Mesh	Vacuum (mm Hg)	Apparent k $\left(\frac{Btu\text{-}in.}{ft^2\text{-}hr\text{-}^oF}\right)$	Temp. of Warm Plate (^oF)	Max. Error Computed $\left(\frac{Btu\text{-}in.}{ft^2\text{-}hr\text{-}^oF}\right)$
Cab-O-Sil	5	ADL	3.5	M-5 (150-200Å)	$<10^{-6}$	0.0102	50	± 0.0006
		NBS	3.7		$<10^{-4}$	0.0145	88	± 0.0007
Perlite	8	ADL	10	Commercial Ungrad.	$<10^{-6}$	0.0105	50	± 0.0006
		NBS	8	-30 + 80	$<10^{-4}$	0.0083	88	± 0.0004
		NBS	6	+ 30 Mesh	$<10^{-4}$	0.0124	88	± 0.0004
Santocel	6	ADL	6	Commercial 250Å	$<10^{-6}$	0.0124	50	± 0.0007
		NBS	6		$<10^{-4}$	0.0145	88	± 0.0007

*Measurements are based on the following values:

Emissivities of cold and warm walls: 0.74

Temperature of cold wall: -320 F.

liquid nitrogen, and the vent lines were connected to the manometers and the oil bath.

Steady state condition was reached in approximately twelve hours. We took at least two readings of the evaporation rate at half-hour to one-hour intervals during the following eight hours. At the same time, we read the manometers, the thermocouples, the vacuum gage, the inlet-water temperatures, and the inlet water rate. (See Appendix, Chapter 4, for a typical test data sheet and calculations.

We had to fill the guard vessel about every three hours to keep the liquid level high; however, the change of the liquid level in the measuring vessel was insignificant during the entire test.

B. 30 LITER DEWAR

1. Construction

A vessel was constructed to test the behavior of high-efficiency insulation under conditions approaching operational use and to investigate the problems of applying the high-efficiency insulation to a container. Figure 17 shows the inside tank, the outside shell with the removable cover, and the pumping equipment. The inside tank is 12-inch OD by 1/8-inch wall and is 25 inches high. It is made of #304 stainless steel and can withstand a pressure of 600 psi. The tank is provided with a 0.002 inch thick aluminum blowout disk which previous pressure tests had shown would blow out at 100 psi when at the temperature of liquid nitrogen. This disk eliminates the possibility of accidents resulting from vacuum failure and the consequent deterioration in the effectiveness of the insulation. Such a failure could cause the gas to boil off fast enough to create a large pressure rise in the dewar.

The inside tank has a concentric ring welded to the bottom so that the tank can rest on three micarta supports, 1/2 inch in diameter x 1-1/2 inches long, attached to the outside shell. The supports have conical ends to minimize the contact area between supports and the tank. Calculations show that the heat-leak through micarta supports should not be more than 1.6 $\frac{Btu}{hr}$. The neck (see Figure 18) is made from stainless steel bellows that are 0.012 inch thick and 3 inches long and have a 1/2-inch ID. The heat-leak to the inside tank through the neck has been calculated to be 0.4 $\frac{Btu}{hr.}$. Both calculations cited are based upon the difference between ambient and liquid nitrogen temperatures.

The outer shell (18-inches OD x 0.250-inch wall) is made of steel. It has a flange at the top with an O-ring groove for an 18-inch OD x 1/4-inch cross-section O-ring. The top cover is bolted to this flange to give a vacuum-tight seal. The outside shell is provided with a safety pop-off valve to release pressure should the inner vessel rupture during test. Ionization and thermocouple gauges are attached to the top cover to measure the vacuum in the insulation space. A 1-inch Veeco

valve at the bottom of the outer shell provides a connection for the rough pumping of the insulation space; a 2-inch diameter connection and a Kinney valve are used for achieving high vacuum. A cold trap, diffusion pump, and fore pump are attached to this connection. The volume of gas boiled off during the test is measured with a standard gas meter capable of measuring a volume of one hundredth of a cubic foot. The complete assembly of the experimental apparatus is shown in Figure 19.

2. Experimental Procedure

Two methods of applying the high efficiency insulation to the dewar were tried.

1. The inner tank was held in a lathe (Figure 20, 21) and the insulation consisting of radiation shields and spacers was rolled onto it. Each radiation shield was one revolution long. Shields were spaced 1/8 inch apart from end to end. Spacer material was a continuous band.

2. A panel consisting of spaced radiation shields was made up. The width of the panel was equal to the height of the inside tank; the length was such that it could be wrapped around the tank exactly one time around (see Figure 22). Each panel was 1/4 inch thick. Four panels were used to obtain an insulation layer that is 1 inch thick. The seams were spaced 90° apart. Four music wires held the insulation on the tank in place.

A band 3 inches wide, made as described in 1., covered the supporting ring on the dewar. The ends of the tank were covered with similarly built insulation in which openings were cut for protruding parts (micarta supports and the neck). The insulated inner tank shown in Figure 23 was lowered into the outside shell (see Figure 24) and sealed with the top cover. Table VII shows the materials which were tested on the 30-liter dewar. The total heat-leak of the installation is calculated from the boil-off rate.

TABLE VII

INSULATIONS TESTED ON 30-LITER DEWAR

No.	Total Thickness	Number of Radiation Shields	Radiation Shield Material	Spacer Material
1	1/4	10	0.002 in. thick H-19 tempered aluminum foil	1/8 x 1/8 mesh 0.020 in. thick resin covered fiberglass
2	1	40	Same	Same
3	1	60	0.00025 in. thick soft aluminum foil	0.008 in. thick Dexter paper
4	1	60	Same	0.008 in. thick 50% open area perforated Dexter paper

VI. TEST RESULTS

A. TESTS WITH SINGLE GUARDED COLD-PLATE APPARATUS

Table VIII is a complete record of all runs (in chronological order) which were made on the thermal conductivity test apparatus. Supplementary tables are used to illustrate particular points of the following discussion.

1. Emissivity of the Materials

We found that the thermal-conductivity apparatus is a useful tool for establishing the mean emissivity of foils or films. To obtain these measurements, we glued the foil to the cold and warm surfaces of the apparatus spaced 1/4 in. apart, and kept one surface at 46 F and the other at -320 F. The space between the surfaces was evacuated to 3×10^{-6} mm of mercury so that radiation was the major portion of the transferred heat. We computed the heat flux between the surfaces, basing our calculations on the observed boil-off rate. The assumption was made that the emissivities of the warm and cold surfaces are equal.

The mean emissivity was established by the Stefan-Boltzmann Equation (equation (3) with n = 0). The calculated heat fluxes and the corresponding mean emissivities are given in Table IX. This table shows that the emissivity, e, of lampblack-Glyptal paint used on the surfaces of the apparatus is 0.74, which is 15% better than the value published by Messrs. Ziegler and Cheung (Reference 16). This difference may be accounted for by the fact that we air dry the paint but do not bake it, which was done in Reference 16. The finished surface is smooth in appearance.

Our value for emissivity of H-19 aluminum foil 0.002 inches thick is approximately three times that of the emissivity of the household type of soft aluminum foil tested by NBS (Reference 11). The thickness of the foil in the NBS tests ranged from 0.00075 to 0.0015 inches. The emissivity values obtained, however, were only 1-1/2 times the emissivity value of the household foil tested by Messrs. Ziegler and Cheung (Reference 16).

2. Evaluation of Materials for Use as Radiation Shields

The materials listed in Table IV were tested as radiation shields. These results are given in Table X (see also Chapter IV, paragraph 1).

The 0.002-inch H-19 tempered aluminum foil is clearly the most effective. A comparison between runs No. 15 and No. 17 and between runs No. 59 and No. 60 shows that the total heat flux increased approximately 0.025 Btu/hr, and 0.030 Btu/hr respectively. In both comparisons the increase must be attributed to the change in radiation shield material since other components (spacer material, number of shields and spacers) remained unchanged. On the basis of emissivity value of H-19 aluminum foil (see preceding paragraph 1 and Table IX), we calculated the emissivity of the

TABLE VIII

TESTS OF INSULATIONS WITH SINGLE GUARDED COLD-PLATE APPARATUS*

LEGEND

1/8 x 1/8 Mesh	-	0.020 in. thick - 1/8 x 1/8 mesh resin-coated fiberglass mesh
Dexter	-	0.008 in. thick glass paper, made by C. H. Dexter and Sons, Inc.
.....% open Dexter	-	0.008 in. thick glass paper, ...% perforated
Fortisan Mesh	-	0.010 in. thick - 1/10 x 1/10 mesh - Fortisan - Acetate
1/4 x 1/4 Mesh	-	0.020 in. thick - 1/4 x 1/4 mesh resin coated fiberglass mesh
H-19 Al	-	0.002 in. thick - H-19 tempered, bright both sides Alcoa aluminum foil
Soft Al	-	0.00025 in. thick, soft Alcoa foil, bright one side

*Measurements are based on the following values:

Emissivities of hot and cold plates: 0.74

Temperature of cold plate: -320 F

Area of sample: 5.81 $in.^2$ (2-3/4 in. diam.)

TABLE VIII - (cont.)

Run. No.	Sample Spec. Assm. Thick. (in.)	Sample Spec. Density (lb/ft^3)	Radiation Shields	Spacers	Vacuum (mm Hg)	Heat Flux (Btu/hr)	App. "k" $\left(\frac{Btu\text{-}in.}{ft^2\text{-}hr\text{-}F}\right)$	Warm Plate Temp. (F)	Remarks
4	5/8	28	(50) H-19 Al	Fortisan Mesh	10^{-5}	0.098	0.0040	50	
5	1/2	3.5	--	Cab-O-Sil	5×10^{-6}	0.304	0.0102	50	Grade M-5
6	1/2	6	--	Santocel	5×10^{-6}	0.370	0.0124	50	Commercial Grade
7.	1/2	5	--	ADL - 16	5×10^{-6}	0.146	0.0049	50	Proprietary Form
8	1/2	10	--	Perlite	10^{-6}	0.315	0.0105	50	Commercial Grade
9	1/4	20	(10) H-1⁄ Al	1/8 x 1/8 mesh	10^{-6}	0.070	0.0012	50	Run No. 24 same as this result reproduced
14	1/8	28	Same	Fortisan Mesh	10^{-6}	0.139	0.0012	50	Run No. 20 - same as thi. Q = 0.202 Btu/hr., k = 0.0017, T_{out} = 56 F
15	1/4	16	Same	Fiberglas AA 8 lb/ft^3	10^{-6}	0.170	0.0028	50	Owens-Corning Fiberglas
16	1/4	16	Same	1/4 x 1/4 mesh	10^{-6}	0.146	0.0024	50	
17	1/4	5	(10)-0.00025 in. Th. Dual-Al Coated Mylar	Fiberglas AA 8 lb/ft^3	10^{-6}	0.195	0.0033	50	Compare to Run No. 15
18	1/4	20	(10) H-19 Al	1/8 x 1/8 mesh	10^{-6}	0.120	0.0020	50	Radiation Shields were exposed to atm. for 1 mo.
19	1/4	20	Same	1/8 x 1/8 mesh	10^{-6}	0.102	0.0017	56	5 new Radiation Shields 5 old Radiation Shields

TABLE VIII (cont.)

Run No.	Sample Spec. Assm. Thick. (in.)	Sample Spec. Density (lb/ft^3)	Radiation Shields	Spacers	Vacuum (mm Hg)	Heat Flux (Btu/hr)	App."k" $\left(\frac{Btu\text{-}in.}{ft^2\text{-}hr\text{-}F}\right)$	Warm Plate Temp. (F)	Remarks
21	1/4	24	(10) H-19 Al	1/8 x 1/8 mesh + ADL-17 powd.	10^{-6}	0.270	0.0044	60	
22	1/4	29	(20) H-19 Al	Nylon Stockg. 0.004 in. thick	2×10^{-6}	0.163	0.0027	60	
23	1/4	22	(10)-0.005 in. thick one side Al-coat Mylar	1/4 x 1/4 mesh	2×10^{-6}	0.284	0.0046	60	Compare with Run No. 16
25	5/16	--	(20)-0,002 in. thick Dual-Al coated Mylar	Polystyrene-bonded glaswool 0.010 in. thick	37% open 2×10^{-6}	0.182	0.0036	70	Dowbeckmun, perforate
27	1/4	9	(13) soft Al	Dexter	10^{-6}	0.200	0.0032	70	
29	1/4	8	Same	25% open Dexter	2×10^{-6}	0.054	0.00086	70	Result is question-able
30	1/8	19	Same	Dexter	10^{-6}	0.560	0.0044	70	15 psi mech. press.
51	5/16	-	(5) H-19 Al (4) 0.005 clear Mylar	1/8 x 1/8 mesh	3×10^{-6}	0.127	0.0027	50	Run No. 52 same as this. No result-vacuu leak
53	5/16	-	(2) H-19 Al (7) 0.005 clear Mylar	Same	8×10^{-6}	0.260	0.0054	50	
54	5/16	-	(9) 0.005 clear Mylar	Same	3×10^{-6}	0.414	0.0086	50	
55a	5/16	-	Apparatus Surfaces	None	3×10^{-6}	2.58	-	50	Emissivity, = 0.74
b	5/16	-	Same	None	6×10^{-4}	2.75	-	50	
c	5/16	-			6×10^{-3}	4.13	-	50	

TABLE VIII (cont.)

Run No.	Sample Spec. Assm. Thick (in.)	Sample Spec. Density (lb/ft^3)	Radiation Shields	Spacers	Vacuum (mm Hg)	Heat Flux (Btu/hr)	App."k" $\left(\frac{\text{Btu-in.}}{ft^2\text{-F-hr}}\right)$	Warm Plate Temp (F)	Remarks
56	5/16	-	H-19 Al Surf. Bright Side	None	10^{-6}	0.128	-	50	Emissivity, = 0.057
57	5/16	-	H-19 Al Surf. Dull Side	None	10^{-6}	0.145	-	50	Emissivity, = 0.063
58	5/16	-	Mylar backed with H-19 Al	None	10^{-6}	0.758	-	50	Emissivity, = 0.23
59	1/4	-	(10) Soft Al	50% Open Dexter	10^{-6}	0.152	0.0025	50	
60	1/4	16.7	(10) H-19 Al	Same	10^{-6}	0.122	0.0020	50	Result reproduced in Runs No. 61 & 69a
61	1/4	16.7	Same	Same	10^{-6}	0.125	0.0020	50	8-3mm I.D.glas tube through guard ring
62	1/4	5.4	(10) 14% Open Soft Al	Same	10^{-6}	0.188	0.0030	50	
63	1/4	19.5	(10) H-19 Al	14% Open Dexter	10^{-6}	0.090	0.0015	50	
65	1/4	19.5	Same	Same	10^{-6}	0.118	0.0019	50	Same as Run 63 result 30% hig er than 63, bu it is more con sistent with60
66	1/4	4.3	None	(13) 50% open Dexter	10^{-6}	0.657	0.0105	60	
67	1/4	5.6	(z) H-19 Al	(11) 50% open Dexter	$2x10^{-6}$	0.284	0.0045	60	
68	1/4	10	(5) H-19 Al	Same	$2x10^{-6}$	0.217	0.0035	60	

TABLE VIII (Cont.)

Run No.	Sample Spec. Assm. Thick (in.)	Sample Spec. Density (lb/ft^3)	Radiation Shields	Spacers	Vacuum (mm Hg)	Heat Flux (Btu/hr)	App. "k" $\left(\frac{Btu\text{-}in.}{Ft^2\text{-}^oF\text{-}hr}\right)$	Warm Plate Temp. (^oF)	Remarks
69a	1/4	16.7	(10) H-19 Al.	50% Open Dexter	10^{-6}	0.118	0.0019	60	
b	1/4	16.7	Same	Same	10^{-4}	0.139	0.0022	60	
c	1/4	16.7	Same	Same	$7x10^{-4}$	0.166	0.0026	60	
70	5/16	11.2	Same	0.015 in. Thick Teflon Washers	$2x10^{-6}$	0.194	0.0038	60	
71	3/8	27.2	Same	0.022 in. Dia. Glass Beads on Mylar	$2x10^{-6}$	0.135	0.0033	60	

TABLE IX

EMISSIVITY OF SURFACES AND FOILS*

Arthur D. Little, Inc.

Material	Heat Flux (Btu/hr)	Mean Emissivity	NBS	W. T. Ziegler
Lamp-Black-Glyptal	2.58	0.74	-	0.86
H-19 Al - Bright Side	0.128	0.056	-	-
H-19 Al - Dull Side	0.145	0.063	-	-
Soft Al - Bright Side	-	-	0.018	-
Soft Al - Dull Side	-	-	0.021	0.043
Aluminum-Backed Mylar	0.758	0.21	-	-

*Measurements are based on the following values

Area of Sample: 5.81 $in.^2$ (2-3/4 in. diameter)

Vacuum: Below 3×10^{-6} mm Hg

Warm Wall Temperature: 46 F

Cold Wall Temperature: -320 F

For ADL Tests Only
(Runs #55-58 - Table VIII)

TABLE X

INFLUENCE OF RADIATION SHIELD CHOICE ON TOTAL HEAT TRANSFER*

	Radiation Shields	Spacers	Heat Flux (Btu/hr)	Approx. Heat Transfer $\frac{Btu\ in.}{(ft^2\text{-}hr\text{-}^oF}$	Warm Plate Temp (^oF)	Run No.	Remarks
1.	(10) H-19 Al	1/8 x 1/8 Mesh	0.070	0.0012	50	9	
2.	(10) H-19 Al	50% Open Dexter	0.122	0.0020	50	60	
3.	(10) Soft Al	Same	0.152	0.0025	50	59	
4.	(10) H-19 Al	Fiberglas AA 8 lb/ft^3	0.170	0.0028	50	15	
5.	(10) - 0.00025-in. thick dual-Al coated Mylar	Same	0.195	0.0033	50	17	
6.	(10) H-19 Al	1/4 x 1/4 Mesh	0.146	0.0024	50	16	
7.	(10)-0.005 in. thick one side Al coated Mylar	Same	0.284	0.0046	60	23	
8.	(20)-0.002 in. thick dual-Al coated Mylar	0.010 in. thick Polystyrene Bonded Glasswool Mat 37% Open	0.182	0.0036	70	25	Sample Thickness is 5/16 in.

*Measurements are based on the following values

AREA OF SAMPLE: 5.81 in.^{2}, (2-3/4 in. diam.)
EMISSIVITY OF HOT AND COLD PLATES: 0.74
TEMPERATURE OF COLD PLATE: -320 F
ASSM. THICKN. 1/4 in.
VACUUM: BELOW 3 x 10^{-6} mm Hg

0.00025-inch soft aluminum foil used in run No. 59 to be 0.18, or 3 times higher than that of the H-19 foil. We may conclude that the 0.00025 in. thick Mylar, coated with aluminum on both sides and used in run No. 17, has approximately the same radiation qualities as the 0.00025-inch soft aluminum foil, since the difference of 0.0005 Btu/hr in the heat-flux increase is relatively insignificant and may be attributable to experimental error or to the use of the different spacer material in runs No. 59 and No. 60. However, Mylar coated on one side only, gives very poor results, as can be seen by a comparison of runs No. 16 and No. 23.

Because Mylar coated on one side only, such as was used in run No. 23, is semitransparent to sunlight, its emissivity could not be established experimentally. We assumed that its emissivity was approximately equal to that of uncoated Mylar backed by H-19 aluminum foil (see run No. 58, Table IX). We, therefore, calculated that the radiation component of heat flux for a system using Mylar coated on one side only as radiation shields would be 0.0617 Btu/hr. The other parts of this system were the same for runs No. 16 and No. 23. The experimentally established difference in heat flux between the runs No. 16 and No. 23, however, is only 0.138 Btu/hr, which indicates that the radiation component of heat flux for run No. 23 is 0.152 Btu/hr or over twice the calculated value (0.0617 Btu/hr). Therefore, it is concluded that semitransparent Mylar transmits considerably more radiation than does a combination of the transparent uncoated material and aluminum backing.

It is concluded that:

1. H-19 tempered aluminum is the most effective radiation shield.

2. Insulation utilizing Mylar is lighter.

3. If Mylar is to be used, a better coating technique and heavier (nontransparent) metal deposits on Mylar surfaces will be required.

3. Contamination of Aluminum Shields

In runs No. 18 and No. 19 (see Table VIII) the increase in heat flux caused by contamination and oxidation of H-19 aluminum shield was observed. In runs No. 9, No. 18, and No. 19, ten aluminum shields of H-19 foil were used. In run No. 9 all shields were new; in run No. 18 all had been exposed to air for over one month; in run No. 19 five new shields were substituted for the old ones. In run No. 18 the heat flux was 0.050 Btu/hr greater than in run No. 9 (i.e., increased by 72% of the total heat flux for the new shield). In run No. 19 it was 0.030 Btu/hr greater than in run No. 9 (i.e., increased by 43% of the total heat flux for new shields). Assuming that the solid conductivity and gas conductivity remained unchanged in runs No. 18, No. 19 and No. 9, we calculated the emissivity of the old H-19 aluminum shield to be 0.25, as compared to 0.06 for the new one.

We can conclude from these tests that the emissivity of the foil will be significantly higher if it is exposed to the ambient air We did not attempt to separate the increase caused by contamination (e.g , dirt or microscopic particles of oil and other substances floating in air and absorbed by the surface) from that caused by oxidation of the surface. Precautions against contamination and oxidation must be taken when aluminum or aluminum-coated shields are used.

4. Effect of Number of Shields on Total Heat Transfer

Two series of runs were made to study the influence of the number of shields on the quality of insulation. In runs No. 51 through No 54, uncoated Mylar sheets were used in place of the removed aluminum shields so that the total specimen thickness was maintained constant. This step was necessary because of the mechanical properties of the spacers The resultant curve of total heat flux versus number of shields is presented as curve (2) of Figure 25. Curve (3) of Figure 25 shows the heat flux calculated on the assumption that the emissivity of the shields is 0 06 and that all other mechanisms of heat transfer remain constant.

The Mylar film used to replace the aluminum shields proved not only to reflect but also to transmit heat radiation, contrary to the literature wherein Mylar film is reported to be 100% opaque to long wave length. On account of this fact, a theoretical correlation of the results was difficult. Another series of tests was conducted (see runs No. 60 and No. 66 to 68) with a spacer material (perforated, 50% open, Dexter paper) that did not require the replacement of removed radiation shields by Mylar sheet. The curve plotted on the basis of this series of tests is shown in Figure 25, curve (1). Theoretically, curves (1) and (3) should be parallel since only the radiation component of the heat transfer is changed by the use of 2, 5, and 10 radial shields The heat transferred by solid spacer and gas is assumed to remain constant since no changes were made in the number of spacers. However, the two curves do not conform to pattern. Curve (1) deviates even more from the theoretical curve (3) than curve (2).

It should be noted that the point calculated theoretically for ten radiation shields of H-19 aluminum combined with 1/8 in. x 1/8 in. resin-covered fiberglass mesh spacers (curve 3) and the point established experimentally for the same insulation system (curve 2) coincide. The point established experimentally for the ten radiation shields of H-19 aluminum and Dexter paper spacers (curve 1) lies higher on the same abscissa. We may assume therefore that the increase in the total heat flux through the latter system is due to the properties of the spacer (e.g., to the conduction through solid or possibly through gas).

With the removal of radiation shields, the insulation qualities of the two systems tested deteriorate more rapidly than calculations indicated. The system utilizing the Dexter paper spacers showed a marked reduction in insulating value when the number of shields was reduced.

It is probable that the deviation of the experimental curves (1) and (2) from the theoretical curve (3) is caused by the effect of heat conduction through the solid upon the temperature of each of the radiation shields. A change in the temperature distribution through the sample would affect the radiation heat transfer. An extensive experimental program is necessary to establish as precisely as possible the extent to which temperature changes within the sample (because of heat conduction through the solid spacer) affect radiation heat transfer.

5. Spacing Methods and Materials

The tests to determine the best possible spacer material for use in the maximum-efficiency insulation system may be separated roughly in two categories: (1) experiments with commercially available materials suited for use as spacer materials and (2) experiments for evaluating new methods in which spacers separate the radiation shields with a minimum contact area.

In the first category the effectiveness of materials such as glass wool (unperforated and perforated), powders, and screens were tested. In the second category, experiments indicated that some of the methods were promising but that there is need for further study. Table V lists all the spacer materials tested under this program. Table XI presents the test results.

a. Screens. Of all the commercially available insulators tested for use as spacer material the most effective were: 0.020 in. thick, 1/8 in. x 1/8 in. mesh, resin-covered fiberglass screen, and 0.010 in. thick, 1/10 in. x 1/10 in. mesh Fortisan-acetate multistrand screen (run No. 9 and No. 14 - Table XI). The lowest value of the mean apparent thermal conductivity obtained for a sample of the insulation system was 0.0012 Btu-in./ ft^2-hr-F. The second material was thinner and a greater number of radiation shields was used but the conduction through the 0.010-inch spacers was greater than through 0.020-inch spacers, thus off-setting the gains effected by the increase in the number of radiation shields per unit thickness.

Table VIII shows that the thinner sample used in run No. 14 is 50% heavier than the sample in run No. 9. Furthermore, the material is more costly and its assembly more difficult. Table XII compares the two runs (No. 9 and No. 14) in detail. The theoretical values of heat flux for different heat transfer mechanisms appearing in this table were calculated as shown in Appendix I.

Theoretically, the use of wider mesh should improve the performance of the insulation system since the contact area is reduced. Accordingly, diverse materials were tested to establish the most effective mesh-size.

We tested 1/4 in. x 1/4 in. mesh screen, and we expected that the results would be four times better than those with 1/8 in. x 1/8 in. mesh spacers. Comparison of run No. 9 (1/8 in. x 1/8 in. mesh) with run No. 16 (1/4 in. x 1/4 in. mesh) shows that, in practice, the wider mesh, probably

TABLE XI

INFLUENCE OF SPACER CHOICE ON TOTAL HEAT TRANSFER*

No.	Spacers	Radiation Shields	Heat Flux (Btu/hr)	Apparent "K" $\left(\frac{\text{Btu-in.}}{\text{ft}^2\text{-}^\circ\text{F-hr}}\right)$	Warm Plate Temp. °F	Run No.	Remarks
1.	Fortisan Mesh	(10) H-19 Al.	0.139	0.0012	50	14	Sample Thickn. 1/8"
2.	1/8 x 1/8 Mesh	Same	0.070	0.0012	50	9	
3.	1/4 x 1/4 Mesh	Same	0.146	0.0024	50	16	
4.	50% Open Dexter	Same	0.122	0.0020	50	60	
5.	Same	(10) Soft Al.	0.152	0.0025	50	59	
6.	Dexter	(13) Soft Al.	0.200	0.0032	70	27	
7.	Nylon Stock 0.004 in. Thick	(20) H-19 Al.	0.163	0.0027	60	22	
8.	Fiberglas AA 8 lb/H^3	(10) H-19 Al.	0.170	0.0028	50	15	
9.	0.002-in. Dia Glass Beads on Mylar	Same	0.135	0.0033	60	71	Sample 3/8-in. Thick
10.	0.015-in. Thick Teflon Washers	Same	0.194	0.0038	60	70	Sample 5/16-in. Thick
11.	1/8 x 1/8 Mesh + ADL-17 Powder	Same	0.270	0.0044	60	21	
12.	37% Open Polystyrene Bond	(20)-0.002-in. Thick - Dual-Al Coat Mylar	0.182	0.0036	70	25	Sample 5/16-in. Thick.

*Measurements are based on the following values:

Emissivity of Hot & Cold Plate: 0.74
Temperature of Cold Plate: -320 F
Vacuum: Below 2 x 10^{-6} mm Hg
Sample Size: 2-3/4-in. Dia. x 1/4 in. Thick

TABLE XII

CALCULATED HEAT TRANSFERRED BY DIFFERENT MECHANISMS THROUGH INSULATED SAMPLE

Measurements are based on following values:

Area of sample: 5.81 $in.^2$ (2-3/4 in. diam)
Warm wall temperature: 50 F
Cold wall temperature: -320 F
Vacuum: 10^{-6} mm Hg.

Run No.	9	14	15
Total Sample Thickness (inches)	1/4	1/8	1/4
No. of Radiation Shields	10	10	10
Kind of Radiation Shield	.002-in. Thick H-19 Tempered Aluminum Foil - Bright on Both Sides		
Spacer Material	Resin Covered Fiber Gl Netting-1/8 x 1/8 Mesh, 0.020-in. Thick,	Acetate-Fortisan Nett. 1/10 x 1/10 Mesh 0.010-in. Thick Multi-Strand	
Radiation (Calc.) Btu/hr	0.014	0.014	0.014
Solid Cond. (Calc) Btu/hr	0.036	0.090	0.140
Gas Conduct. (Calc.) Btu/hr	0.003	0.004	---
Edge Loss (Calc.) Btu/hr	0.014	0.014	0.014
Total Heat Flux (Calc.)	0.067	0.122	0.168
Total Heat Flux (Exp.)	0.070	0.139	0.169

See Appendix 1 for sample calculation

due to looser weave and thus to larger area of contact with the radiation shields at each point of contact, conducts more heat than the closer mesh. The use of a close-woven nylon mesh of 0.004-inch thickness (comparison of run No. 22 to run No. 9) also proved unsatisfactory, as we expected, since points of contact were too numerous.

b. Fibrous Materials and Powders. In runs No. 15, No. 21 and No. 27 we tested the two fibrous materials and a powder: Owens-Corning fiberglass AA having a density of 8 lb/ft^3, Dexter glass paper, and ADL-16 powder. Table VIII shows that the Owens-Corning fiberglass and Dexter paper spacers are approximately of the same quality. Our calculations based on data in Reference 1 indicate that the heat conduction through the fibrous materials is very close to the experimental values. Table XII shows that the heat conducted through the solid is approximately four times greater for the fiberglass than for the screen discussed in (5a).

In run No. 21, in which we used the powder, the solid conduction is even higher than in the runs with fibrous materials. A total of 0.231 Btu/hr is conducted through the powder and the 1/8 in. x 1/8 in. mesh screen (which was necessary to keep the powder in place). Assuming that 0.030 Btu/hr is conducted through the screen (see run No. 9), we find that 0.212 Btu/hr is conducted through powder as compared to 0.140 Btu/hr for the glass wool spacer.

Additional evidence that a powder is poorly suited for use as a spacer in maximum efficiency insulation system may be found from run No. 7, in which ADL-16 powder insulation was tested without radiation shields, but with different radiation-attenuating materials. The apparent "k" for run No. 21 is about 10% less than that for run No. 7. This decrease shows that the radiation-attenuating materials employed in ADL-16 powder are almost as effective as 10 radiation shields, when the shields are used in combination with a powdered spacer material. It is clear that neither the powders nor the fibrous spacers are as effective insulation as are screens. The mean apparent thermal conductivity for the fibrous and powder spacers is approximately three to four times as much as that for spacers of 1/8 in. x 1/8 in. mesh.

c. Perforated Spacers. A comparison of runs No. 27 and No. 59 shows that the use of a perforated spacer material decreases the total heat flux. In run No. 27 a solid 0.008 inch thick Dexter paper spacer was used; in run No. 59 the same Dexter paper was perforated with 3/16-inch diameter holes in such a way as to remove 50% of the paper surface. Radiation shields of the same soft aluminum were used in run No. 59 and No. 27. Thirteen shields were used in run No. 27, and ten in run No. 59. If ten radiation shields had been used in run No. 27 we would have increased the total heat flux by approximately $n_{13}/n_{10} = 1.3$, or from 0.200 Btu/hr to 0.260 Btu/hr (see equation (4a)). The total heat flux for the insulation system in run No. 59 was 0.152 Btu/hr. Since the decrease in the heat loss is solely due to the decrease in the area of the spacer, we may assume that the heat conduction through the original spacer is approximately

twice the difference between heat transported in run No. 27 (corrected for ten radiation shields) and run No. 59.

$2(0.260 - 0.152) = 0.216$ Btu/hr

It follows that the heat conducted by the spacer is 85% of the total heat flux in run No. 27 and 71% in run No. 59.

Run No. 29 with perforated 25% open Dexter paper spacer and soft aluminum radiation shields resulted in our lowest value of mean apparent thermal conductivity, 0.00086 Btu-in./ft^{2}hr-$^\circ$F. However, this value was never reproduced in repeated tests (see runs No. 59 to No. 65) with perforated Dexter paper having different percentages of open area. In run No. 63, when perforated Dexter paper of 14% open area was used as a spacer, the "k" value obtained (0.0015 Btu-in./ft^{2}hr-$^\circ$F) was lower than expected. It is possible that the efficiency of this type of perforated spacer may be a maximum for some value of open area between 14% and 50%.

More tests would be necessary to establish the true relationship of percent open area to performance. At this point we do not consider run No. 29 to be reliable. In general, the decrease in heat flux introduced by perforation is sufficient to warrant an investigation of the effect of perforation on the insulating efficiency of other materials.

d. New Methods. The scope of the work in this area was limited and only two approaches were investigated.

In runs No. 70 and No. 71 washers and beads were used as spacers. The resulting "k" values, although not exceptional, are sufficiently low to warrant further work.

In run No. 70 teflon washers, 0.050-inch OD, 0.027-inch ID, and 0.015-inch thick, were spaced 3/4 inches apart and kept in place by a nylon thread (see Figure 26 to 28). The calculations show a fair agreement with the results of the run (see Appendix, Chapter 5).

In run No. 71 glass beads 0.022 inches in diameter were glued with Glyptal to Mylar sheet which had indentations 1/4 inch apart. The beads were glued into every second indentation (see Figure 29-31). Heat flux of 0.135 Btu/hr was quite low; however, the beads were too large and hence the total thickness of the sample with ten radiation shields proved to be too great for a low value. Teflon beads of smaller diameter (e.g., approximately 0.015 inches) would certainly give better results, since the thermal conductivity of teflon is between 1/4 and 1/6 that of glass. In addition, the smaller bead size would decrease the effective heat transfer area and allow the use of more radiation shields per unit thickness.

e. Comparison of Results. Comparison of the computed values for the heat transfer through spacer (see Appendix 1 for the computation of the heat transfer - 0.030 Btu/hr - for run No. 9) with the actual values of

heat conducted (as shown by interpolation of results achieved in runs No. 59, No. 60, and No. 9 as well as other tests for which we made calculations) shows that the actual values are consistently greater than the theoretical ones.

As we already remarked in the chapter dealing with the radiation shields, we based our calculations on the assumption that the heat transfer by conduction through the solid and the heat transfer by radiation are independent. Since the real temperature distribution through the sample is different from the distributions obtained for pure conduction or for pure radiation, the heat transfer rate by conduction is affected by the presence of radiation and vice versa.

6. Effect of Vacuum on the Heat Conduction Through Gas

a. Run No. 55. We conducted run No. 55 to check calculations of the heat conduction through gas. During this test we used two 0.74 emissivity surfaces and no sample between the apparatus surfaces. We made measurements at pressures of 3×10^{-6} mm, 6×10^{-4} mm, and 6×10^{-3} mm of mercury. The corresponding values of the total heat flux were 2.58 Btu/hr, 2.75 Btu/hr, and 4.13 Btu/hr. We used equation (2) to calculate the heat conducted by gas at all three vacuum levels. The theoretical curve is shown as curve (1), Figure 32.

We calculated the heat conducted by the gas to be 0.001 Btu/hr at a pressure of 3×10^{-6} mm of mercury. This value is negligible with respect to the total heat flux of 2.58 Btu/hr obtained at a pressure of 3×10^{-6} mm of mercury. Thus, if we subtract 2.58 Btu/hr from the two other values of total heat flux the differences should represent the amount of heat conducted by gas at 6×10^{-4} mm and 6×10^{-3} mm of mercury. Figure 32, curve (2), was based on the two points obtained in this manner. As Figure 32 shows, the computed values (curve (1)) lie very close to the experimentally obtained points; in fact, the experimental values lie well within the range of experimental error.

b. Run No. 69. In run No. 69 we repeated the experiment except that a sample of maximum-efficiency insulation was placed between the apparatus surfaces.

We calculated the effect of the vacuum changes on this sample by means of equation (2a) and we plotted curve (3) of Figure 32 on this basis. Applying the same reasoning as in a. to the experimentally obtained readings and assuming the heat conduction through the solid and heat transfer by radiation to remain constant, we establish two points of reference as shown by the single points in Figure 32. Note that the difference between the calculated curve and the data points increases as the apparent pressure is reduced. We conclude that the ionization gauge may indicate a better vacuum than the vacuum actually within the specimen. Thus the assumption may be correct that heat conduction through the gas produces negligible heat transfer through the insulation.

Tests on the 30-liter dewar, described in detail later, also indicate that a problem is posed by vacuum conditions inside the insulation system boundaries. Additional tests are necessary to establish the actual vacuum within a specimen.

c. Runs No. 60 and No. 61. In runs No. 60 and No. 61 we investigated the influence of the guard ring on the vacuum between the measuring and guard vessels. In all of the runs we measured the vacuum by an ionization gauge on the outer jacket of the single-guarded cold-plate apparatus. It is possible that the vacuum between the inner measuring and outer guard vessels was higher than the gauge reading due to the pressure drop through the glass-wool guard ring. We inserted six 1/8-inch ID glass tubes through the guard ring as illustrated in Figure 33. We measured no decrease in the heat flux, which indicates that no appreciable pressure drop existed through the guard ring and that the vacuum between the vessels was of the same magnitude as we measured by the ionization gauge.

7. Mechanical Pressure on the Insulation

The influence of the mechanical pressure on the specimen was investigated in runs No. 27 and No. 30.

A load simulating the atmospheric pressure on an evacuated insulation system was applied to a specimen consisting of thirteen soft aluminum shields and spacers of 0.008-inch thick Dexter paper. The specimen was compressed from an initial thickness of 1/4 inch to a final thickness of 1/8 inch. Therefore, even though the total heat flux increased from 0.200 Btu/hr to 0.560 Btu/hr, the mean apparent "k" value increased only from 0.0032 Btu-in./ft^2-hr-F to 0.0044 Btu-in./ft^2-hr-F; both values are better than the corresponding values for the best available evacuated powder mixtures (see run No. 7).

Figures 34 and 35 show the compressibility of the insulations used in runs No. 9 and No. 27 respectively. The tests were performed on 12 x 12 x 1-inch thick insulation sample. Radiation shields used in run No. 9 were impressed with the screen under pressure; neither of the two insulations regained the original thickness, but both received a certain permanent set after the first load had been taken off. However, after application of the repeated load, both insulations became completely elastic.

8. Reproducibility of the Tests

We repeated some tests several times to establish the reproducibility of the results. Each time we manufactured a new sample from the same materials. We repeated run No. 9 in run No. 24; we repeated run No. 60 in run No. 61 and again in run No. 69a (see Table VIII).

It is important to note at this point that the tests performed by NBS on the insulation sample built from the same materials as those used

in run No. 27 showed results which are ten times better than ours. Two variables, which are hard to control, may be the cause of the difference in results:

1. A high-efficiency insulation is not a homogeneous insulation; e.g., the heat resistance in one direction - perpendicular to the radiation shield planes - is several magnitudes higher than the resistance to the heat flow in the direction parallel to the radiation shields. In the type of the apparatus used by NBS, a slight temperature difference between the measuring and guard vessels may, due to this characteristic of the insulation system, produce a considerable difference in the results.

2. As we pointed out in paragraph 6-b, we do not know the actual gas pressure inside our specimen. It is possible that NBS achieved better vacuum than we did. We tried to pump the same specimen for different lengths of time, but an increase in the pumping time from one day to five days produced no improvement in vacuum reading or in the achieved heat flux.

B. TESTS ON 30-LITER DEWAR

Having accumulated sufficient information, by testing small samples, to warrant a study of the practical applications of this insulation system to a cryogenic liquid container, we built the experimental dewar described in Chapter V-B. Separate tests were run with liquid nitrogen and with liquid hydrogen in the tank.

Table XIII summarizes the results we obtained during these tests. The calculations of the mean apparent thermal conductivity are based on the mean logarithmic area of the insulation, and on the assumption that the temperature of the outer layer of insulation is equal to that of the surrounding air as measured by the thermometer. The temperature of the outer wall of the dewar, when measured by the thermocouple during the tests, was found to be identical with the air temperature.

The test with 0.008-inch thick unperforated Dexter paper spacer and 0.00025-inch thick soft aluminum radiation shield produced approximately the same results as those obtained by the test with the small 1/4-inch thick sample. Likewise, the test with perforated Dexter paper and liquid nitrogen in the dewar produced approximately the same results as those obtained by a test with a small, 1/4-inch thick sample. It is interesting to note that when the same insulation systems were tested with liquid hydrogen the total heat flux decreased. The higher heat loss during the test with liquid nitrogen supports the supposition that the pressure between radiation shields may be higher than that read by the ionization gauge on the outer shell. It is possible that the narrow spacing between radiation shields allows the residual gas to be trapped inside the spacer or that outgassing of the aluminum and the separators may continue for many days. When liquid hydrogen is used, a cryopumping effect is produced; hence, the vacuum is better. The cryopumping effect is less with liquid nitrogen.

TABLE XIII

TESTS ON 30-LITER DEWAR

Run No.	Sample	Vacuum (mm Hg)	Evapor. Rate (Scfh)	Total Heat Flux (Btu/hr)	App. "k" $\left(\frac{\text{Btu-in.}}{\text{ft}^2\text{-hr-}^\circ\text{F}}\right)$	Outside Temp ($^\circ$F)	Value From Table VIII	Liquid in Dewar	Total Thickness of Insul. (inches)
1	.00025 in Th. Soft Al. .008 in. Th. Dext. Pap.	8×10^{-6}	2.14	14.2	.0036	79	.0032	Nitrogen	1
2a	.00025 in. Th. Soft Al.	4×10^{-6}	1.82	12.1	.0032	82	.0025	Nitrogen	
2b	.008 in. Th. Dext. Pap. 50% Open	3×10^{-6}	7.25	7.9	.0018	45		Hydrogen	1
3a	.002 in. Th. H-19 Al.	2×10^{-6}	2.21	14.7	.0037	73	.0012	Nitrogen	1
3b	1/8 x 1/8 Mesh	6×10^{-7}	9.5	10.4	.0024	41		Hydrogen	
4	Same 1/4 in. thick	5×10^{-7}	3.36	22.4	.0016	76	.0012		1/4

The difference in heat loss between runs No. 3a with liquid nitrogen and No. 3b with liquid hydrogen is approximately 4.3 Btu/hr.

Assuming that this difference is due entirely to gas conduction, we can use equation (2a) to calculate the minimum effective pressure inside the insulation during the nitrogen test: it is 1.7×10^{-3} mm Hg rather than a value of less than 4×10^{-6} mm Hg as was indicated by the ionization gauge on the outer cover of the tank. The calculations show that the vacuum of 3×10^{-3} mm Hg would be enough to raise the meanapparent thermal conductivity value from 0.0012 Btu-in./ft^2-hr-$^{\circ}$F (obtained from a small sample of the same insulation system in our single-guarded cold-plate apparatus) to 0.0032 Btu-in./ft^2-hr-$^{\circ}$F (obtained on the dewar with 1-inch thick insulation system during the run No. 3a with liquid nitrogen). Calculations also show that 1.4×10^{-3} mm of mercury would be enough to raise the mean apparent thermal conductivity from 0.0012 to 0.0019 Btu-in./ft^2-hr-$^{\circ}$F (obtained during the run No. 3b with liquid hydrogen).

Note that the pressure between layers may increase as the distance from the cold wall increases. It is possible that cryopumping is most effective within the layers adjacent to the inside tank filled with cryogenic liquid, and that the effect decreases in the subsequent layers. For liquid nitrogen the effect of the cryopumping is much smaller than for the liquid hydrogen, which would explain the lower heat flux obtained in tests with liquid hydrogen.

Let us compare run No. 3a, in which we used an insulation system 1 inch thick with run No. 4, in which we used the same type insulation system but in which the thickness was reduced to 1/4 inch. In run No. 4, cryopumping of a liquid-nitrogen container operates on a higher percentage of the insulation thickness. The fact that the value of the apparent "k" is smaller in run No. 4 reinforces the supposition that the vacuum inside the radiation insulation may be higher than the value indicated by the ionization gauge.

Figure 36 shows a curve of the mean apparent thermal conductivity as a function of pressure as measured by the ionization gauge. We wrapped 1-inch thick insulation consisting of 60 layers of 0.00025-inch thick soft aluminum foil for radiation shields and 61 layers of 0.008-inch thick Dexter paper for spacers. It is of interest that even at atmospheric pressure this insulation is somewhat better than the fine glass wool.

C. OUTGASSING OF INSULATING MATERIAL

During the tests with the 30-liter tank, we found that the outgassing properties of unbaked Dexter paper in combination with the outgassing of the outer steel wall make it very difficult to achieve vacuums higher than 3×10^{-4} mm Hg. Even after one month of pumping with a 2-inch diffusion pump, a vacuum of only 4×10^{-5} mm Hg was reached. We conducted a limited study of outgassing phenomenon. We came to the following conclusions, based on the literature survey and tests on the 30-liter dewar:

1. The unbaked insulation may outgas for a long time. Records show that high outgassing rates of unbaked systems have been sustained for periods of more than ten days.

2. The passages between the radiation shields are too long and too narrow. Wrinkles or small apertures in the radiation shields, to allow passage of the gas across the shields, would decrease considerably the pumping time and improve the ultimate vacuum.

3. Coatings (especially Glyptal) should not be used on the metal surfaces exposed to vacuum. The outgassing of the metal surface under the coating will not be stopped but only slowed down, and the time required to outgas the unit will be increased even more. The Glyptal also contributes some outgassing.

Several tests on the 30-liter dewar for investigation of the outgassing were performed and are described in the following paragraphs.

1. The Pressure Rise Test on the Outer Tank

The outer steel tank was tested for outgassing after the inner vessel and insulation wrapping were removed.

1. With Glyptal film covering the inside surface of the tank.

2. With cleaned inside wall (sand blasted).

We closed the Kinney valve (see Figure 17), separating the vacuum space on the tank from the pumping system. The pressure rise was observed for one hour. The results are presented in Figure 37, which shows that outgassing from the clean steel surface is less than that from the Glyptal-coated one (see page 60).

2. The Pressure Rise Test on Insulation

The inner vessel was wrapped with insulation and replaced inside the outer tank.

The test was performed as described above under paragraph C-1, but in this test the pressure rise was observed for four days (see Figure 38). The test revealed the outgassing rate to be 2×10^{-12} mm/sec-cm^2, which, according to literature, is to be expected for an unbaked system.

Figure 39 compares pumping characteristics of a one-inch thick insulation system using 1/8 in. x 1/8 in. mesh resin-coated fiberglass spacers with an insulation system using Dexter paper spacers. The insulating system using the fiberglass spacers was pumped down to 1×10^{-4} mm in 36 hours. At this point the pumping speed apparently reached equilibrium with the outgassing rate of the plastic spacers so that further pumping did not improve the vacuum. The dewar was then filled with liquid nitrogen

1. The unbaked insulation may outgas for a long time. Records show that high outgassing rates of unbaked systems have been sustained for periods of more than ten days.

2. The passages between the radiation shields are too long and too narrow. Wrinkles or small apertures in the radiation shields, to allow passage of the gas across the shields, would decrease considerably the pumping time and improve the ultimate vacuum.

3. Coatings (especially Glyptal) should not be used on the metal surfaces exposed to vacuum. The outgassing of the metal surface under the coating will not be stopped but only slowed down, and the time required to outgas the unit will be increased even more. The Glyptal also contributes some outgassing.

Several tests on the 30-liter dewar for investigation of the outgassing were performed and are described in the following paragraphs.

1. The Pressure Rise Test on the Outer Tank

The outer steel tank was tested for outgassing after the inner vessel and insulation wrapping were removed.

1. With Glyptal film covering the inside surface of the tank.

2. With cleaned inside wall (sand blasted).

We closed the Kinney valve (see Figure 17), separating the vacuum space on the tank from the pumping system. The pressure rise was observed for one hour. The results are presented in Figure 37, which shows that outgassing from the clean steel surface is less than that from the Glyptal-coated one (see page 60).

2. The Pressure Rise Test on Insulation

The inner vessel was wrapped with insulation and replaced inside the outer tank.

The test was performed as described above under paragraph C-1, but in this test the pressure rise was observed for four days (see Figure 38). The test revealed the outgassing rate to be 2×10^{-12} mm/sec-cm^2, which, according to literature, is to be expected for an unbaked system.

Figure 39 compares pumping characteristics of a one-inch thick insulation system using 1/8 in. x 1/8 in. mesh resin-coated fiberglass spacers with an insulation system using Dexter paper spacers. The insulating system using the fiberglass spacers was pumped down to 1×10^{-4} mm in 36 hours. At this point the pumping speed apparently reached equilibrium with the outgassing rate of the plastic spacers so that further pumping did not improve the vacuum. The dewar was then filled with liquid nitrogen

and the pressure in the vacuum space dropped to 2×10^{-6} mm. With Dexter paper, it took five days of pumping to reduce the vacuum within the insulation system to 1×10^{-4} mm; however, the vacuum continued to improve with continued pumping. On the 13th day it reached 5×10^{-5} mm; the dewar was then filled with liquid nitrogen, and the pressure in the vacuum space dropped to 1×10^{-5} mm and then rose again to 5×10^{-5} mm. Preliminary heating of both insulation systems would improve the final vacuum since heating speeds up the outgassing rate. A test was performed with a sample of the insulation system having 1/8 x 18 in. mesh resin-coated fiberglass spacers 1/4 inch thick. The insulation system was simultaneously heated and pumped for four days. Final vacuum reached was 10^{-4} mm of mercury. Liquid nitrogen was then introduced and the pressure in the vacuum space dropped to 5×10^{-7} mm. We found that the techniques presently available for obtaining high vacuum present many difficulties and unsolved problems.

VII. MANUFACTURING AND HANDLING TECHNIQUES

A. RADIATION SHIELD MATERIALS

In the process of handling materials necessary for high-efficiency insulation we ascertained some of the qualities and shortcomings of these materials. This phase of our investigation will assume special importance when the high-efficiency insulation outgrows the laboratory and becomes an industrial item.

We found that 0.00025-inch thick aluminum foil, which gave us the lightest sample, is too thin for non-laboratory use and that the foil should be at least 0.0005 inches thick.

The thin foils, however, in practically applied insulation systems, require the use of a continuous spacer such as Dexter paper since the radiation shields are not self-supporting.

On the other hand, 0.0015-inch or even 0.0010-inch thick hardened foils may be successfully substituted for 0.002-inch thick aluminum foil in the system utilizing 1/8 x 1/8-inch mesh screen spacers. This substitution will decrease the weight of such insulation systems without adversely influencing the thermal properties.

We found that 0.002-inch thick hardened aluminum foil can be supported by point contacts as far as 3/4 inches apart.

Mylar 0.00025 inches thick and coated with aluminum on both sides showed good handling properties and suitable weight, but the cost is much higher than the cost of aluminum foils.

B. SPACER MATERIALS

Resin-covered fiberglass screen, with a 1/8 x 1/8-inch mesh is a strong and an easily handled spacer material. However, it is slippery when used with aluminum, and the insulation assembly must be kept in place by some external means.

Dexter paper is hard to handle because it does not possess an adequate tensile strength and it is easily stretched and ripped. Perforated Dexter paper is almost impossible to handle even under laboratory conditions. It may be considered impractical in commercial application.

C. APPLICATION METHODS

Two methods of application of high-efficiency insulation system are suggested: winding and paneling.

Winding is useful for small cylindrical or prismatic tanks. The tank is held in a lathe or another rotatable fixture. The spacer is wound in

a continuous band. Each radiation shield is one revolution long, and each is separated by a 1/8 in. gap from the previous shield. (See Figures 20 and 21.)

Paneling is useful for large tanks and shapes which cannot be covered by a winding method.

A panel of a standard size (or, when necessary, of shape and size that conforms to requirements) is prepared in a given thickness. The tank is insulated by layers of these panels applied in a brickwork pattern, so that the seams of the first layer are covered with panels of the second layer, etc.

VIII. LITERATURE SURVEY

A survey of the available literature showed that the idea of a multiple radiation shield insulation system can be traced back to Dewar. The first laboratory application of such a system was made by Peter Petersen of University of Lund (Sweden) in 1946 (Reference 7). Both the fiberglass spacer and radiation shields were spiraled. The heat-leak through the spiral aluminum radiation shield was apparently very high since the total heat flux through the insulation was high and the reported values were unexceptional. We found no report of any work in this field until the 1959 Cryogenic Conference published several articles on high-efficiency insulation systems (see References 6, 18, 19, 20, and 21), among which the work by NBS is outstanding. The mean apparent thermal conductivities reported by NBS are consistently about one-tenth the values reported by us for the same samples (see runs No. 25 and No. 27, Table VIII) in our paper published by the same Conference at the same time. (See discussion in this report in Chapter VI, paragraph A-8).

Works by Linde and NRC give the results without a description of the insulation system. It is apparent from these papers that the same NBS apparatus was used in all tests - (Paragraph A-8 of Chapter VI).

IX. FURTHER DEVELOPMENT

We feel that the basic data, the theory, and the trends for maximum efficiency insulation system were established in the course of this project. Guide lines for further research were clearly indicated.

Further investigation of the outgassing phenomenon in high efficiency insulation system, of ways to improve pumping techniques so as to reduce pumping time and improve vacuum, and of a possible way to retain the vacuum for longer periods of time without repumping is necessary.

Development of load-supporting, high-efficiency insulation systems, i.e., cryogenic vessels which are in effect self-insulating, is feasible (see Chapter VI A-7). The mean apparent thermal conductivity of such insulation systems will not reach the mean apparent thermal conductivity of an unloaded insulation, but they will eliminate the need for a heavy supporting structure. The resultant reduction in the total weight of the system will compensate for loss in the mean apparent thermal conductivity.

X. CONCLUSIONS

On the basis of our experimental work we can draw the following conclusions:

1. A good agreement exists between thermal conductivity data obtained in the single-plate thermal conductivity apparatus and the 30-liter insulated container.

2. We established the superiority of the multilayer radiation shield insulation system under laboratory conditions.

3. Immediate use of the multilayer radiation shield insulation system in selected cases is possible and the wide spread industrial use is feasible.

4. Radiation shield-spacer combination suitable for a specific use may be selected on the basis of the obtained information.

5. Insulation effectiveness is greatly influenced by the degree of vacuum actually obtained in the insulation system. The vacuum is influenced by the prior history of outgassing, and the materials used for the spacers and radiation shields of the insulation. The degree of the cryopumping influences the effectiveness of the system.

X. CONCLUSIONS

On the basis of our experimental work we can draw the following conclusions:

1. A good agreement exists between thermal conductivity data obtained in the single-plate thermal conductivity apparatus and the 30-liter insulated container.

2. We established the superiority of the multilayer radiation shield insulation system under laboratory conditions.

3. Immediate use of the multilayer radiation shield insulation system in selected cases is possible and the wide spread industrial use is feasible.

4. Radiation shield-spacer combination suitable for a specific use may be selected on the basis of the obtained information.

5. Insulation effectiveness is greatly influenced by the degree of vacuum actually obtained in the insulation system. The vacuum is influenced by the prior history of outgassing, and the materials used for the spacers and radiation shields of the insulation. The degree of the cryopumping influences the effectiveness of the system.

XI. LIST OF REFERENCES

1. J. D. Verschoor and P. Greebler, "Heat Transfer by Gas Conduction and Radiation in Fibrous Insulation," Transactions of the ASME, Vol. 74, p. 961, August 1952.

2. R. M. Lander, "Gas is an Important Factor in Thermal Conductivity," Transactions of the American Society of Heating and Ventilating Engineers, Vol. 60, p. 121, 1954.

3. M. Smoluchowski, "Sur la Conductibilite Calorifique des Corps Pulverises," Bulletin Int. de L'Academie des Sciences de Cracovie, Series A, p. 129, 1910.

4. R. M. Christiansen, M. Hollingsworth, Jr., and H. N. Marsh., Jr., "The Performance of Glass Fiber Insulation under High Vacuum," Proceedings of 1959 Cryogenic Engineering Conference, University of Colorado Press.

5. R. H. Kropschot, B. J. Hunter, J. E. Schrodt, and M. M. Fulk, "Evacuated Powder Insulation," Proceedings of 1959 Cryogenic Engineering Conference, University of Colorado Press.

6. I. A. Black, A. A. Fowle, and P. E. Glaser, "Development of High-Efficiency Insulation," Proceedings of 1959 Cryogenic Engineering Conference, University of Colorado Press.

7. P. Peterson, "The Heat-Tight Vessel, a Transport and Storage Vessel for Liquid Oxygen and Liquid Nitrogen," Office of Naval Intelligence Translation No. 1147, December 1951.

8. P. Peterson, "Some Means to Improve the Vacuum Insulation of the Dewar Flask," Sartryck ur TVF 29 (1958); 4, p. 151 (Sweden).

9. R. B. Scott, Cryogenic Engineering, D. van Nostrand Company, 1959.

10. R. P. Mikesell and R. B. Scott, "Heat Conduction through Insulating Supports in Very Low Temperature Equipment," Journal of Research of National Bureau of Standards, Vol. 57, No. 6, December 1956.

11. D. B. Chelton and D. B. Mann, Cryogenic Data Book, University of California Press, May 1956.

12. W. H. McAdams, Heat Transmission, McGraw-Hill Book Company, New York, 1954.

13. Max Jakob, Heat Transfer, New York, John Wiley & Sons, 1950, Chapter 9.

14. Gordon B. Wilkes, Heat Insulation, New York, John Wiley & Sons, 1950, Chapter 3.

15. F. T. Zimmerman, "Total Emissivities and Absorptivities of Some Commercial Surfaces at Room and Liquid-Nitrogen Temperatures," Journal of Applied Physics, Vol. 26, No. 12, pp. 1483-88, December 1955.

16. W. T. Ziegler and H. Cheung, "Total Emissivity of Some Surfaces at 77° K," Proceedings of the 1956 Cryogenic Engineering Conference, U. S. Department of Commerce, National Bureau of Standards, p. 100.

17. M. M. Fulk, M. M. Reynolds, and O. E. Park, "Thermal Radiation Absorption by Metals," Proceedings of the 1954 Cryogenic Engineering Conference.

18. M. P. Hnilicka, "Engineering Aspects of Heat Transfer in Multi-Layer Reflective Insulation," Proceedings of 1959 Cryogenic Engineering Conference, University of Colorado Press.

19. R. H. Kropschot, J. E. Schrodt, and M. M. Fulk, "Multiple Layer Insulation," Proceedings of 1959 Cryogenic Engineering Conference, University of Colorado Press.

20. P. M. Riede and D. I-J. Wang, "Characteristics and Applications of Some Superinsulations," Proceedings of 1959 Cryogenic Engineering Conference, University of Colorado Press.

21. S. T. Stoy, "Cryogenic Insulation Development," Proceedings of 1959 Cryogenic Engineering Conference, University of Colorado Press.

22. N. A. Lange, Handbook of Chemistry, Handbook Publishers, Inc., Sandusky, Ohio, 1952.

23. Pittsburgh Corning, Foamglass Catalog.

24. E. I. du Pont de Nemours & Company, Catalog.

APPENDIX

I. SAMPLE CALCULATION

Assume: Emissivity of cold and warm walls = 0.74
Sample area, A_{mean} = 37.5 cm^2 = 5.81 $in.^2$
11 spacers: 1/8 x 1/8-in. mesh plastic netting with thread 0.010 of an inch thick.
n = 10 aluminum shields, 0.002 of an inch thick with emissivity
e_s = 0.06 on both sides
T_2 = 283 K, 510 R, or 50 F
T_1 = 77 K, 140 R, or -320 F

A. GAS CONDUCTION (EQUATIONS 2 and 20)

$C = 30.9$ Btu/hr-lb_f-$(^oR)^{1/2}$

$a_1 = 1$; $a_2 = 0.85$ (accommodation coefficients for air)

$A_1 = A_2 = A_{mean} = 5.81\ in.^2 = 0.0404\ ft^2$

$\gamma = 1.4$ (air)

$M = 29$ (air)

$T_P = 293$ K or 527 R

$P = 0.1$ micron Hg or $0.000288\ lb_f/ft^2$

$$Q_{gas} = 194 \frac{0.85\ (1)}{0.85 + (1 - 0.85)\ (1)} \frac{1.4 + 1}{1.4 - 1} \frac{0.000288}{\sqrt{29\ (527)}} \frac{510 - 140}{10 + 1} 0.0404$$

$Q_{gas} = 194\ (.85)\ (6)\ 2.32\ (10^{-6})\ (33.6)\ (0.0404)$; $Q_{gas} = 0.0031$ Btu/hr

B. HEAT RADIATION (EQUATION 3)

$A_{mean} = 0.0404\ ft^2$

$\sigma = 0.1713 \times 10^{-8}$ Btu/hr-ft^2-$^oR^4$

$$Q_{rad} = 0.1713 \times 10^{-8}\ (0.0404) \frac{510^4 - 140^4}{10(\frac{2}{0.06} - 1) + (\frac{2}{0.74} - 1)} \qquad (3)$$

$$= 0.1713 \times 10^{-8}\ (0.0404) \frac{(650 - 3.8)\ 10^8}{323 + 1.7}$$

$= 0.0142$ Btu/hr

C. CONDUCTION THROUGH SOLID SPACER (EQUATION 4a)

Assume: $K_{140}^{510} = 1.5$ Btu-in./$^{\circ}$R-ft^2-hr

Area: $0.01 \times 0.01 = 1 \times 10^{-4}$ in.^{2} (64 points/in.^{2} of insulation)

$L = (n + 1)\ell = 11\ (0.02) = 0.22$ inches

$$Q_{solid} = \frac{1}{\sqrt{10}} \quad \frac{(1.5)\ (10^{-4})\ 64}{(144)\ 0.22} \quad (510 - 140)$$

$$Q_{solid} = 0.0355 \text{ Btu/hr}$$

D. TOTAL HEAT LOSS

$$Q_{gas} + Q_{rad} + Q_{sol} = 0.003 + 0.014 + 0.036 = 0.053 \text{ Btu/hr}$$

II. MANUFACTURERS CONTACTED IN CONNECTION WITH HIGH-EFFICIENCY INSULATION

A. RADIATION SHIELDS

1. Alcoa
   Pittsburgh, Pa.
   (Aluminum Foil)

2. Reynolds Metal Co.
   Louisville, Ky.
   (Aluminum Foil)

3. DuPont de Nemours & Co., Inc.
   Wilmington, Delaware
   (Mylar)

4. Eastman Kodak Co.
   Rochester, N. Y.
   (Plastic Films)

5. Minnesota Mining & Mfg. Co.
   St. Paul, Minnesota
   (Metallized Plastics)

6. Hy-Sil
   Revere, Mass.
   (Metallized Plastics)

7. Coating Products
   Englewood, N. J.
   (Metallized Plastics)

8. Hastings & Co.
   Philadelphia, Pa.
   (Metallized Plastics)

9. Bemont Papers
   Bennington, Vermont
   (Aluminized Saran)

10. National Research Corp.
    Cambridge, Mass.
    (Metallized Plastics)

11. Dow-Beckman Co.
    Cleveland, Ohio
    (Metallized Plastics)

12. Mylam Electric
    Providence, R. I.
    (Coated Mylar Laminations)

13. Aluminseal Corp.
    New York, N. Y.
    (Aluminum Foil Laminated Mylar)

14. Sumner Specialties
    Littleton, Mass.
    (Aluminum Foil Laminated Paper)

15. Walco Bead Co.
    New York, N. Y.

16. Anaconda Aluminum Co.
    Louisville, Ky.

B. SPACERS

1. Joseph P. Ott Mfg. Co.
   Pawtucket, R. I.
   (Manufacturer of Fiberglass Screens)

2. Celanese Corp. of America
   New York, N. Y.
   (Fortisan-Acetate Screens)

3. American Copper Sponge Co
   Woonsocket, R. I.
   (Weavers of Metal Supported Fiberglass Net)

4. Ruse Liberty Mica
   Peabody, Mass.
   (Fiberglass Yarn)

5. Owens-Corning
Huntington, Pa.
(Fiberglass Wool and other products)

6. Linen Thread Co.
Boston, Mass.
(Weavers, Fish Net)

7. Melo Product Co
Chicago, Illinois
(Hair Nets)

8. Helen Cornell, Distributor
Boston, Mass.
(Hair Nets)

9. Sears Roebuck & Co.
Cambridge, Mass.

10. Exeter Manufacturing Co.
Exeter, N. H.
(Fiberglass Material)

11. Haines Co.
(Nylon Stockings)

12. Walco Bead Co.
New York, N. Y.

13. C. H. Dexter & Sons, Inc.
Windsor Locks, Conn.
(Glass Paper)

14. Cataphote Corp.
Jackson, Miss.
(Glass beads)

15. National Perforation Corp.
Clinton, Mass.

III. EQUIPMENT ACCURACY

Computation of possible heat-leaks into the measuring vessel.

A. RADIATION FROM 510 R DOWN THE NECK (Q_{R-N})

Neck diameter = 11/32 in. or 0.344 in.

Area = 0.0928 $in.^2$ or 6.45×10^{-4} ft^2

Emissivity of the hot wall (e_w) = 0.1 (copper)

Emicsivity of stainless steel (e_s) = 0.30

$$Q_{R-N} = \sigma \frac{e_w e_s A}{e_w + (1 - e_w) e_s} (T_w^4 - T_s^4)$$

$$= 0.1713 (10^8) \frac{(0.1) (0.3) (6.45) (10^{-4})}{0.1 + 0.3 (1 - 0.1)} (510^4 - 140^4)$$

$$= \frac{0.1713 (0.193) 10^{-4} (646)}{0.37} = 0.0057 \text{ Btu/hr}$$

B. RADIATION FROM GUARD VESSEL

Assume $\Delta T = 1$ K

Measuring vessel = 2-3/4 in. dia. x 6 in. long

Guard vessel enclosure = 2-7/8 in. dia. x 12 in. long

Mean area (A) = 600 cm^2 or 0.645 ft^2

Emissivity of stainless steel at 140 R (e) = 0.05

$$Q_{rad} = 0.1713 (10^8) \frac{0.05}{2 - 0.05} (0.645) \left[140^4 - 138.2^4\right] = 0.00055 \text{ Btu/hr}$$

C. GAS CONDUCTION BETWEEN MEASURING AND GUARD VESSELS

$\Delta T = 1$ K $\quad a_1 = a_2 = 1$, $P = 0.1$ micron Hg or 0.000288 lb_f/ft^2

$$Q_{gas} = 194 (6) \frac{(0.000288)}{\sqrt{29 (510)}} (1.8) (0.645) = 0.0032 \text{ Btu/hr}$$

III. EQUIPMENT ACCURACY

Computation of possible heat-leaks into the measuring vessel.

A. RADIATION FROM 510 R DOWN THE NECK (Q_{R-N})

Neck diameter = 11/32 in. or 0.344 in.

Area = 0.0928 $in.^2$ or 6.45×10^{-4} ft^2

Emissivity of the hot wall (e_w) = 0.1 (copper)

Emissivity of stainless steel (e_s) = 0.30

$$Q_{R-N} = \sigma \frac{e_w e_s A}{e_w + (1 - e_w) e_s} (T_w^4 - T_s^4)$$

$$= 0.1713 (10^8) \frac{(0.1)(0.3)(6.45)(10^{-4})}{0.1 + 0.3 (1 - 0.1)} (510^4 - 140^4)$$

$$= \frac{0.1713 (0.193) 10^{-4} (646)}{0.37} = 0.0057 \text{ Btu/hr}$$

B. RADIATION FROM GUARD VESSEL

Assume ΔT = 1 K

Measuring vessel = 2-3/4 in. dia. x 6 in. long

Guard vessel enclosure = 2-7/8 in. dia. x 12 in. long

Mean area (A) = 600 cm^2 or 0.645 ft^2

Emissivity of stainless steel at 140 R (e) = 0.05

$$Q_{rad} = 0.1713 (10^8) \frac{0.05}{2 - 0.05} (0.645) \left[140^4 - 138.2^4\right] = 0.00055 \text{ Btu/hr}$$

C. GAS CONDUCTION BETWEEN MEASURING AND GUARD VESSELS

ΔT = 1 K $\quad a_1 = a_2 = 1$; P = 0.1 micron Hg or 0.000288 lb_f/ft^2

$$Q_{gas} = 194 (6) \frac{(0.000288)}{\sqrt{29 (510)}} (1.8) (0.645) = 0.0032 \text{ Btu/hr}$$

D. CONDUCTION THROUGH STAINLESS-STEEL NECK

ΔT = 1 K or 1.8 R

$K_{ss} = 54 \frac{\text{Btu-in.}}{\text{ft}^2\text{-hr-}^\circ\text{R}}$

Tubing = 3/8-in.O.D. x 0.015-in. wall

Area = 0.1103 - 0.0925 = 0.0178 in.^2

$Q = 54 \frac{(0.0178)}{144\ (6)}\ (1.8) = 0.002$ Btu/hr

E. TOTAL POSSIBLE HEAT-LEAK TO MEASURING VESSEL

$Q_{total} = 0.006 + 0.0006 + 0.003 + 0.002 = 0.0116$ Btu/hr

F. UNCERTAINTIES IN MEASURED VALUES

Water temperature: $\pm$ 1/2 F

Cold plate temperature: $\pm$ 1/2 F

Ambient temperature: $\pm$ 1 F

Boil-off rate: $\pm$ 15 ccm/hr

Barometric pressure: $\pm$ 1 mm Hg

Thickness of specimen: $\pm$ 1/64 inches

Diameter of specimen: $\pm$ 1/64 inches

Positive pressure in vessel: $\pm$ 0.05 in. H_2O

IV. DATA SHEET AND CALCULATIONS

Test No. 9

Sample: ten 0.002 in. thick H-19 tempered aluminum shields

eleven 0.020 in. thick - 1/8 x 1/8 mesh resin covered fiberglass

Sample size: 2-23/32 in. dia. x 1/4 in. thick

Guard insulation: glass wool

A. DATA SHEET

Date and Time	WATER (WARM PLATE) Inlet T (^{o}F)	BRRL T (^{o}F)	#30 T.C. (μV)	#32 T.C. (μV)	Rate (gpm)	LIQ. LN_2 BOIL. Grad. (ccm)	Rate (ccm/hr)	Vac. (mm Hg)	Pressure (in. H_2O)	Operation
Mar 2										
11:30a					0.23					Start diff.pump
12:00a								0.52×10^{-3}		
2:30p								1.20×10^{-4}		Start LN_2 transfer
3:00p								1.7×10^{-5}		Finish LN_2 transfer
4:00p								7.4×10^{-6}		
5:00p	47				0.23			7.4×10^{-6}	5.9	
5:30p	46				0.23			7.4×10^{-6}	5.8	
Mar 3										
9:15a	45	55	0.370	0.362	0.23			2.7×10^{-6}	5.2	3½ in. of LN_2 in measuring dewar 2½ in. LN_2 in guard dewar
9:45a	45	55	0.372	0.367	0.23	0		2.3×10^{-6}	5.1	Start test (a)
15min.	45	55	0.372	0.367	0.23	85	340	2.2×10^{-6}	5.1	
30min.	45	55	0.375	0.370	0.23	160	320	2.2×10^{-6}	5.3	
45min.	45	55	0.375	0.370	0.23	230	310	2.1×10^{-6}	5.3	
1 hr.	45	55	0.373	0.367	0.23	310	310	2.1×10^{-6}	5.3	Finish test 3½ in. of LN_2 in measuring dewar, 1 in. of LN_2 in guard dewar Guard dewar topped
11:30a	45	55	0.367	0.369	0.23	0		2.1×10^{-6}	5.3	Start test (b)
15min.	45	55	0.369	0.367	0.23	83	320	2.1×10^{-6}	5.3	
30min.	45	55	0.376	0.372	0.23	175	350	2.1×10^{-6}	5.4	
45min.	45	55	0.374	0.372	0.23	260	350	2.1×10^{-6}	5.4	
60min.	45	55	0.374	0.367	0.23	340	340	2.1×10^{-6}	5.4	Finish test

B. CALCULATIONS

1. Area of sample = 5.81 $in.^2$ (2-23/32 in. dia.)

2. Thickness = 1/4 inch

3. Heat of vaporization of nitrogen = 0.235×10^{-3} Btu/ccm @ 0 C and 760 mm Hg

4. Temperatures: Ambient = 70 F
   Cold plate = -320 F
   Warm plate = 49 F

5. Evaporation rates:

   a. 310 ccm/hr @ (762.7 mm Hg - 11.25 in. H_2O)

   $$\text{Std. rate} = 310 \frac{(762.7 - 11.25 \times 1.87)}{760} \times \frac{492}{530} = 282 \text{ sccm/hr}$$

   b. 340 ccm/hr @ (763 mm Hg - 5 inches W.C.)

   $$\text{Std. rate} = 340 \frac{(763 - 5 \times 1.87)}{760} \times \frac{492}{530} = 314 \text{ sccm/hr}$$

6. Mean std. evaporation rate =

   $$\frac{282 + 314}{2} = 298 \text{ sccm/hr}$$

7. Heat loss through sample (Q) = $0.235 \times 10^{-3} \times 298 = 0.070$ Btu/hr

8. Mean apparent conductivity

   $$K\Big|_{-320^\circ}^{49^\circ} = \frac{0.07 \times 0.25 \times 144}{5.81\ (49 + 320)} = 0.0012 \text{ Btu-in./ft}^2\text{-hr-}^\circ\text{F}$$

V. CALCULATION OF TEST NO. 70

Data:

Emissivity of cold and warm walls = 0.74

Sample area (A_{mean}) = 37.5 cm^2 or 0.0404 ft^2

n = 10 aluminum shields 0.002 inch thick of e = 0.06 emissivity (both sides)

Spacers: 0.050-inch O.D. x 0.02-inch I.D. Teflon tubing, 13 pieces

Total thickness of sample: 0.215 in.

T_2 = 289 K or 520 R; T_1 = 77 K or 140 R

1. Gas conduction (equation 2 and 20, also sample calculation in paragraph I-A above).

$$Q_{gas} = 194\ (0.85)\ 6\ \frac{0.000288}{\sqrt{29\ (527)}}\ \frac{(520 - 140)}{10 + 1}\ 0.0404 = 0.0032 \text{ Btu/hr}$$

2. Heat radiation (equation 3 and paragraph I-B above).

$$Q_{rad} = 0.1713\ (10^8)\ (0.0404)\ \frac{520^4 - 144^4}{10\ (\frac{2}{0.06} - 1) + (\frac{2}{0.74} - 1)} = 0.0160 \text{ Btu/hr}$$

3. Conduction through solid spacer (equation 4a and paragraph I-C above).

Teflon K - 1.7 Btu-in./ft^2-hr-^oR

$$\text{Area} = \frac{\pi}{4}\ (D_0^2 - D_1^2) = 0.785\ (0.050^2 - 0.020^2) = 0.00165 \text{ in.}^2$$

Length of Teflon tubing: 0.215 - 10 (0.002) = 0.195 inches

$$Q_{solid} = \frac{1}{\sqrt{10}}\ \frac{(1.7)\ (0.00165)\ (13)}{144\ (.195)}\ (520 - 140) = 0.156 \text{ Btu/hr}$$

Total calculated heat loss: $Q_{total} = Q_{gas} + Q_{rad} + Q_{solid} + Q_{edge}$

$$Q_{total} = 0.003 + 0.016 + 0.156 + 0.015 = 0.190 \text{ Btu/hr}$$

Total heat loss found during test: $Q_{total\ exp.} = 0.194$ Btu/hr

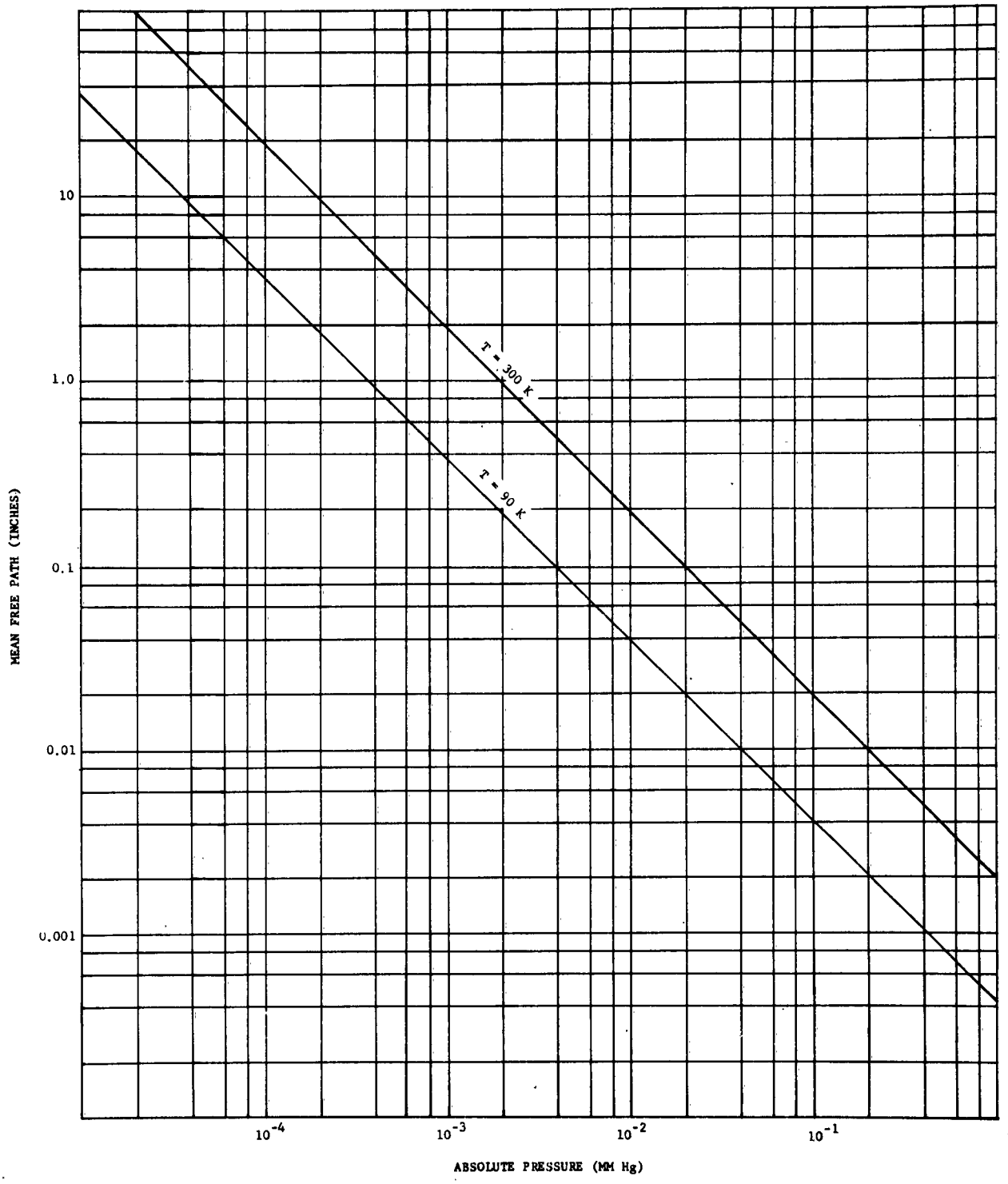

Figure 1. Mean Free Path for Air

Arthur D. Little, Inc.

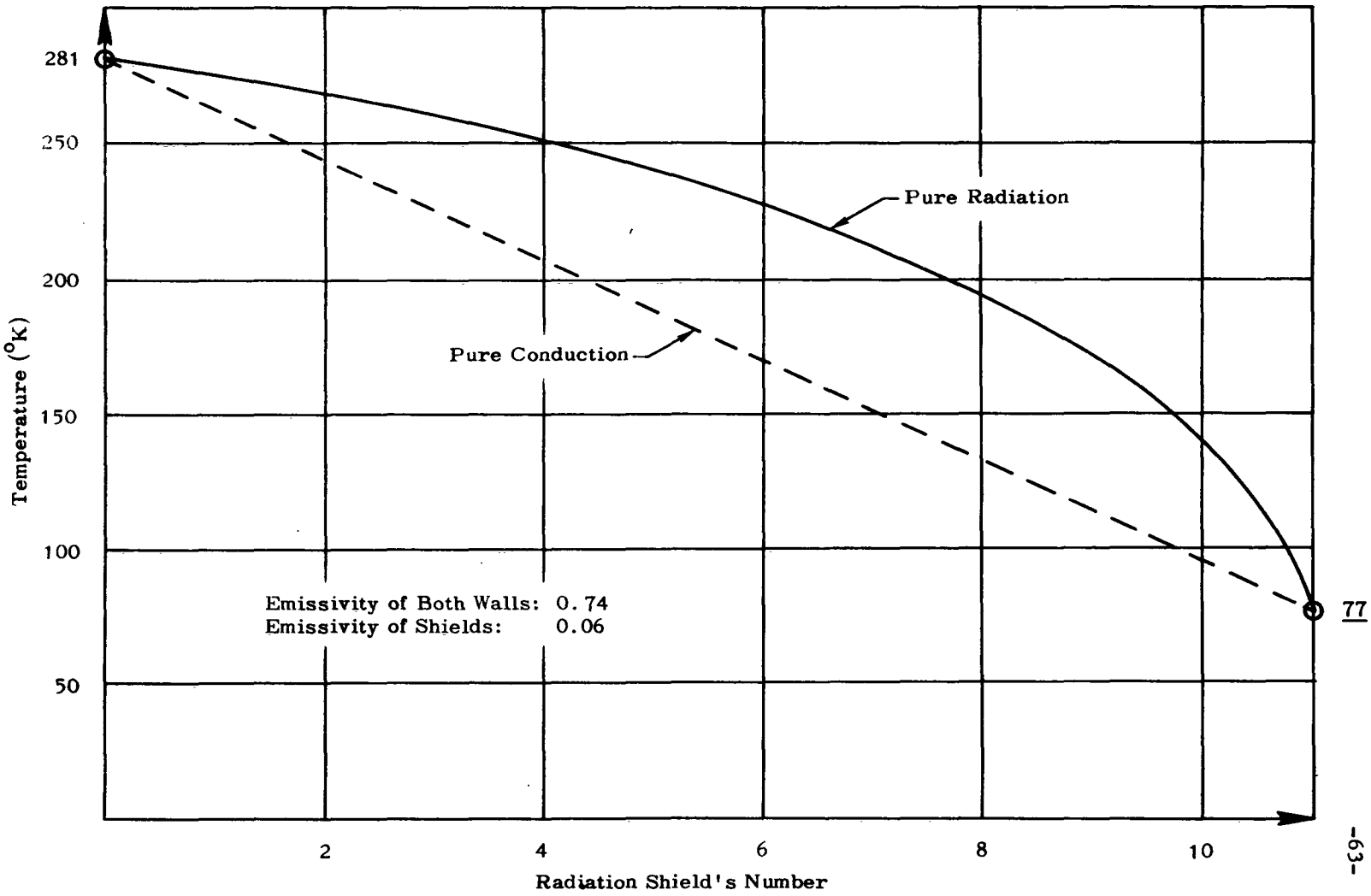

Figure 2. Theoretical Temperature Distribution Through 10 Radiation Shields Spaced in Vacuum

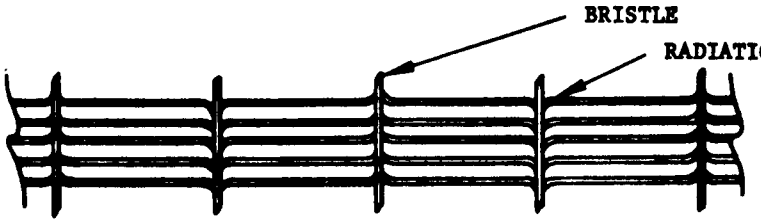

SECTION THRU BRISTLE-BONDED SHIELDING

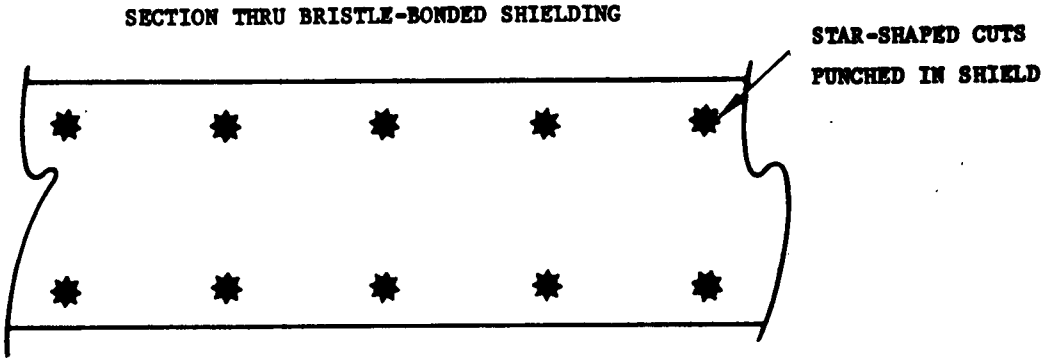

SHIELD PREPARED FOR INSERTION OF BRISTLES

If star-shaped "fingers" do not bind sufficiently against bristles, it may be necessary to string beads on bristles between shields in order to keep the shields separated. In this case a simple punched hole could replace the "star."

It will be difficult to apply this shielding to curved surfaces. Each succeeding shield will have to be larger, and the spacing between bristles larger to prevent crimping of shields near the surface.

Figure 3. Bristle-Bonded Radiation Shielding

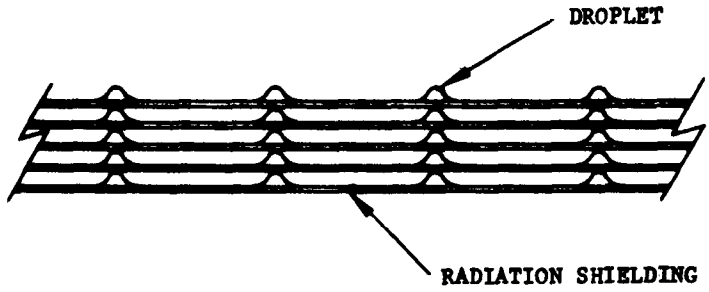

Each shield is prepared beforehand by distributing on one of its surfaces a network of droplets. For application to the surface to be insulated, the shields are stacked on top of one another.

For random distribution of droplets, a colloidal suspension of droplets could be sprayed or painted on. Care would have to be taken in the selection of the suspension system to prevent blemishing of the reflective surfaces.

For a specified lattile of droplets, the droplets might be applied to the shielding surfaces by a perforated, roller-type device, or by a network of extrusion tubes.

Figure 4. Droplet-Spaced Shielding

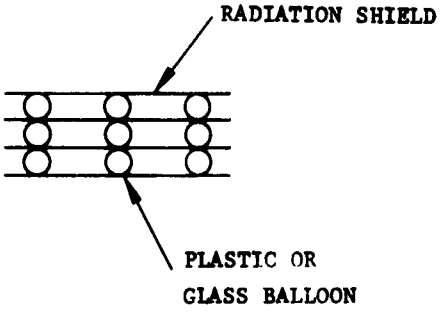

Figure 5. Balloon-Spaced Shielding

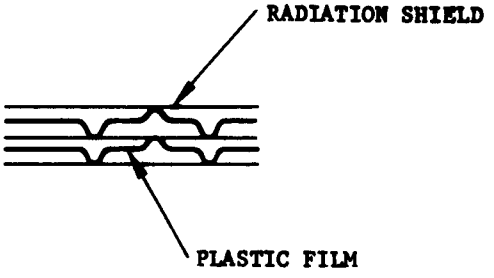

Figure 6. Shielding Spaced with Plain Embossed Plastic Film

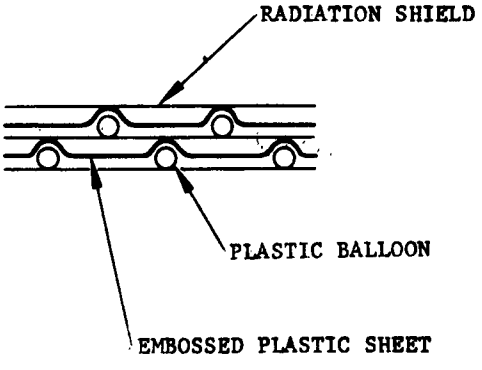

Figure 7. Shielding Spaced by Embossed Plastic Film and Balloons

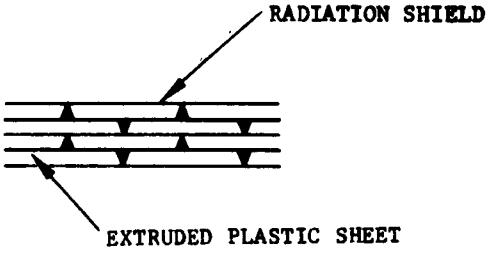

Figure 8. Shielding Spaced with Extruded Plastic Sheet

See Figure 4 for Configuration

In the stickum-globule method, some type of adhesive is applied in the desired spots on the shielding surface. Preformed droplets are then sprinkled on the surface, sticking only where the adhesive is applied. Excess droplets would be blown off.

The net result will be much the same as Figure 4, i.e., droplets on shielding surface. However, this method may be more successful in the event that a suitably viscous, air-hardening droplet material can not be found, or if the droplets do not adhere to the shielding surfaces.

Figure 9. Stickum-Globule Method

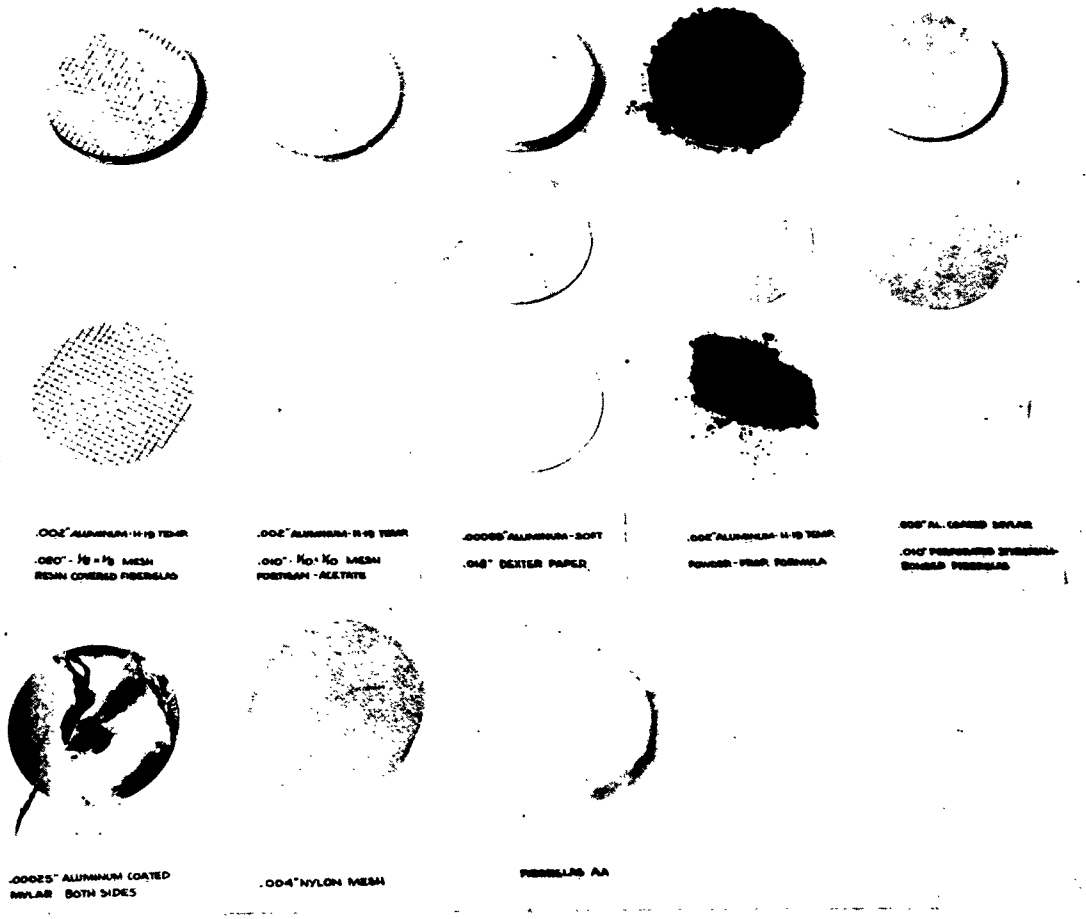

Figure 10. Component Parts of Multiple-Layer Radiation Insulation

Figure 11. Prefabricated Panel Consisting of 60 Layers per Inch of 0.00025-Inch Thick Soft Aluminum Foil and 0.008-Inch Thick Dexter Spacers

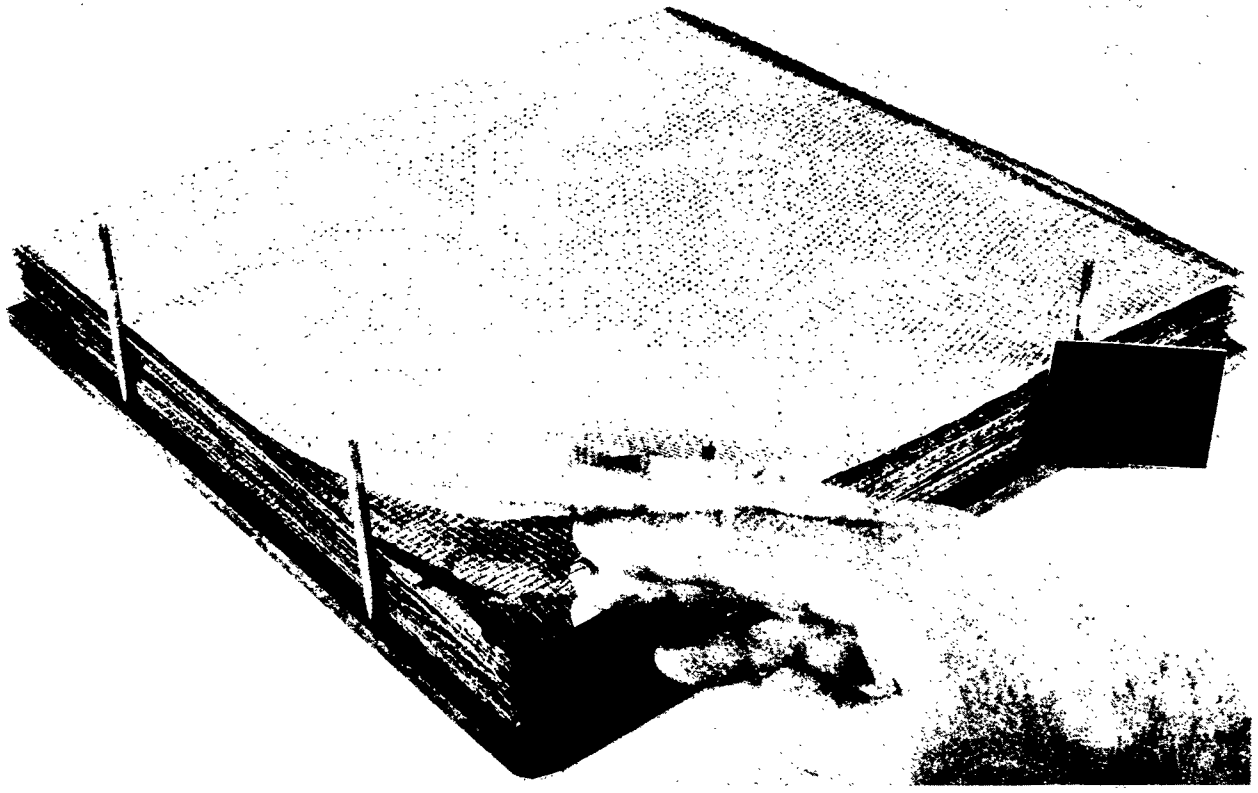

Figure 12. Prefabricated Panel Consisting of 40 Layers per Inch of 0.002-Inch Thick Aluminum Foil and 0.020-Inch Thick 1/8 x 1/8-Inch Plastic Mesh Spacers

Figure 13. Test Setup

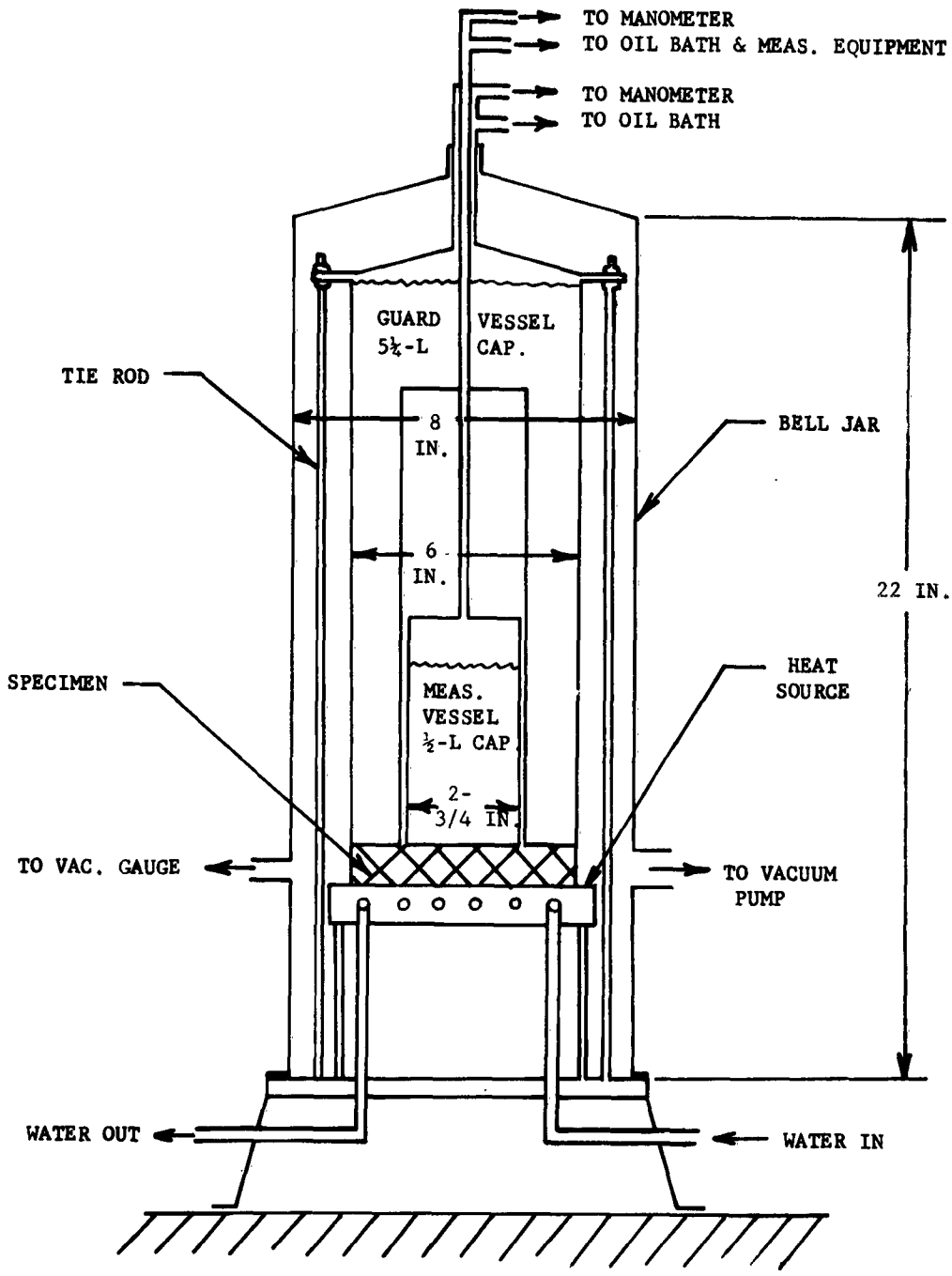

Figure 14. Single Guarded Cold Plate Apparatus

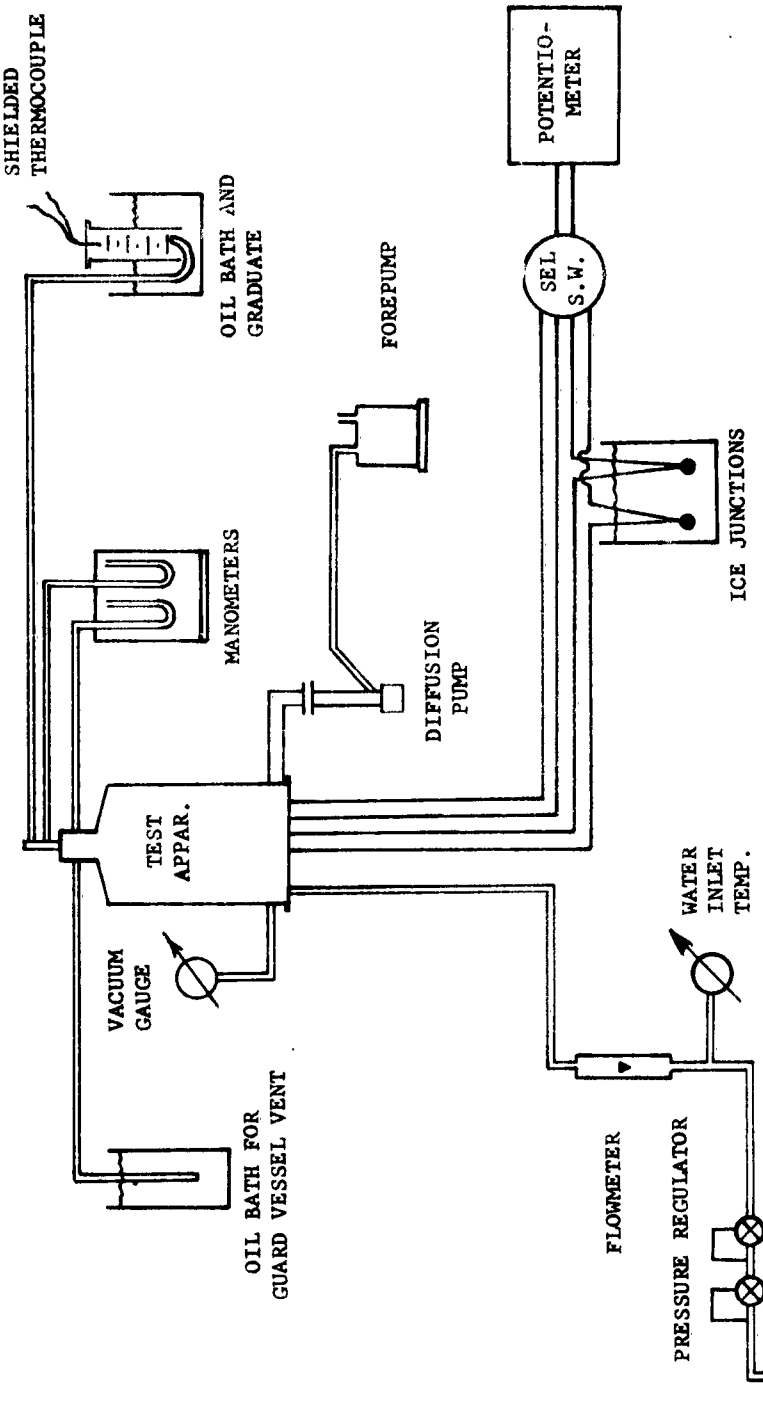

Figure 15. Test Setup of Single, Guarded, Cold-Plate Apparatus

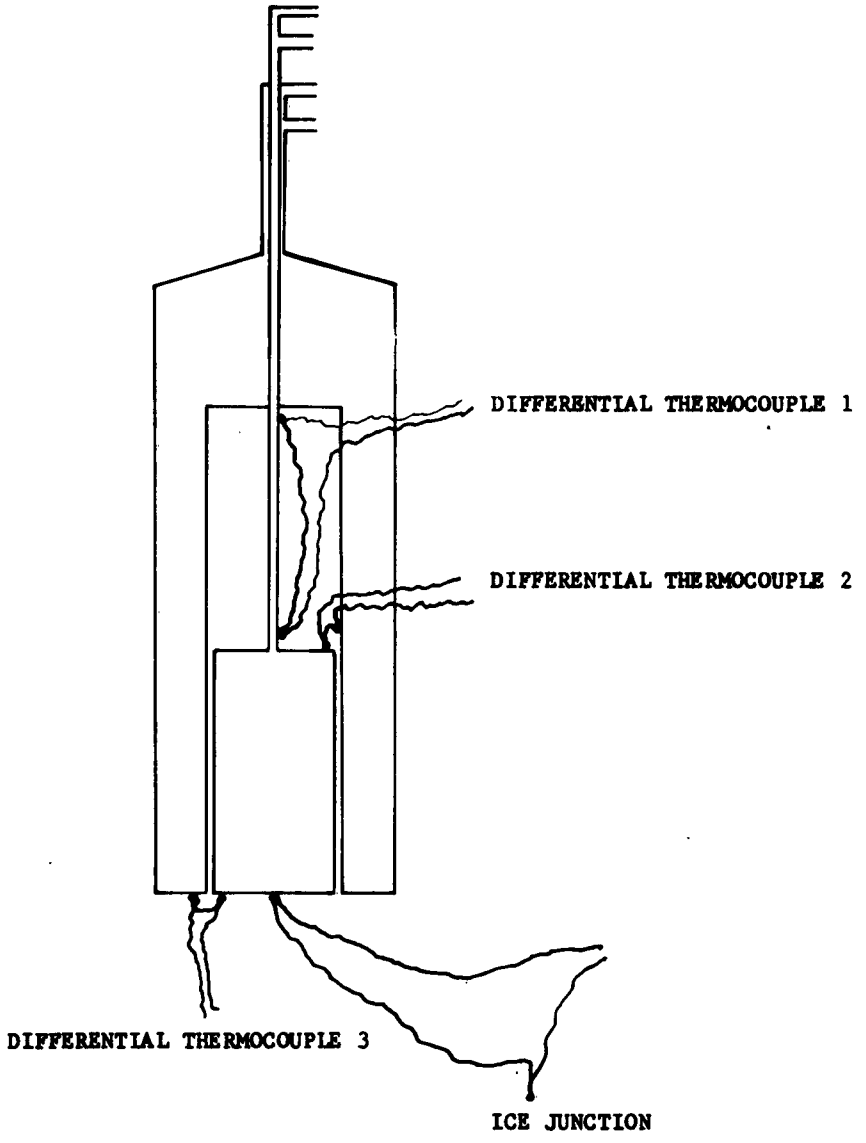

Figure 16. Location of Check Thermocouples

Figure 17. Disassembled 30 Liter Dewar

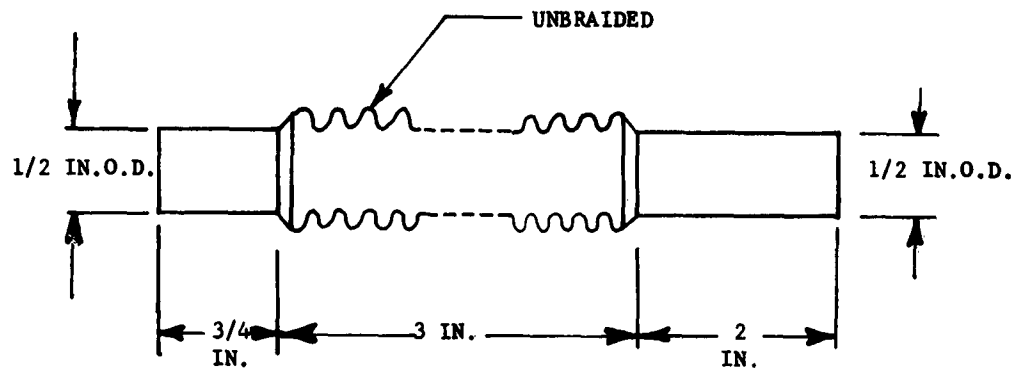

NO. 321 - STAINLESS STEEL BELLOW - SS-0

NIPPLES - 1/2 IN. O.D. x 0.028 WALL -

NO. 304 OR NO. 321 STAINLESS

Figure 18. The Neck for the 30-Liter Dewar

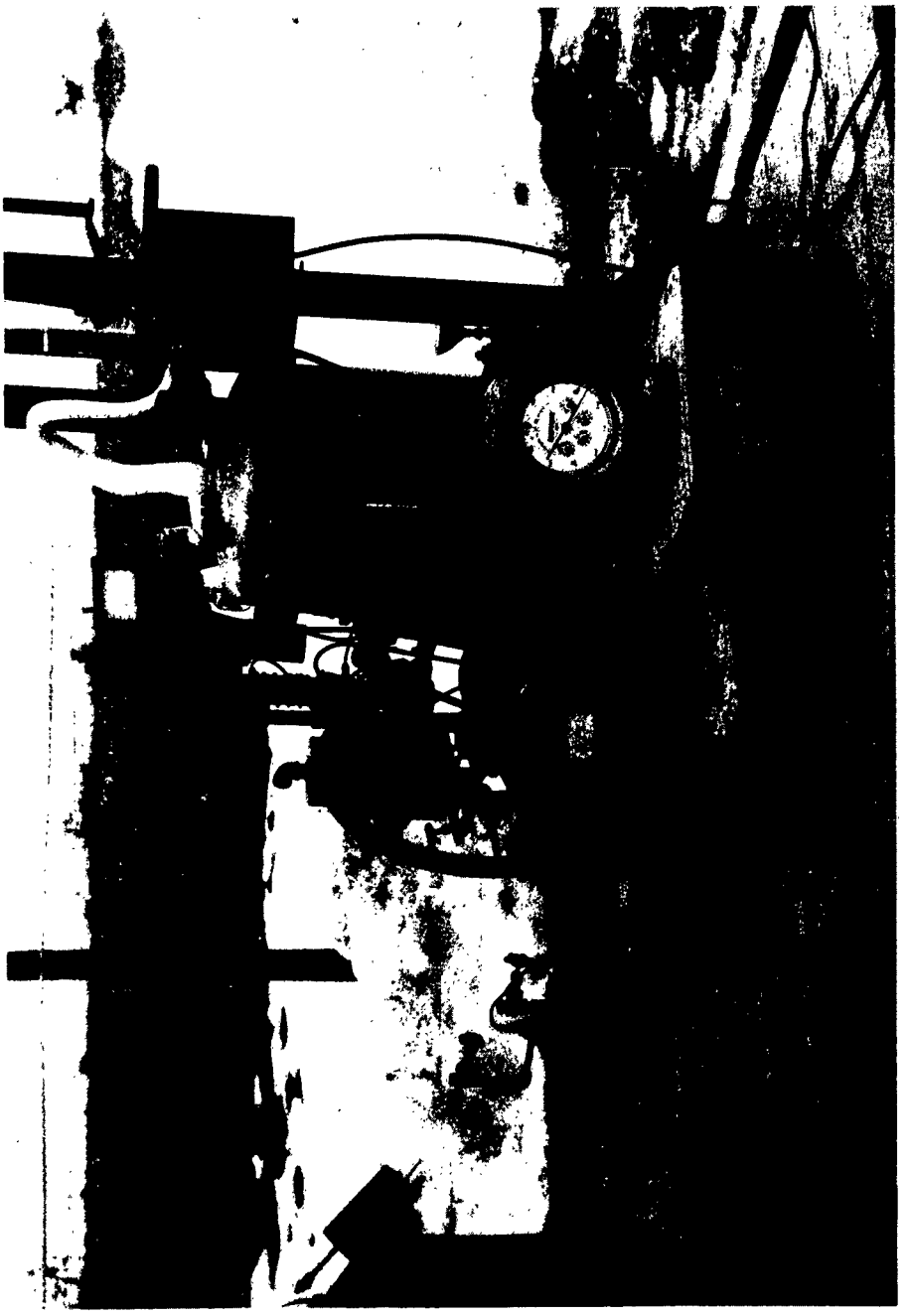

Figure 19. 30-Liter Dewar Test Setup

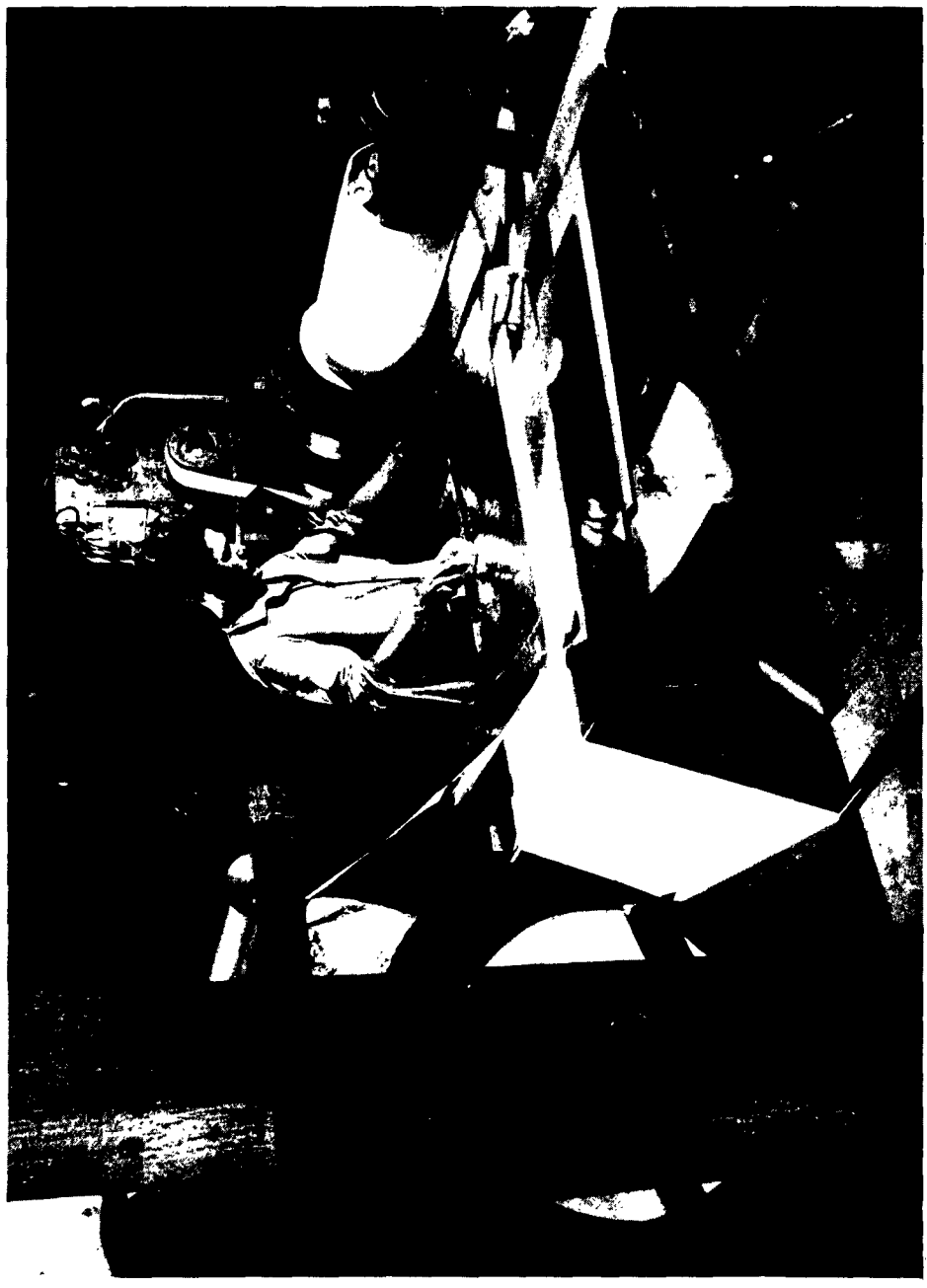

Figure 20. Winding of Insulation Using Dexter Paper Spacer

Figure 21. Winding of Insulation Using 1/8 x 1/8-Inch Mesh Plastic Spacer

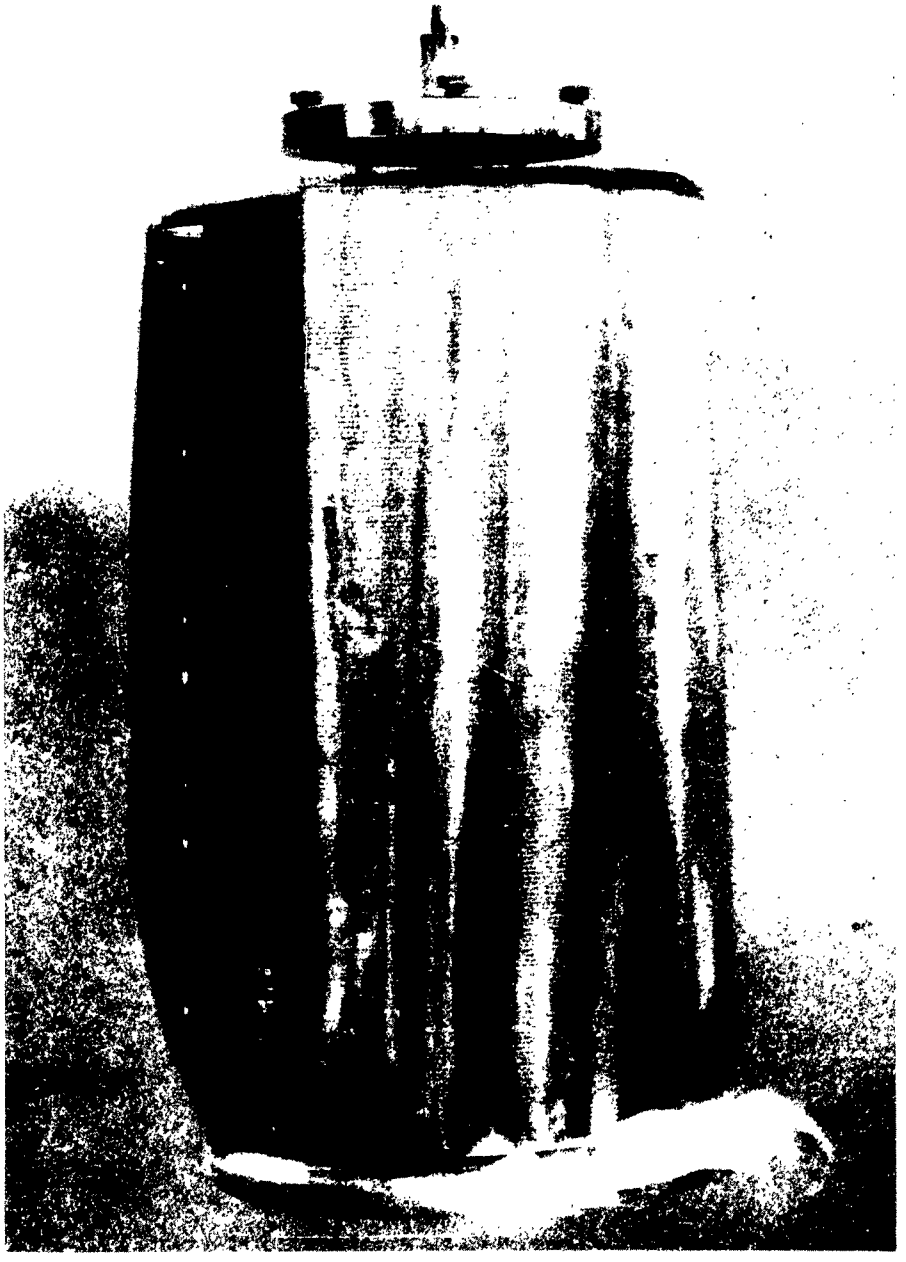

Figure 22. Insulation of 30-Liter Dewar With Prefabricated Panels

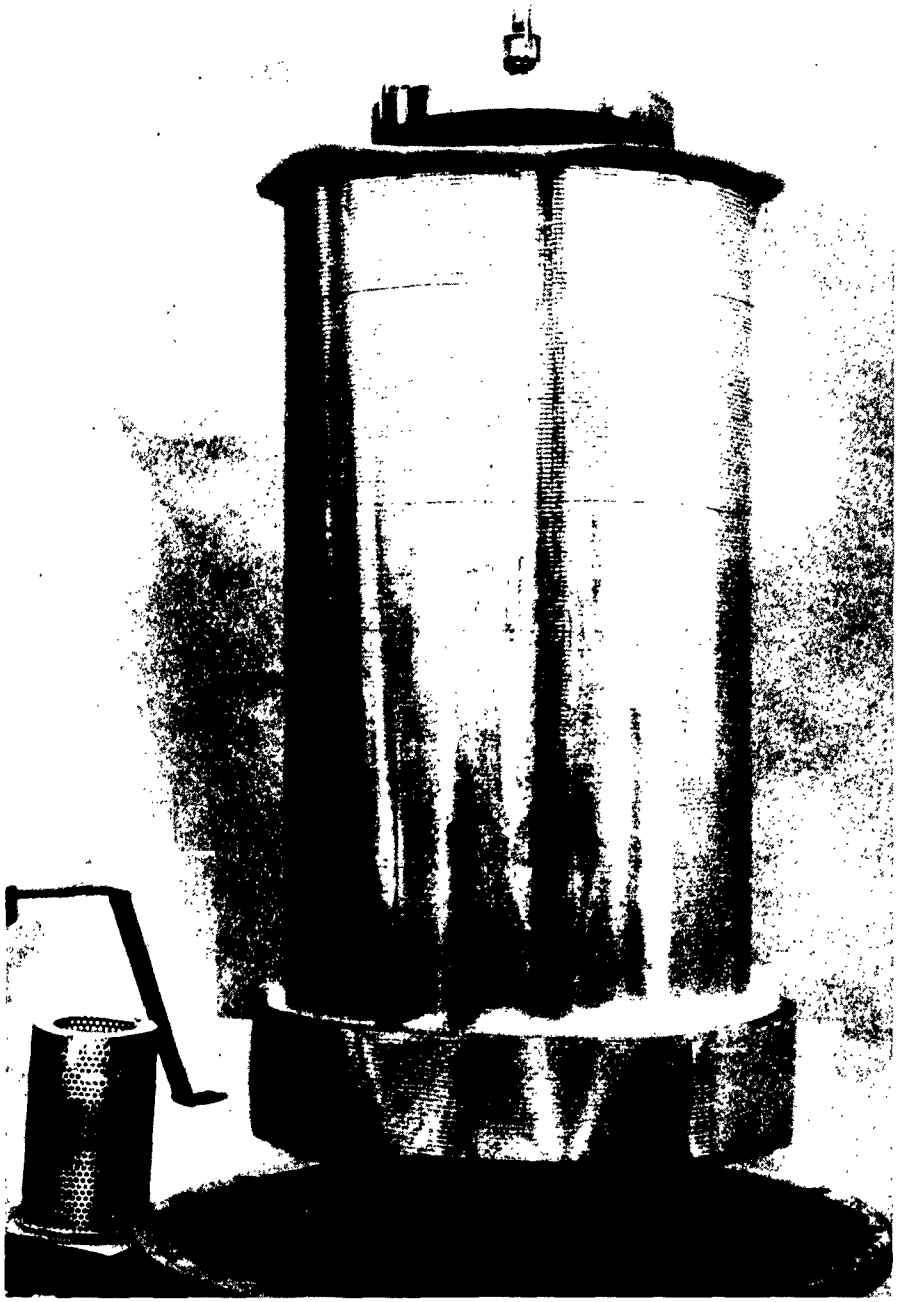

Figure 23. Inside Tank of 30-Liter Dewar with Insulation in Place

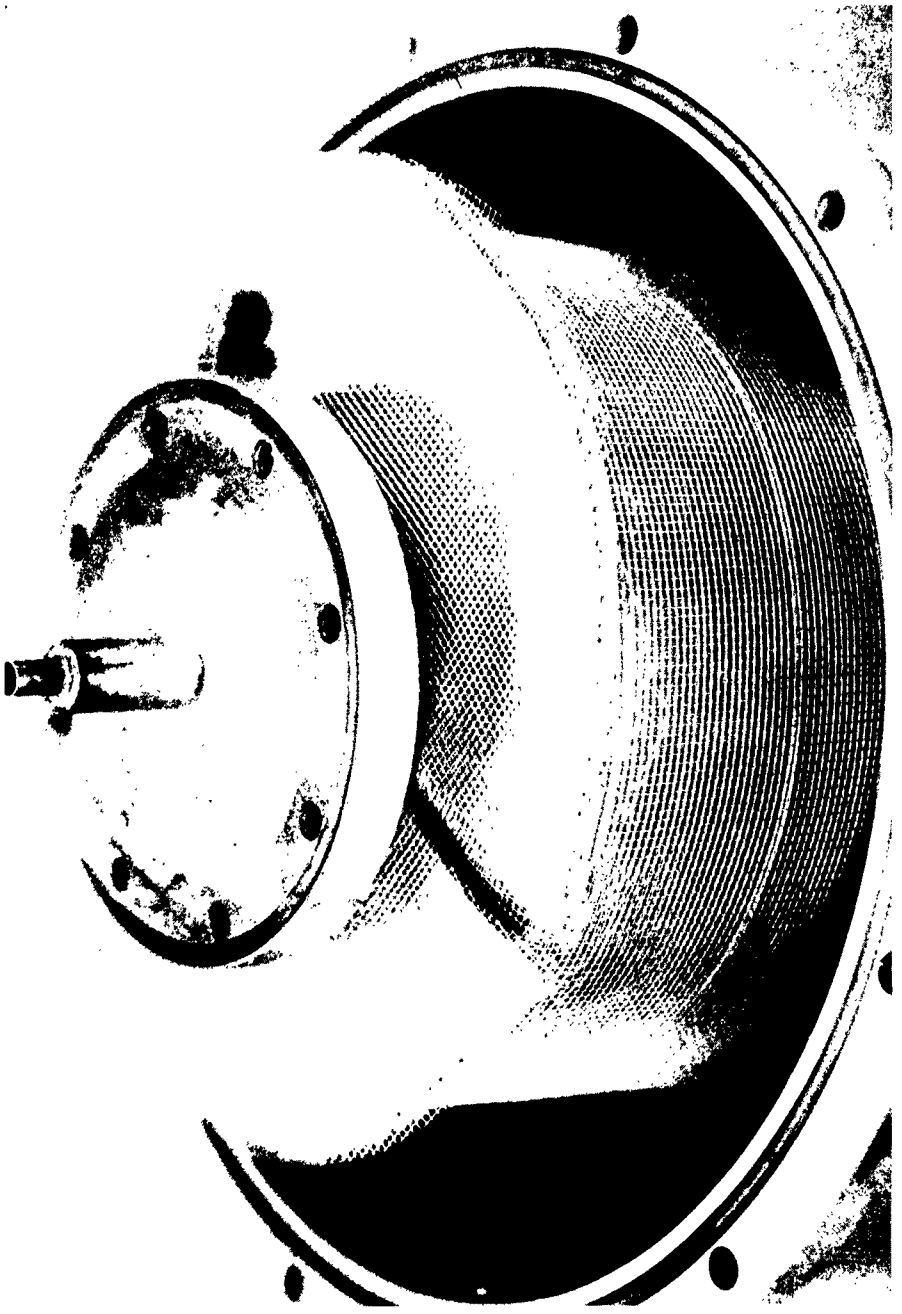

Figure 24. Top View of the 30-Liter Dewar with the Cover Off

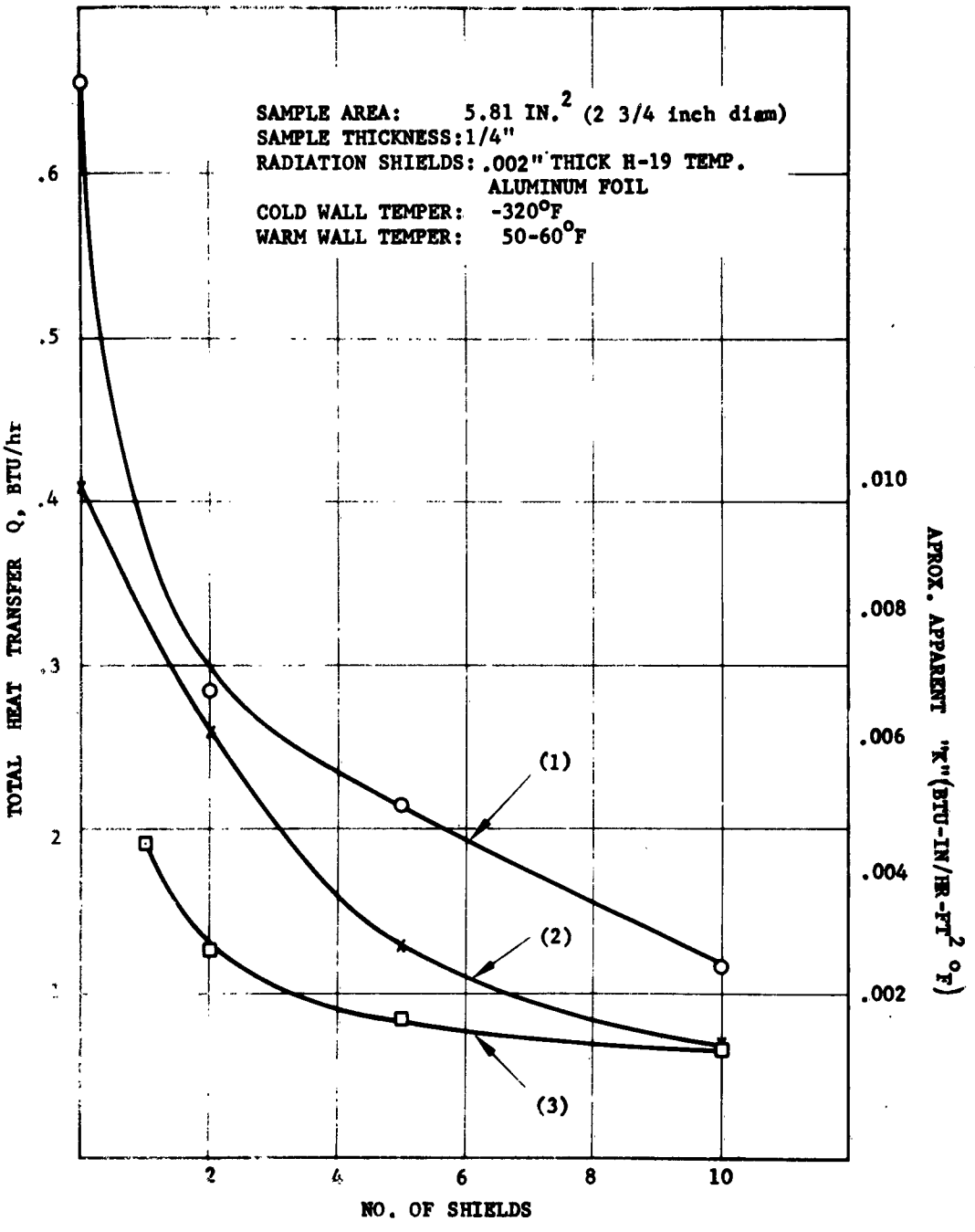

Figure 25. Influence of Number of Shields on Total Heat Transfer Through the Sample

Figure 26. Multiple-Layer Radiation Insulation Using Teflon Washers for Spacers (Top View)

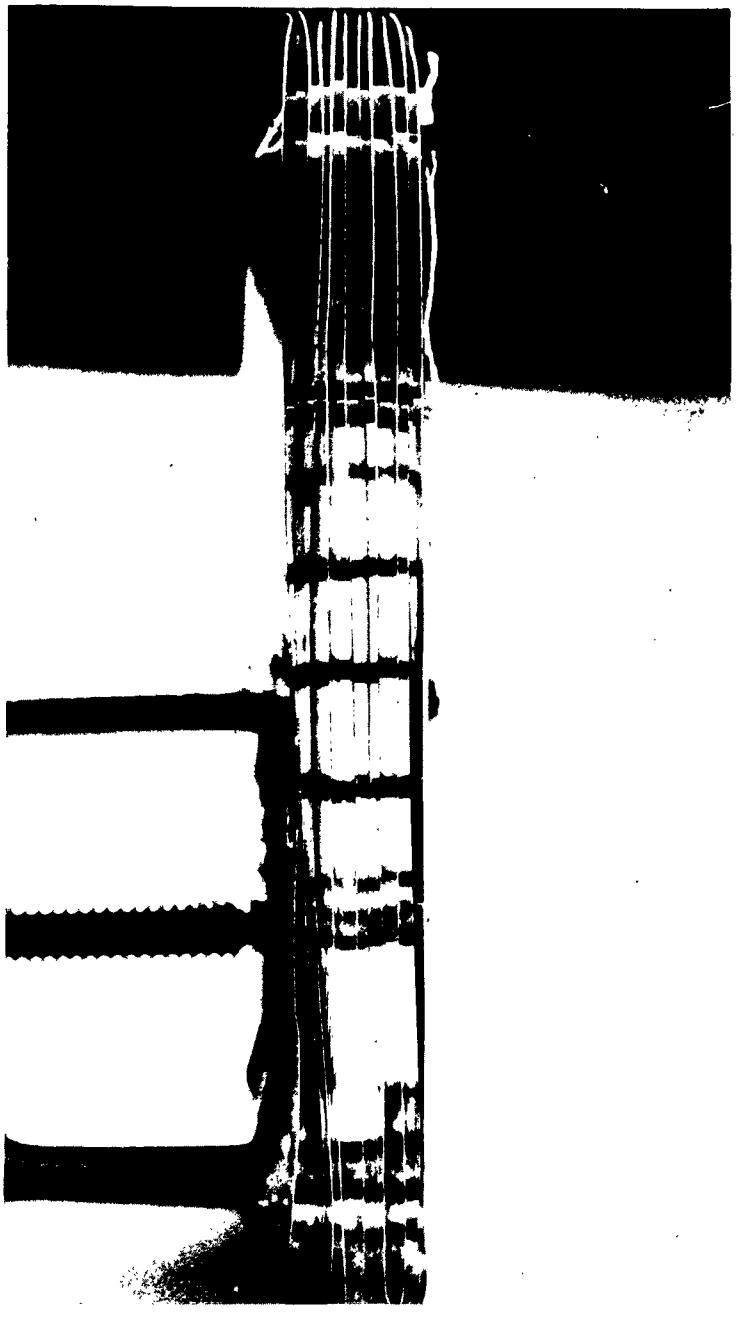

Figure 27. Multiple-Layer Radiation Insulation Using Teflon Washers for Spacers (Side View)

Figure 28. Multiple-Layer Radiation Insulation Using Teflon Washers for Spacers (Bottom View)

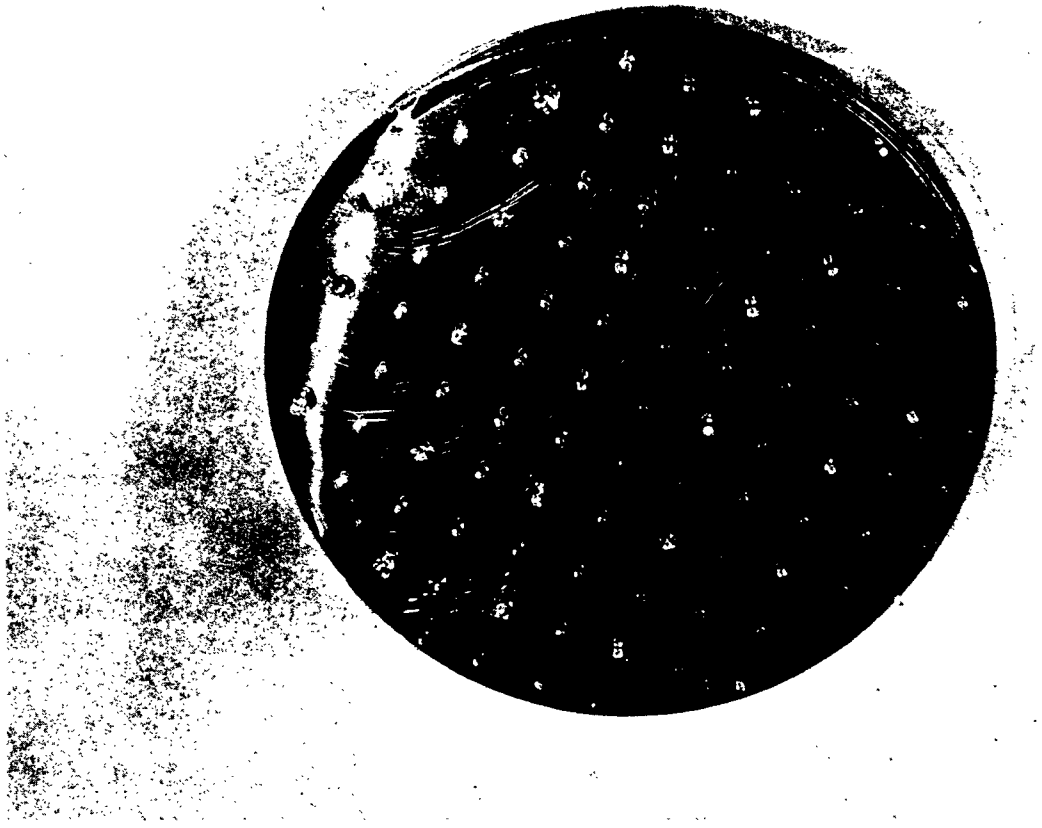

Figure 29. Multiple-Layer Radiation Insulation Using Embossed Mylar Sheets With Glass Spheres Glued into Every Second Embossment (Top View)

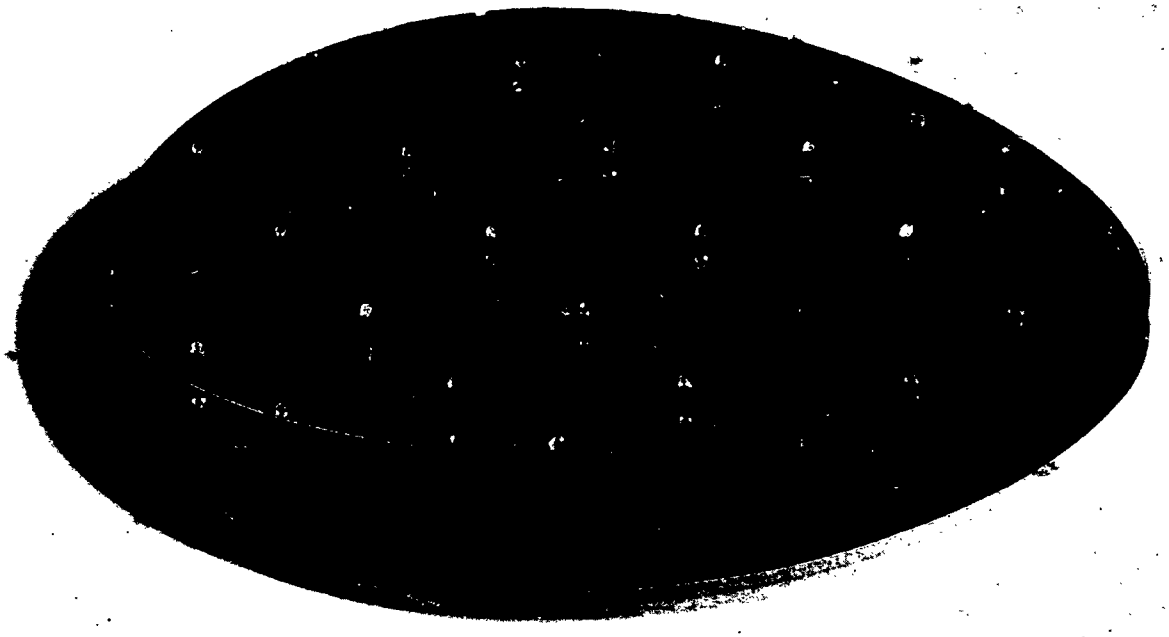

Figure 30. Multiple-Layer Radiation Insulation Using Embossed Mylar Sheets With Glass Spheres Glued into Every Second Embossment (Bottom View)

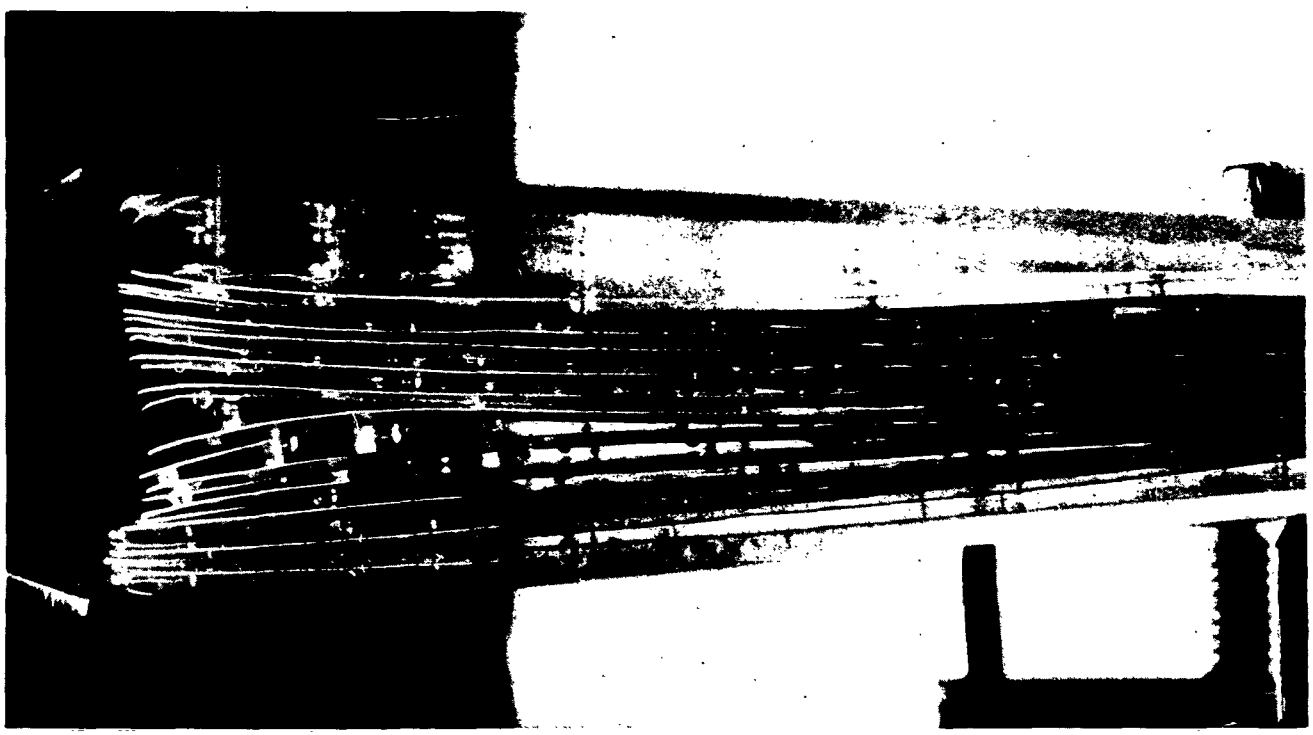

Figure 31. Multiple-Layer Radiation Insulation Using Embossed Mylar Sheets With Glass Spheres Glued into Every Second Embossment (Side View)

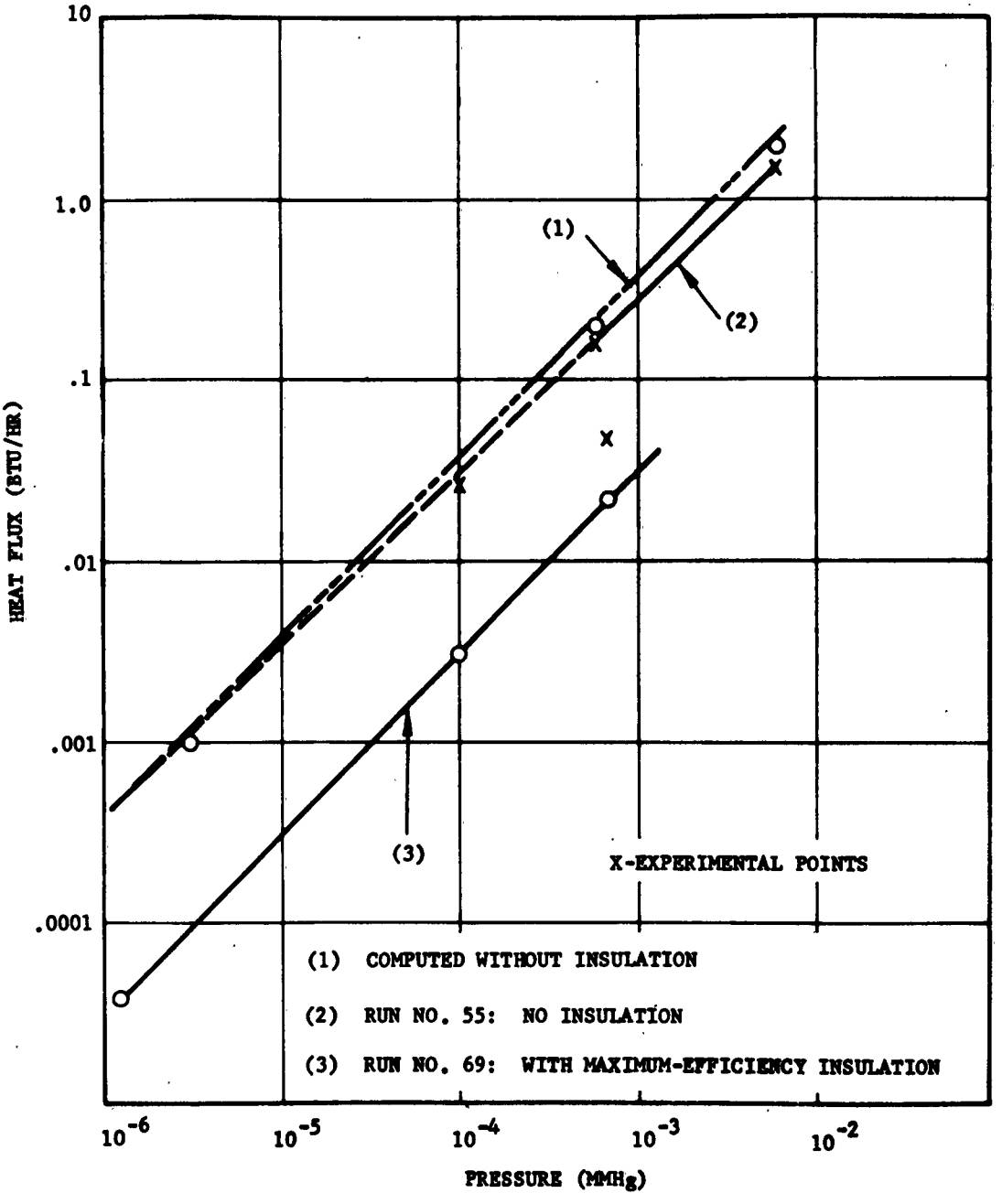

Figure 32. Gas Conduction Through Vacuum Space

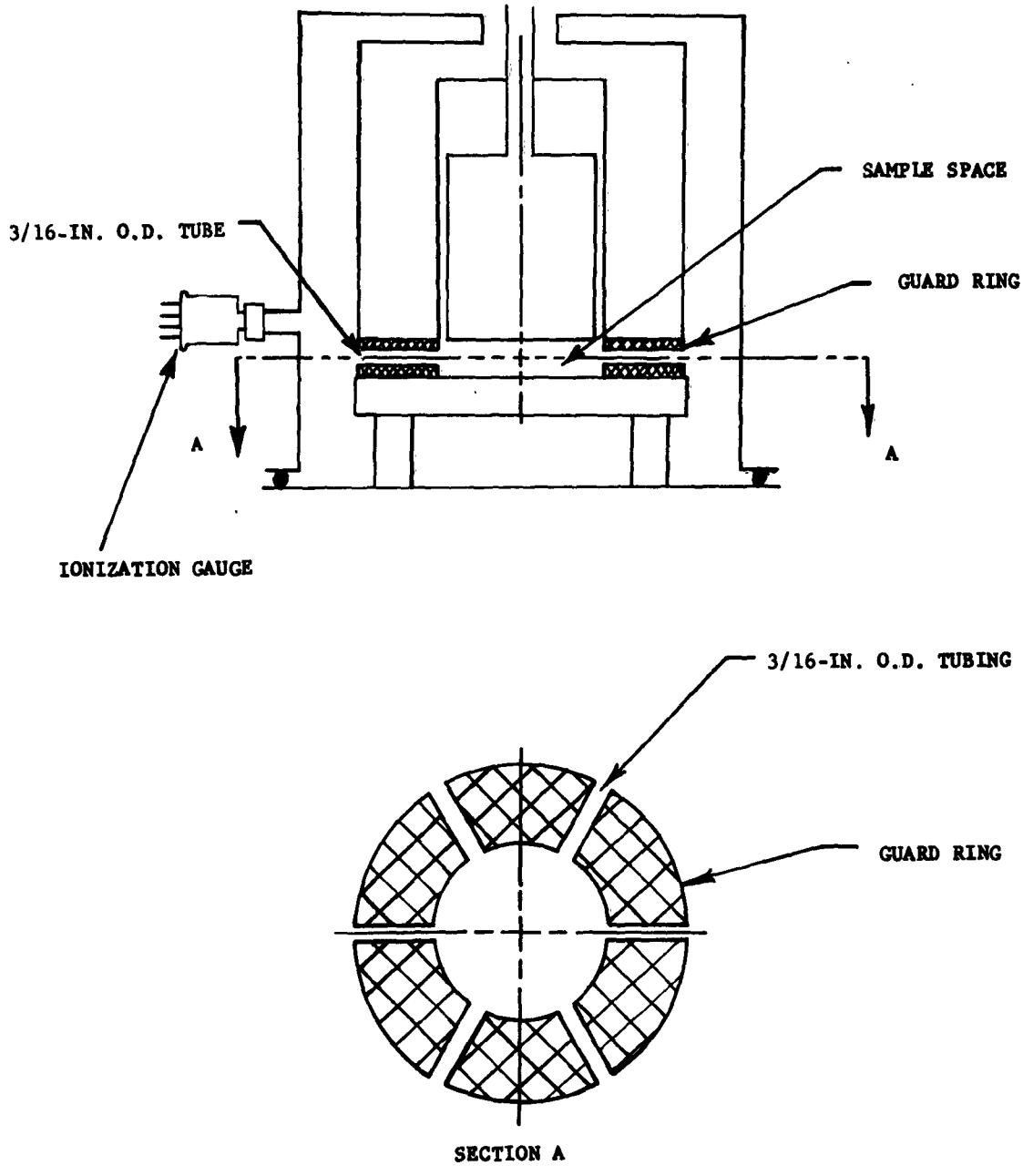

Figure 33. An Attempt to Improve Evacuation of Sample Space by Penetration of the Guard Ring with Glass Tubes

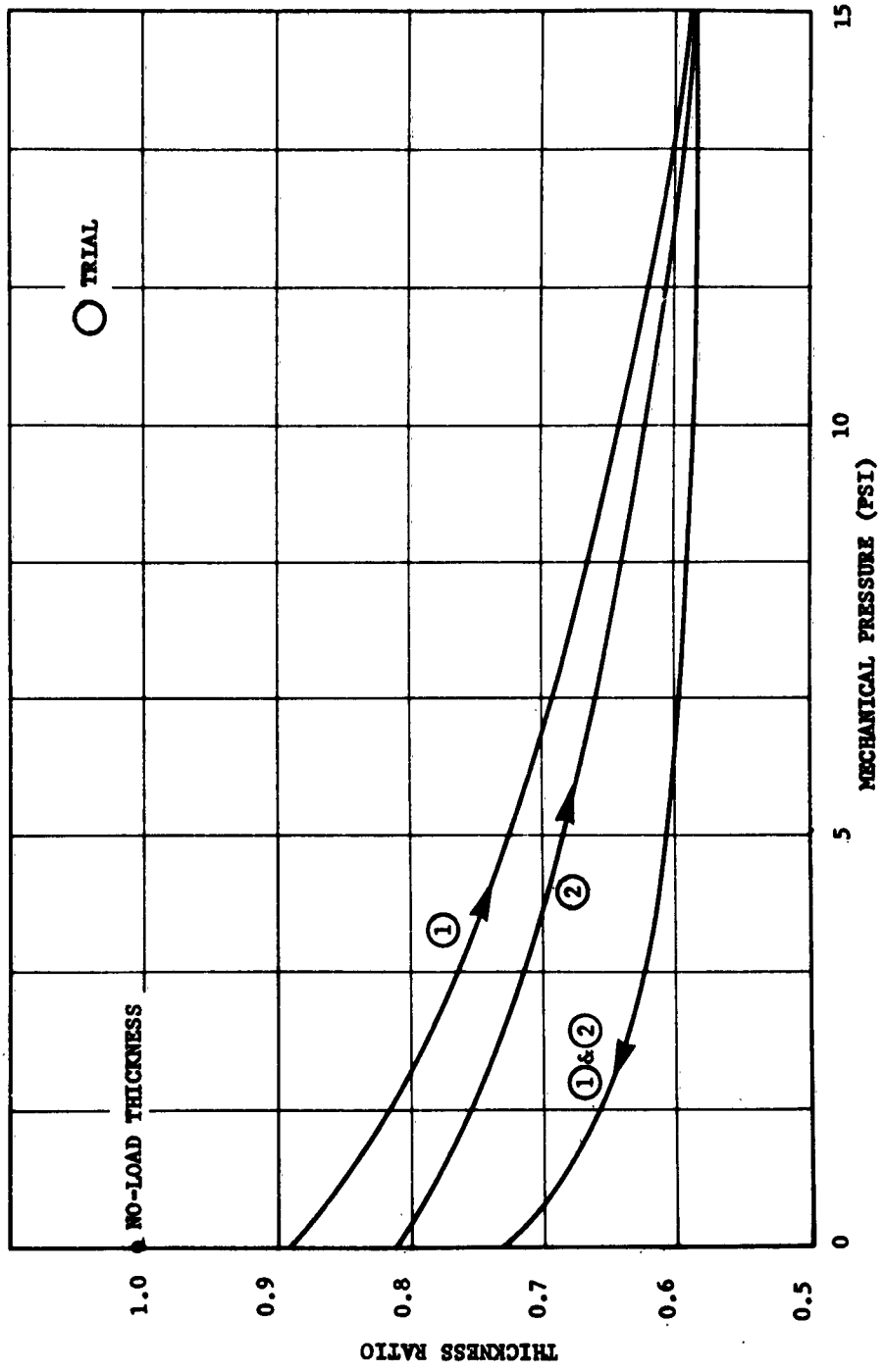

Figure 34. Compressibility of Radiation Insulation Used in Run No. 9

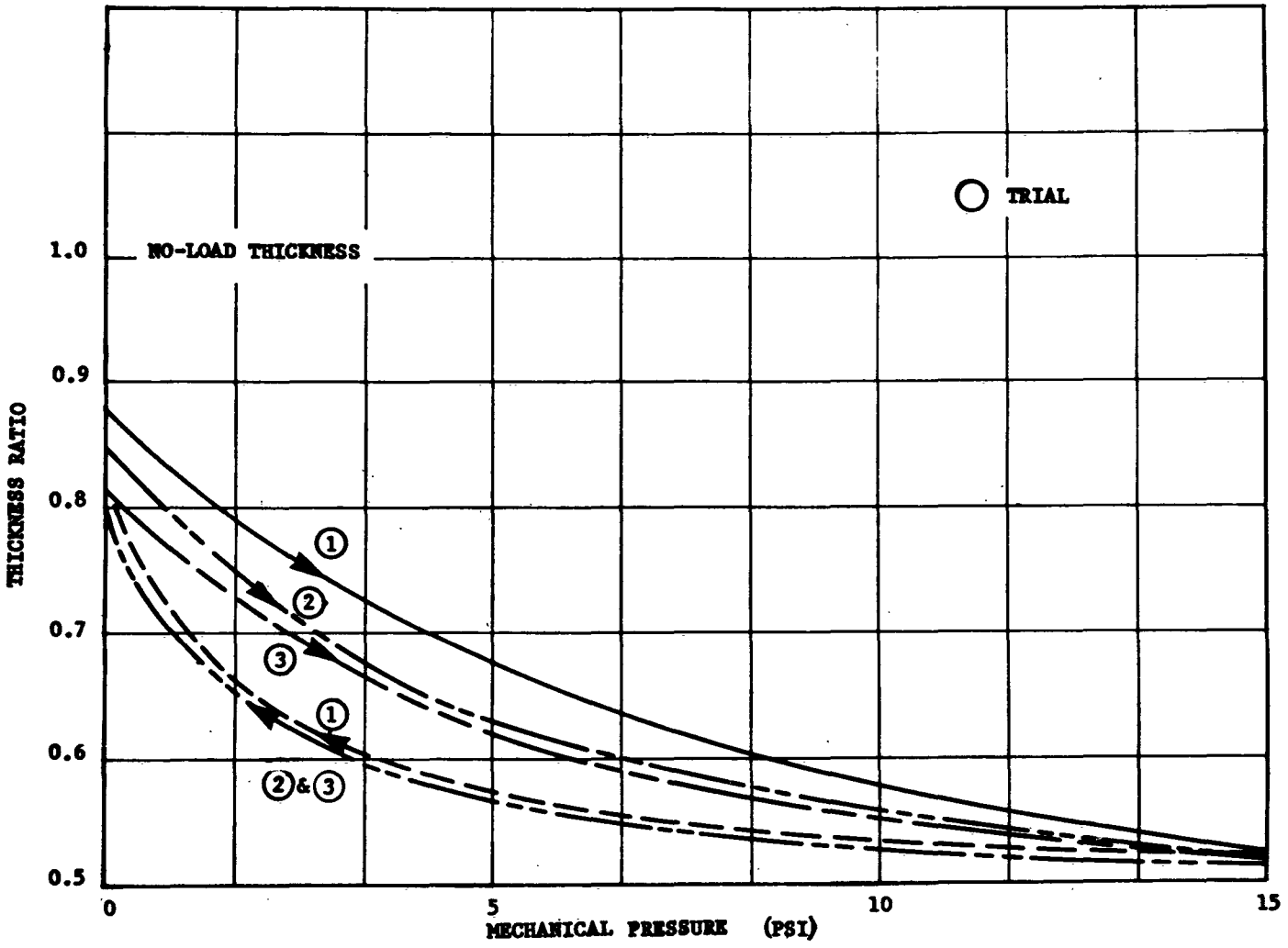

Figure 35. Compressibility of Insulation Used in Runs No. 27 & 30

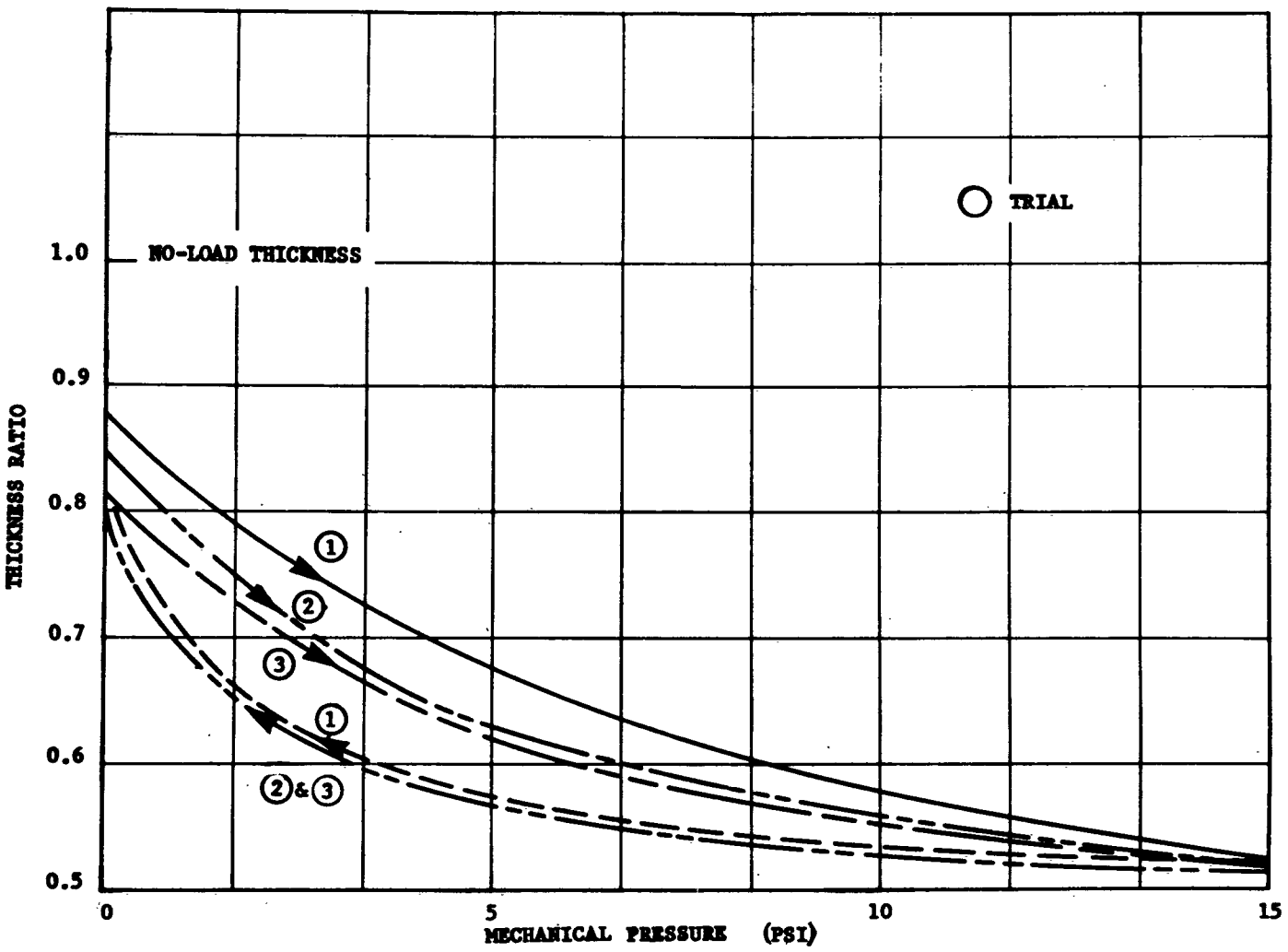

Figure 35. Compressibility of Insulation Used in Runs No. 27 & 30

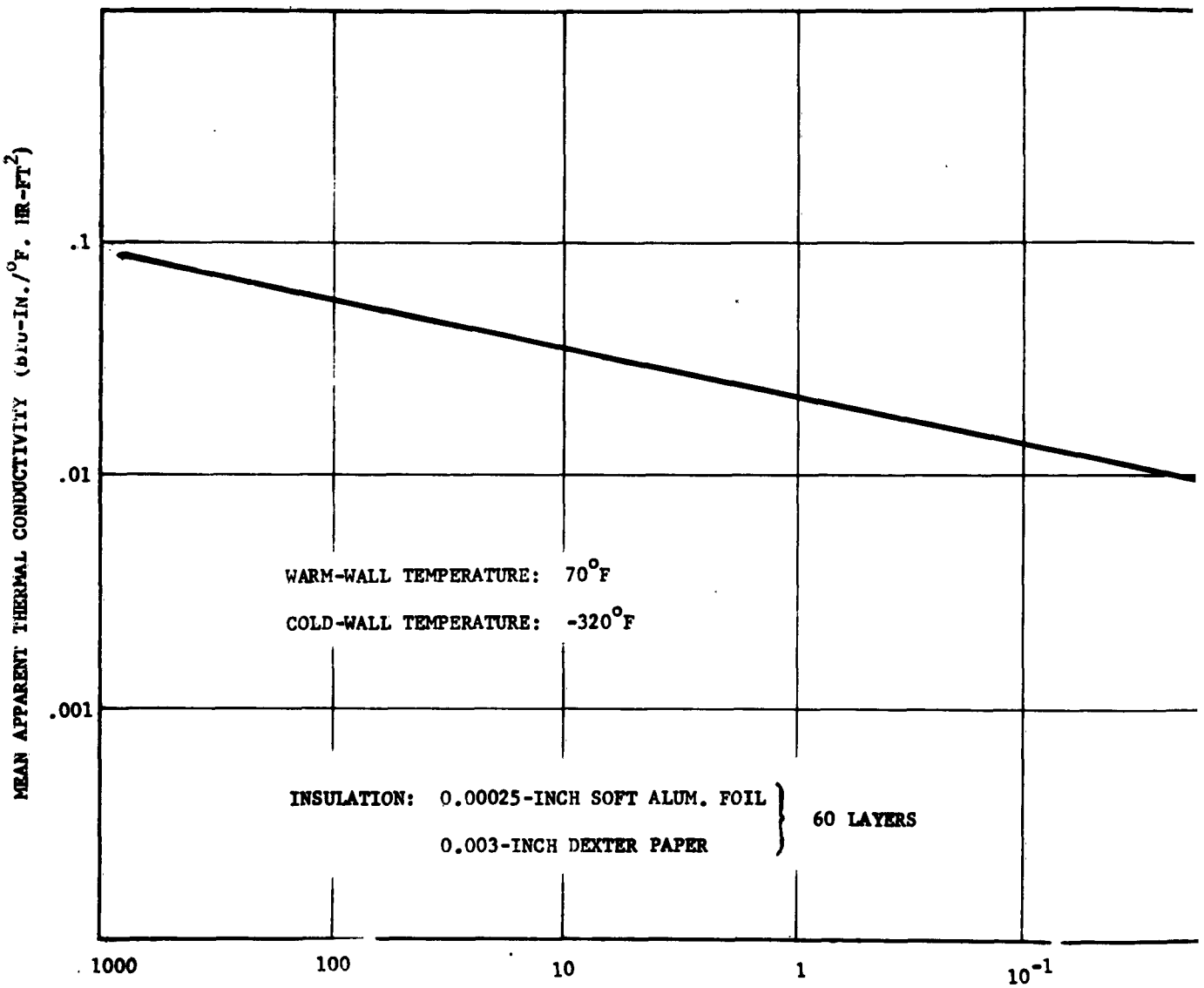
MEAN APPARENT THERMAL CONDUCTIVITY (BTU-IN./°F. HR-FT²)
.1
.01
.001
WARM-WALL TEMPERATURE: 70°F
COLD-WALL TEMPERATURE: -320°F
INSULATION: 0.00025-INCH SOFT ALUM. FOIL
0.003-INCH DEXTER PAPER
60 LAYERS
1000
100
10
1
10⁻¹
PRESSURE (MM O

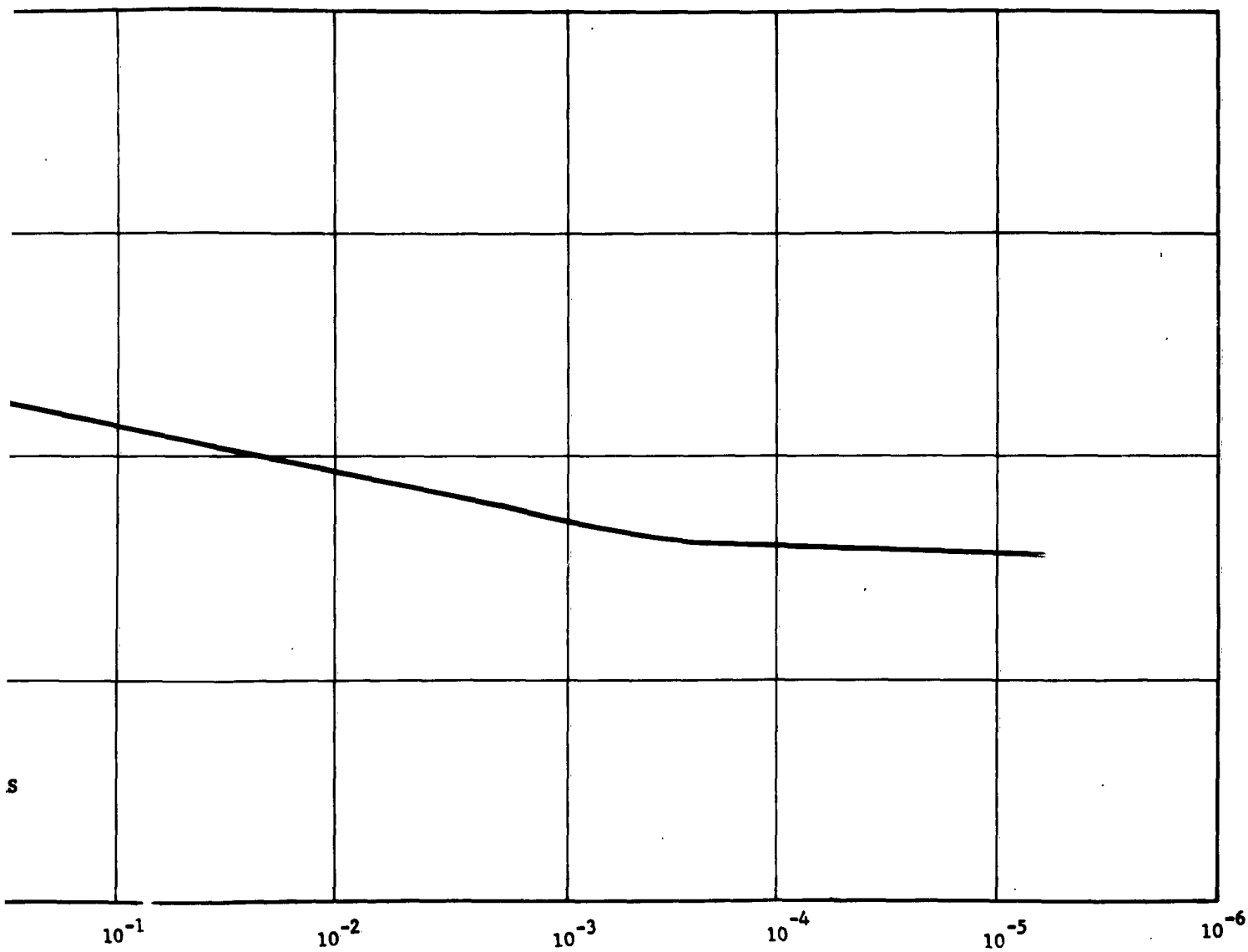

Figure 36. Mean Apparent Thermal Conductivity of Insulation

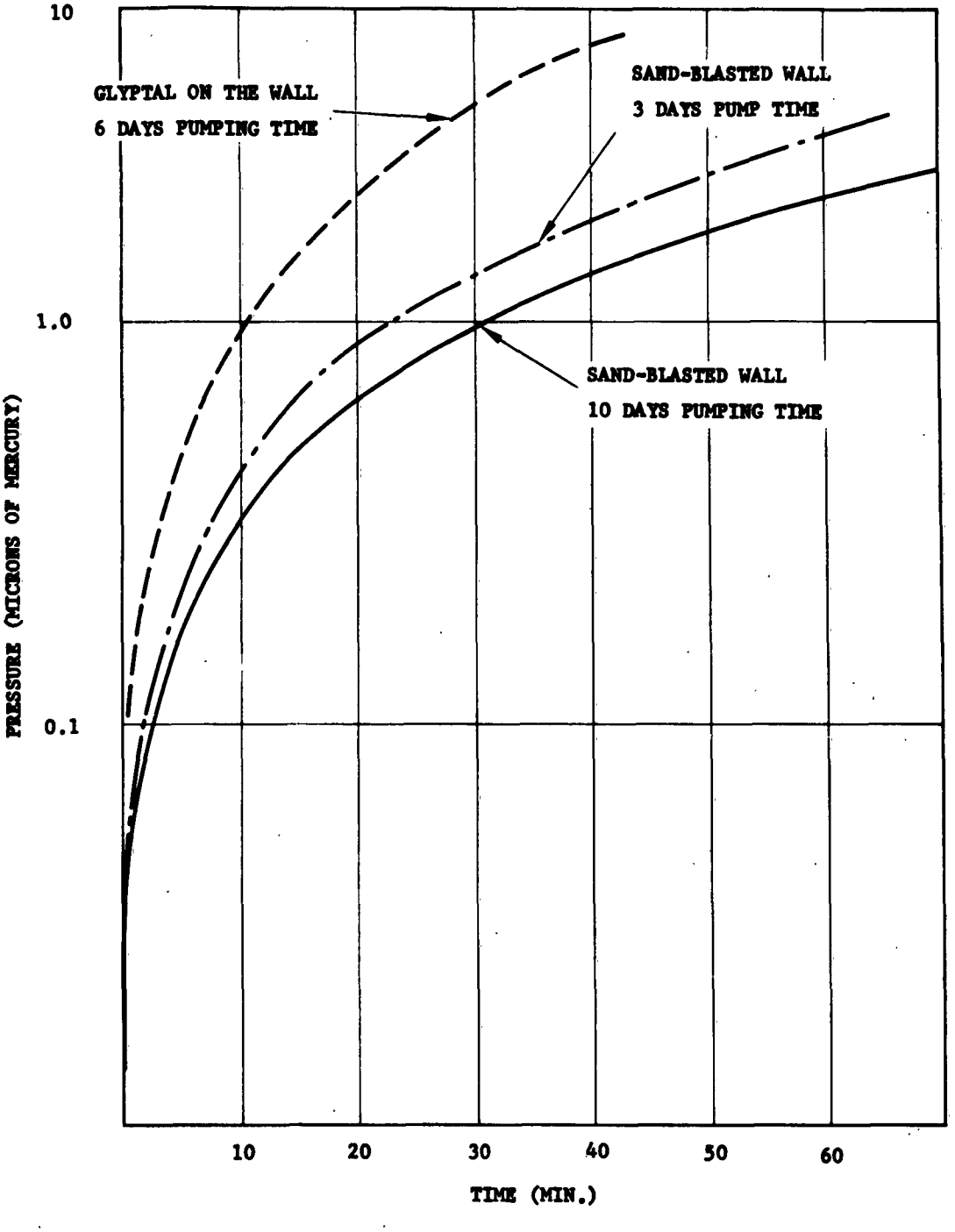

Figure 37. Pressure Rise Inside Outer Steel Tank of 30-Liter Dewar

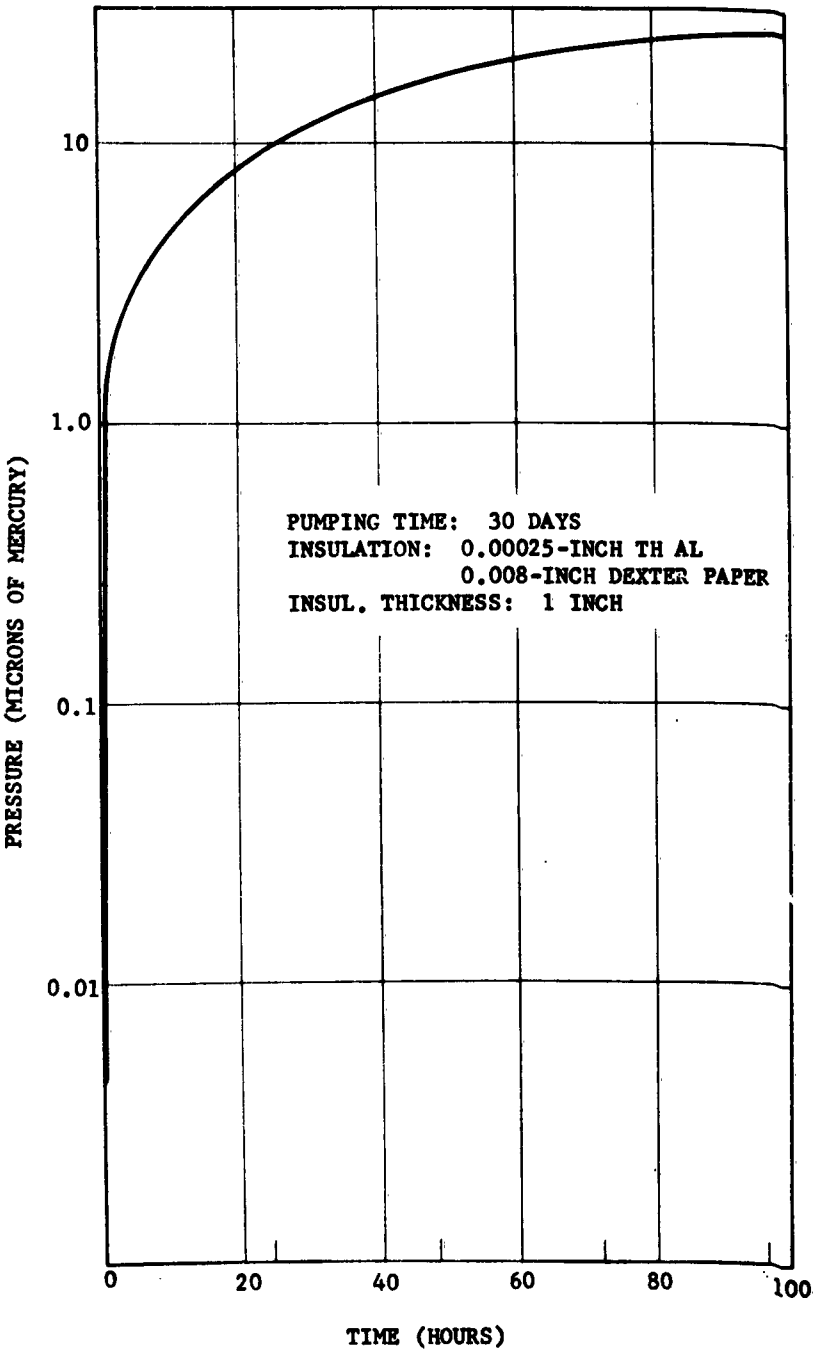

Figure 38. Pressure Rise in 30-Liter Dewar

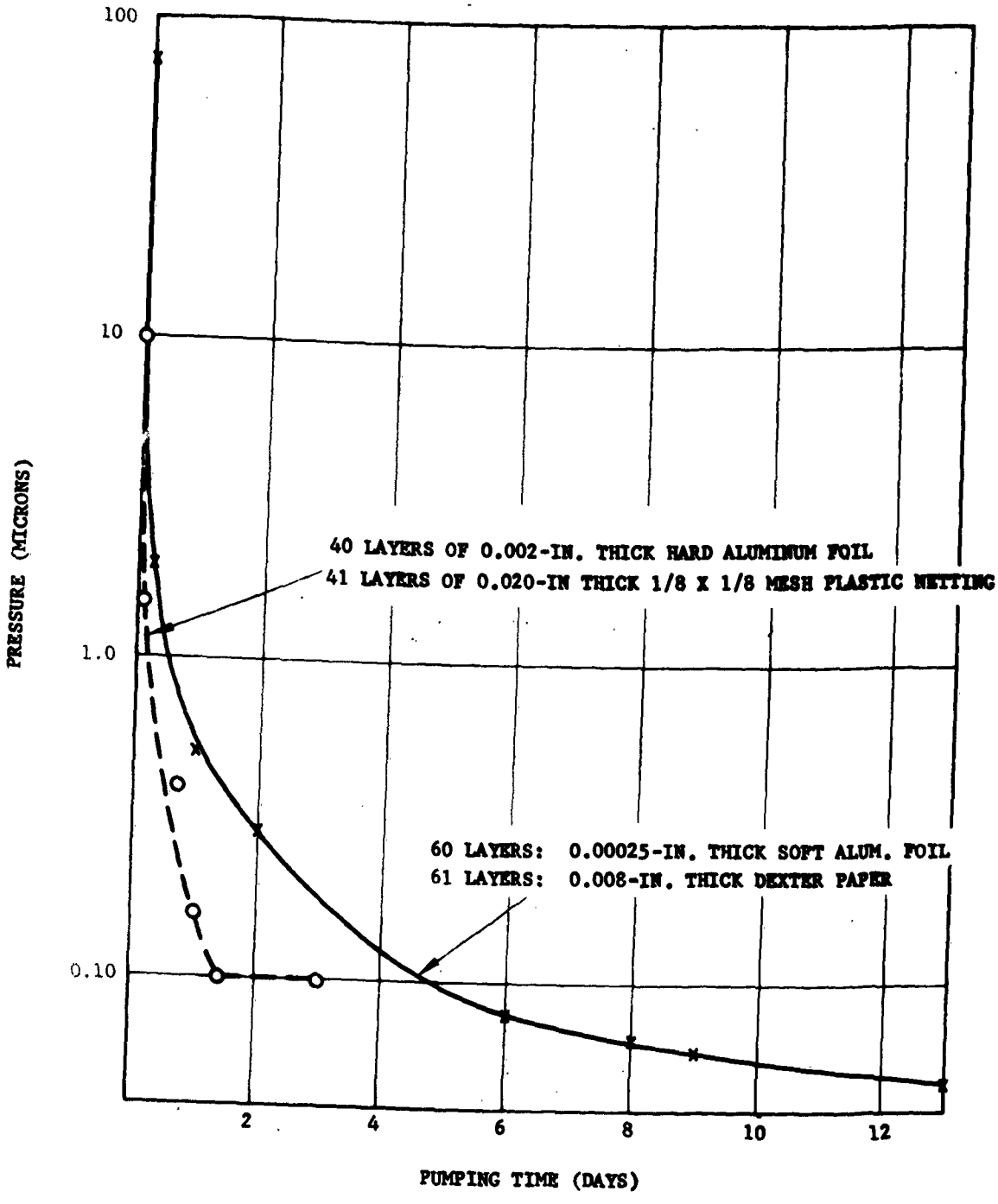

Figure 39. Pumping of High-Efficiency Insulation on 30-Liter Dewar